ISSN 1732-9353 (suspended)
eISSN 2543-7496

Scientific Review

Engineering and Environmental Sciences

Przegląd Naukowy
Inżynieria i Kształtowanie Środowiska

Vol. 30 (4) 2021 Issue 94
Quarterly

SCIENTIFIC REVIEW
ENGINEERING AND ENVIRONMENTAL SCIENCES
Quarterly

EDITORIAL OFFICE ADDRESS
Wydział Budownictwa i Inżynierii Środowiska SGGW, ul. Nowoursynowska 159, 02-776 Warsaw, Poland
tel. (+48 22) 59 35 363, 59 35 210, 59 35 302
e-mail: srees@sggw.edu.pl
https://srees.sggw.edu.pl

ISSN 1732-9353 (suspended)
e-ISSN 2543-7496

Electronic version of the Scientific Review Engineering and Environmental Sciences is primary version

All papers are indexed in the data bases as follows: AGRO(Poznań), BazTech, Biblioteka Nauki, **CrossRef**, **DOAJ**, **Google Scholar**, **Index Copernicus**, INFONA, POL-Index, **SCOPUS**, SIGŻ(CBR)

Scientific Review

Engineering and Environmental Sciences

Przegląd Naukowy

Inżynieria i Kształtowanie Środowiska

Vol. 30 (4) 2021 Issue 94

Contents

Editorial work – Anna Dołomisiewicz, Violetta Kaska

ISSN 1732-9353 (suspended) eISSN 2543-7496

Scientific Review – Engineering and Environmental Sciences (2021), 30 (4), 511–524
Sci. Rev. Eng. Env. Sci. (2021), 30 (4)
Przegląd Naukowy – Inżynieria i Kształtowanie Środowiska (2021), 30 (4), 511–524
Prz. Nauk. Inż. Kszt. Środ. (2021), 30 (4)
https://srees.sggw.edu.pl
DOI 10.22630/PNIKS.2021.30.4.43

Mohamed Saad ABBADI, Nouzha LAMDOUAR
Mohammed V University in Rabat, Mohammadia School of Engineers

Multi-objective optimization of elastomeric bearings to improve seismic performance of old bridges using eigen analysis and genetic algorithms

Key words: seismic isolation, OpenSees, genetic algorithms, Eurocode 8

Introduction

Bridges are a vital link in a road transport network, and their closure during extreme events such as earthquakes poses a threat to emergency services. In addition, the economic consequences can be severe in case of prolonged closure of these structures. Because of their importance for access to and evacuation of earthquake-affected areas, bridges and viaducts must remain operational with minimum capacity criteria after an earthquake. Some old bridges in Morocco are 40 years old or more. Consequently, they were designed without considering important seismic details that have been incorporated in recent codes and are not in conformity with the new seismic hazards. In addition, the effect of corrosion on transverse and longitudinal reinforcement of the piles contribute heavily on the reduction of the strength and ductility of the structure.

Many attempts have been made to provide old bridges additional ductility and strength, and seismic isolation remains the most practical and effective way to achieve it. The interest of an isolation system is the gain in lateral flexibility of the connection between the deck and the supports. This additional flexibility allows the fundamental period of vibration of the structure to be shifted to larger ranges of values. The seismic response of the structure is reduced and can approach the elastic range or with limited ductility.

However, an excessively prolonged period of vibration of the isolated bridges, using over flexible bearings, could lead to higher displacements

between the deck and the piers, causing great damage on joints and bearings, spacing and discontinuity of the deck, and in some critical cases the unseating of the superstructure.

Many studies found in literature on optimal design of the seismic isolation system have been conducted during past decades. For example, Alhan and Gavin (2005) studied the seismic risk analysis of vital equipment by specifying the reliability of each component of the isolation system by considering the reliability of the entire isolated structure, for different seismic hazard levels. It includes uncertainties such as isolation system and ground motion characteristics by mean of Monte Carlo simulation techniques to determine failure probabilities. Léger, Rizzian and Marchi (2017) performed a multi-objective reliability-based design optimization of reinforced concrete structures with elastomeric base isolators, considering vertical loads and isolator damping as sources of uncertainties, and having the objective of minimizing displacement and forces at the floor level to limit damage. Mishra, Roy and Chakraborty (2017) considered optimizing the reliability of isolation systems at the base to overcome the damaging effects of seismic action and taking into consideration the uncertainties of the system. The concept of total probability theory is used to evaluate the unconditional response of structures under parameter uncertainty and a multi-story building isolated with elastomeric bearings to illustrate the effects of parameter uncertainties on the optimal performance of isolation systems. Roy and Chakraborty (2015) performed a robust optimization of the base isolation systems considering random parameters of the isolators, the structure and the seismic action. This optimization is conducted by minimizing the sum of the maximum displacement values of the structure floors and their standard deviation. Scozzese, Dall'Asta and Tubaldi (2019) analyzes this problem by proposing a general framework to explore the seismic risk sensitivity of structural systems with respect to system properties that vary within defined ranges. The results obtained show that the response of the structure varies considerably with damping properties. Scruggs, Taflanidis and Beck (2006) proposes a probabilistic approach to isolation systems based on structures modeled as linear dynamic systems subjected to stochastic seismic loads. Matsagar and Jangid (2004) studied the seismic response of bridges isolated by elastomeric bearings subjected to bi-directional seismic loads.

This research aims to provide a good understanding of the effects of seismic isolation as a rehabilitation method on the seismic performance of typical bridges, by formulating a multi-objective optimization problem, in order to efficiently design isolation system to retrofit exiting bridges, and determine a set of optimal compromising solutions that took into consideration the conflicting objectives cited before.

This procedure is coupled with a three-dimensional numerical model of the structure created using OpenSees, which allows a very detailed representation of the behavior of the structures, in order to quantify the effect of vibration period extension on seismic analysis results (displacements and stresses) (Alkhamis, Ghasemi, Gholinezhad, Shabakty & Abdullah, 2018).

Elastic response spectra

The reference representation of the seismic action in the Eurocodes is in the form of response spectra of an equivalent single degree of freedom system, with a viscous damping of 5% as a reference. In addition, Eurocode 8 adopt reference peak ground acceleration (PGA) on rock from zonation maps, developed using a probabilistic approach. Maps of statistical values (median, mean, 15th and 85th percentiles) were derived at return periods Tncr of 50, 225, 475 and 975 years and were finally used to propose a new seismic zonation supporting the regulation for the seismic of bridges (Fig. 1), these accelerations correspond to return periods Tnrc, for the design of the seismic action of bridges of medium importance. For bridges of Class III, PGAs are multiplied by the importance factor, recommended as 1.3, considered having major economic and social impact, and are crucial for communications and immediate post-earthquake period.

Probability of not being exceeded during a defined return period and present the different limit states summarized as follows (Table 1):

– The operational limit state advocating a frequent seismic action, with a return period of 50 years relative to a duration less than the service life of the structure.
– The immediate use limit state advocating occasional seismic action, with a return period corresponding to a duration equivalent to twice the service life of the structure, which is 225 years.

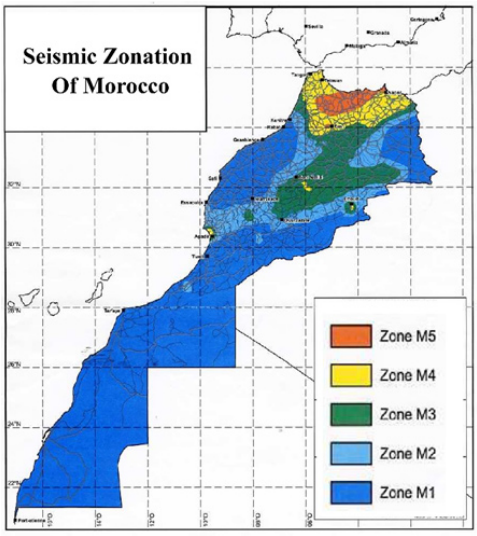

FIGURE 1. Seismic zonation map of Morocco

– The limit state of structural safety advocating a rare seismic action, with a probability of not being exceeded of 10% corresponding to a return period of 475 years.
– The near-collapse limit state advocating a very rare seismic action with a probability of not being exceeded of 2% with a return period of 975 years.

TABLE 1. PGAs adopted for the bridge study example

Parameter	Operational	Immediate use	Life safety	Near collapse
Tncr [year]	50	225	475	975
PGA [m·s^{-2}]	0.65	0.91	1.26	1.91

Two types of spectra shape for each ground type are adopted in accordance to Eurocode 8, type 1 for moderate to large magnitude earthquakes and type 2

for low-magnitude ones at close distance (Table 2; Kolias, Fardis, Pecker & Gulyanessian, 2012)

TABLE 2. Standard horizontal elastic response spectra recommended in the EC8

Ground type	Spectrum type 1				Spectrum type 2			
	S	Tb	Tc	Td	S	Tb	Tc	Td
A	1.00	0.15	0.40	2.00	1.00	0.05	0.25	1.20
B	1.20	0.15	0.50	2.00	1.35	0.05	0.25	1.20
C	1.15	0.20	0.60	2.00	1.50	0.10	0.25	1.20
D	1.35	0.20	0.80	2.00	1.80	0.10	0.30	1.20
E	1.40	0.15	0.50	2.00	1.60	0.05	0.25	1.20

Consequently, the elastic response spectrum adopted to conduct seismic analyses, for ground type B, are summarized in Figure 2.

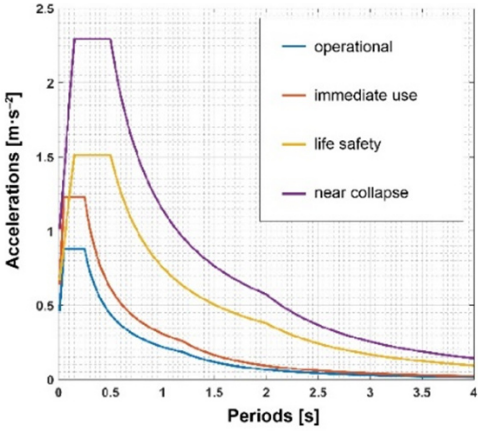

FIGURE 2. Elastic spectrum for different limit states

Low-damping elastomeric bearings

Elastomeric bearings (Fig. 3) are used as an effective and simple means of providing partial isolation of the structure. The vibration period of the structure is shifted to higher values due to the increased flexibility provided by the elastomers. And thus the seismic demand in terms of seismic forces is reduced. In practical, the reduction of the horizontal stiffness of the total system (K_{eff}) increases its fundamental period $T_{eff} = 2\pi\sqrt{\frac{M}{K_{eff}}}$ relative to that of the initial structure. The acceleration spectrum shows that this period shift brings about a substantial reduction in the spectral acceleration. However, the displacement spectrum clearly shows that the displacement is also increased substantially.

FIGURE 3. Laminated elastomeric bearings

The elastomers show an elliptical hysteretic behavior with an equivalent viscous damping of 6% and their shear behavior can be considered as linear. This behavior is defined by the stiffness modulus of the elastomers. The damping they offer is consistent with the default value of 5% used in linear analysis.

Such bearings are designed to resist all non-seismic horizontal and vertical actions. Consequently, different types of ultimate limit states verifications must be done for all types of elastomeric bearings, and are detailed thereafter. The main physical parameter of the elastomer used in the design of the bearing is its conventional shear modulus (G), with a nominal value G of the conventional shear modulus is 0.9 MPa.

The dimensions in plan, the thickness and the number of elastomer layers determines the population of standard sized bearings meeting previous non-seismic requirements. The incredible number of feasible solutions make the computational time cost unrealistic, guiding us to use a multi-objective optimization approach using genetic algorithm (Xie & Zhang, 2018).

Multi-objective optimization

The use of isolation and damping techniques is an effective means of achieving the desirable level of seismic performance and safety. However, it is difficult to achieve the desired design objectives at each of the seismic hazard levels while taking full advantage of the benefits offered by isolation and damping systems. In practice, the design is performed for a single-hazard performance level, typically corresponding to the highest seismic hazard, and the consequences of that design on performance for lower seismic hazard levels are accepted, without any optimization. Such a design approach generally results in seismic protection solutions that provide no or very limited improvement in the performance of the bridge structure for more frequent and smaller seismic events, because the isolation system is unlikely to be activated during such earthquakes. Damage prevention under frequent events will require that the bridge needs to be designed to respond elastically to this level of seismic hazard. If, instead, the protection system is designed to fully engage under the lower level event, the bridge is susceptible to excessive deformation through the isolation system and, therefore, significant damage or even the possibility of collapse under a stronger earthquake. Ideally, a bridge protection system based on isolation and damping should have a positive impact on the seismic performance at the different hazard levels (Rizzian, Léger & Marchi, 2017). In a context of structure design based on the performance approach, multi-objective optimization allows to take into consideration the achievement of several objectives simultaneously (Dezfuli & Alam, 2013). This capability is all the more useful when these objectives behave in a conflicting way, i.e. the improvement of one objective cannot be done without deteriorating the performance of the remaining objectives. The multi-criteria optimization problem is expressed by the following relation (Ohsaki, Yamakawa, Fan & Li, 2019):
Minimize

$$y(x) = \{f_1(x), f_2(x), ..., f_n(x)\}, x \in \theta \quad (1)$$

Subject to

$$h(x) \leq 0 \quad (2)$$

where:
x – input variables of the considered system,
f – function reflecting an objective,
n – number of objective functions,
h – constraint function.

The result of the multi-objective optimization is a set of solutions representing the best compromise of the different objective functions. The Pareto front is the graphical representation of these optimal solutions (Kwag & Ok, 2013). To deal with multi-objective optimization

problems, GA toolbox, a MATLAB optimization toolbox was used. It incorporates the NSGA-II (non-dominated sorting genetic algorithm II). This algorithm has shown good results in solving complex multi-objective optimization problems, being able to find diverse solutions of the Pareto front with little computational effort. The algorithm begins by generating a population of 50 individuals in the design space. The values of the objectives are calculated for the different individual solutions and the optimization criterion is chosen from the set of options such as the number of generations, the limit calculation time, and the tolerance function (Pourzeynali, Salimi & Kalesar, 2013). The individuals are then ranked according to the objective values. It creates an order among the individuals by mean of fitness assignment. A selection criterion filters out the candidate solutions with poor fitness and retains those with acceptable fitness to enter the reproduction process with a higher probability. A new generation in the genetic algorithm is created through reproduction from the previous generation. Three mechanisms (elitist, crossover, and mutation) are primarily used to create a new generation. The algorithm finished by obtaining best individuals that satisfies the termination criteria (Pourzeynali, Malekzadeh & Esmaeilian, 2012).

Description of the bridge

In order to investigate the effectiveness of the proposed optimization of the seismic performance of the structure, a reinforced concrete girder bridge (Fig. 4) located in the city of Casablanca, Morocco, is selected.

FIGURE 4. Reinforced concrete girder bridge

An investigation program is conducted in order to determine material characteristics of the supports, carrying out exhaustive surveys of damage, in-situ tests, and laboratory tests on concrete cores and finally inspecting the state of corrosion of the reinforcements (Table 3; Abbadi & Lamdouar, 2019). The distribution of the reinforcement inside piles (Fig. 5) is evaluated using magnetic auscultation with pachometer, the device also provides an estimate of the cover and the diameter of the detected reinforcement. For the characterization of the concrete properties, sclerometric auscultation is conducted confirmed with core tests (Table 4; Abbadi & Lamdouar, 2018).

TABLE 3. Main characteristics of the bridge study example

Property	Description
Year of construction	1978
End supports	abutment with front wall with integrated header and return walls for support on the landside
Intermediate supports	piers with multiple piles (05), tied by headbands
Superstructure	11 reinforced concrete beams
Support devices	laminated elastomer: 11 for each support
Number of spans	4
Bias	100 g
Total length	49.36 m
Overall width	10.25 m
Rolling width	7 m
Air draft	5.33 m

FIGURE 5. Visual examination of columns

TABLE 4. Mean values ($\bar{x}$) and standard deviations (*SD*) of material properties

Property	$\bar{x}$	*SD*
Longitudinal reinforcement spacing [cm]	17	3
Transverse reinforcement spacing [cm]	15	2
Longitudinal reinforcement diameter [cm]	25	0
Transverse reinforcement diameter [cm]	8	0
Concrete cover [cm]	3	0.5
Compressive concrete strength [MPa]	31.1	5.4

Verifications of elastomeric bearings

Four types of ultimate limit state verification must be made for elastomeric laminated bearings of any type:

- the maximum total distortion at any point in the bearing is limited;
- the thickness of the shrink discs must be sufficient to withstand the tension they are subjected to;
- the stability of the support device must be ensured against rotation, buckling and sliding;
- the actions applied by the bearing device on the rest of the structure must be checked (direct effect of the bearing device on the structure and indirect effect due to the deformations of the bearing device).

The verifications are carried out for several horizontal deformations of the elastomer, corresponding to the displacements that it undergoes during a seismic event (Fig. 6). A reduced area (A_r) (Fig. 7) is calculated as follow:

$$A_r = A' \cdot \left(1 - \frac{v_x}{a'}\right) \tag{3}$$

where:
A' – effective area of the elastomer,
v_x – lateral displacement,
a' – dimension in plane of the elastomer.

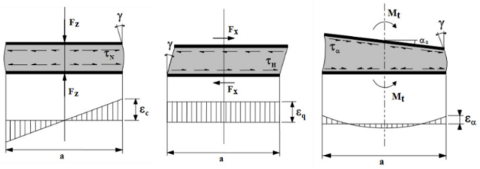

FIGURE 6. Illustrations of the verifications

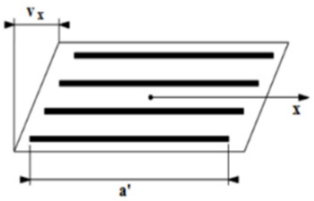

FIGURE 7. Reduced area due to horizontal strains

Numerical study

The deck is modeled by beam-column elements with linear behavior. The modulus of elasticity is determined for a concrete with a characteristic strength of 34 MPa. The supports are modeled for characteristic concrete strengths according to the state of confinement of each pier composing these supports (Table 5; Abbadi & Lamdouar, 2018). Each support is composed of five piles connected by a common beam. The Popovics

behavior law is used to model the concrete, referenced as "concrete04" in OpenSees. The bearings are modeled as "zero length" elements with a linear elastic behavior law. The modulus of elasticity in the lateral directions corresponds to that of elastomers, while that in the vertical direction is infinitely stiff.

TABLE 5. Material properties of concrete and reinforcement for different levels of corrosion

Parameter	Column				
	C0	P1	P2	P3	C4
Core concrete					
E [GPa]	13.21	7.94	10.16	13.21	10.16
f'_{cc} [MPa]	31.05	38.6	34.04	31.05	34.04
ε'_{cc} (10^{-3})	2.35	3.86	3.35	2.35	3.35
ε_{cu} (10^{-3})	3.55	5.60	4.56	3.55	4.56
Cover concrete					
E [GPa]	15.87	21.11	17.41	15.87	17.41
f'_{c0} [MPa]	22.23	29.56	24.38	22.23	24.38
ε'_{c0} (10^{-3})	1.4	1.4	1.4	1.4	1.4
ε_{cu} (10^{-3})	2.1	2.1	2.1	2.1	2.1
Reinforcement					
Yield stress [MPa]	235	235	235	235	235
ε_{cu} (10^{-3})	3.55	5.60	4.56	3.55	4.56

Multi-objective analysis using 3D OpenSees Model

A finite element analysis with a 3D model coupled with a multi-objective analysis is conducted to obtain periods and eigen modes. The algorithm generate a population of 50 individuals in the design place, issued from a custom function that respect calculated stiffness's (Fig. 8). Pushover analysis determines the performance points consisting on moment-displacement values for each limit states in the longitudinal (Fig. 9) and transverse directions (Fig. 10). Tournament option is chosen to execute the selection process, and a crossover fraction of 0.8 is taken to produce the next generation. Thereafter mutation process intervene where small random changes in the individuals in the population are created, which provide genetic diversity and enable the genetic algorithm to search a broader space, and arithmetic function crossover is used to create children's that are a random arithmetic mean of two parents.

The objectives to be optimized simultaneously are expressed as follows:

$$f_{d,i\in\{OP,IU,LS,NC\}} = Disp_{Acc\in\{OP,IU,LS,NC\}} \quad (4)$$

$$f_{f,i\in\{OP,IU,LS,NC\}} = Forces_{Acc\in\{OP,IU,LS,NC\}} \quad (5)$$

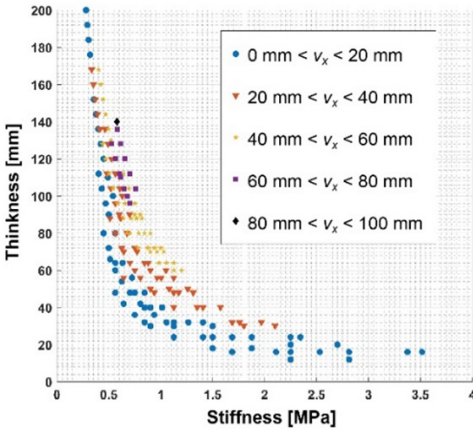

FIGURE 8. Flowchart of feasible elastomeric bearings characteristics and the corresponding allowable maximum displacements

The Pareto fronts of optimal solutions are presented as a set of points that represented the best compromising responses in terms of displacements and moments for the four limit states considered in the transverse (Fig. 11a) and longitudinal directions (Fig. 11b).

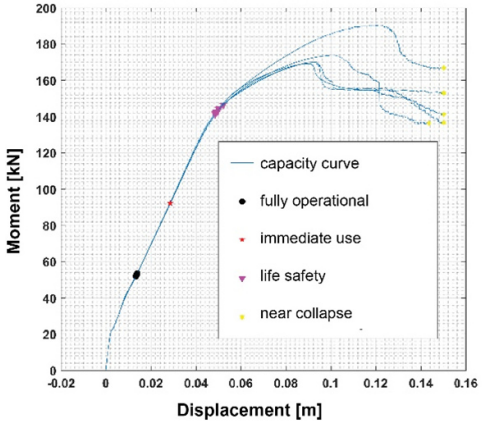

FIGURE 9. Limit states at longitudinal direction

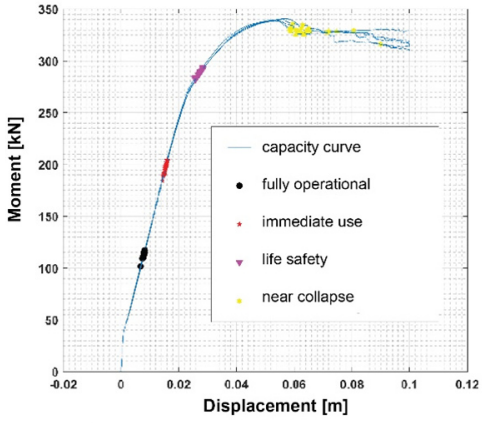

FIGURE 10. Limit states at transverse direction

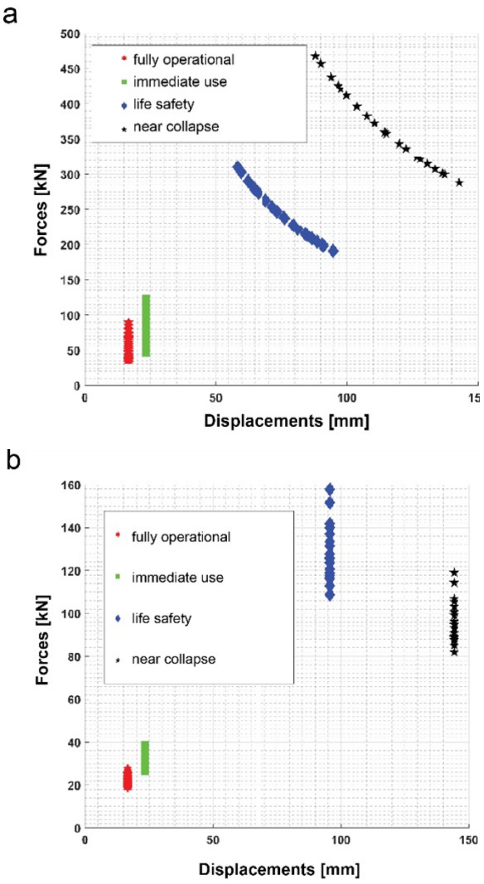

FIGURE 11. Optimal values of accelerations and displacements for various bearing stiffness's in the transverse (a) and longitudinal (b) direction

Multi-objective analysis using two degree of freedom model

The seismically isolated bridge is assumed to be fixed at the base of the columns and the bridge superstructure is assumed to be relatively rigid with respect to the bridge bearings and columns. Therefore, the isolated regular bridge is modeled as a system with two degrees of freedom in the lateral and transverse direction (Jara & Casas, 2006).

The multi-objective optimization is conducted according to the same procedure of the analysis using 3D OpenSees model and the results are summarized in Figure 12a for the transverse and Figure 12b for the longitudinal direction.

The results of the optimization show that the objectives in terms of ductility and forces are considerably improved. In the transverse direction, the demand for forces is reduced by more than 100%, while the ductility

demand is reduced by 50% for large seismic actions. In the longitudinal direction, the improvement is less important, about 50% for forces and almost stable for ductility. It should be noted that the results of the optimization based on the simplified model in two degrees of freedom are in agreement with the results of the optimization based on numerical modelling.

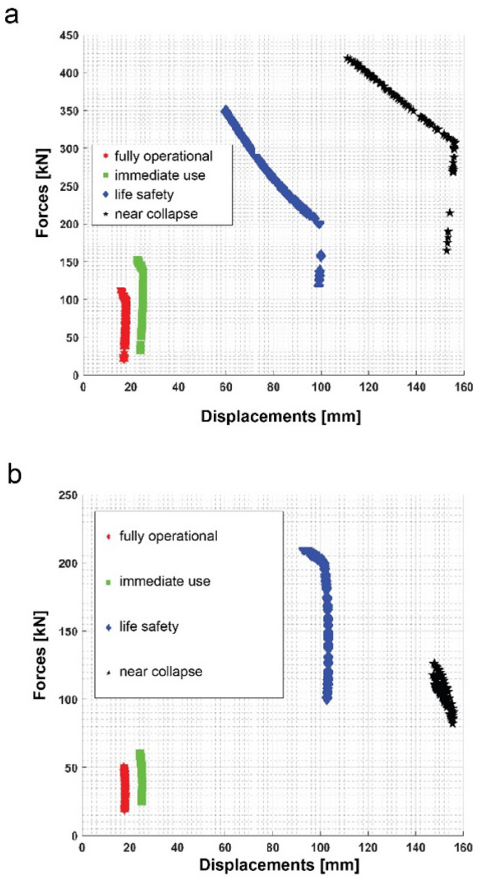

FIGURE 12. Optimal values of accelerations and displacements for various bearing stiffness's in the transverse (a) and longitudinal (b) direction

Multi-objective analysis using equivalent single degree of freedom analysis

The use of simple equivalent single degree of freedom systems (Fig. 13) has been recognized for many decades as the simplest way to obtain information on the dynamic response of isolated structures subjected to seismic excitations. For the analysis of bridge structures in the longitudinal and transverse directions, it is common to divide the structure into two model elements: the substructure and the superstructure. Most of the mass of the bridge is located at the deck (superstructure), and the effect of the substructure mass is neglected when Conversely, the stiffness of the substructure has a significant effect on the behavior of the structure and must be considered accurately. The superstructure is modelled as a rigid body with infinite axial stiffness. For straight bridges, the motion of the superstructure in the longitudinal and transverse directions can be considered decoupled. Using these simplifying assumptions, SDOF analyses can be used for the seismic analysis of most isolated ordinary bridges, and consequently in order to check eigenvalue analysis in OpenSees. Thus, the entire bridge is represented as a simple oscillator that consists of the total mass concentrated at the upper end of a single pole with the same stiffness and damping properties as the bridge substructure. k1 and c1 are the lateral stiffness and viscous damping coefficients. Both coefficients represent the contribution of substructure elements, including intermediate supports, abutments, and isolation and damping devices.

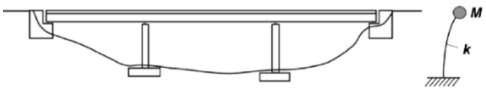

FIGURE 13. SDOF modeling of bridges

For a bridge design with isolation at the top of the piers and abutments, the equivalent stiffness is determined according to Equation (6). The two terms in this expression represent two springs placed in series. The first term is the stiffness contribution of the piers and their bearings, while the second term represents the two abutments and their bearings.

$$k_{eq} = \sum_{j=1}^{n} \frac{k_{pier,j} \cdot k_{isol,j}}{k_{pier,j} + k_{isol,j}} + \sum_{j=1}^{2} \frac{k_{abut,j} \cdot k_{isol,j}}{k_{abut,j} + k_{isol,j}} \quad (6)$$

Assuming that the abutments are infinitely rigid with respect to the piers, the equation becomes:

$$k_{eq} = \sum_{j=1}^{n} \frac{k_{pier,j} \cdot k_{isol,j}}{k_{pier,j} + k_{isol,j}} + \sum_{j=1}^{2} k_{isol,j} \quad (7)$$

Consequently, the Pareto fronts are plotted as presented in the transverse (Fig. 14) and longitudinal (Fig. 15) directions.

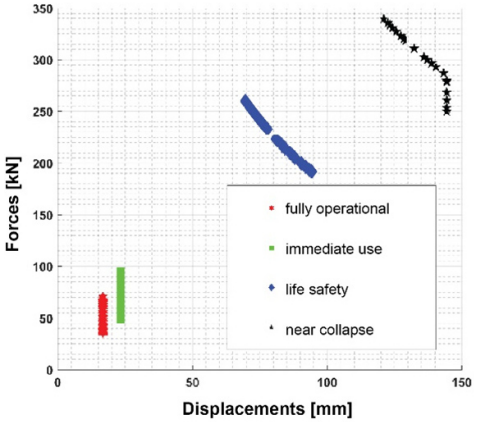

FIGURE 14. Optimal values of accelerations and displacements for various bearing stiffness's in the transverse direction

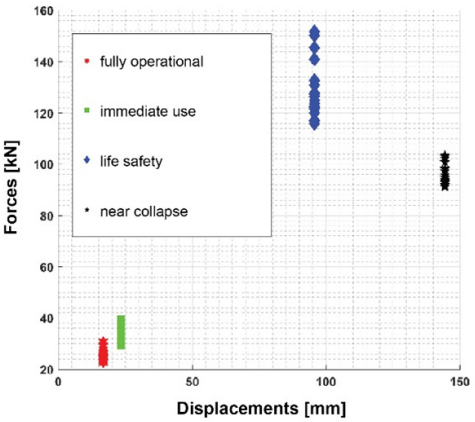

FIGURE 15. Optimal values of accelerations and displacements for various bearing stiffness's in the longitudinal direction

The results of the optimization based on the equivalent single degree of freedom model are in agreement with the two degree of freedom model and also with the results of the optimization based on numerical modelling, which allows to validate the adapted methods.

Results and discussion

This study proposes an optimal design method of the seismic isolation system for existing bridges. The method combine finite element methods with multi-objective optimization approach, enabling two major advantages. First, the multi-objective optimization using genetic algorithms can handle mutually multiple conflicting objectives with affordable computational cost, producing a set of optimal solutions helping the designer to choose between multiple alternatives. Second, the use of linear analysis allow the assessment of the structure in the elastic range using

elastomeric bearings, in such a way that displacements, representing service conditions of the bridge, remains acceptable. Third, the actual behavior of the columns materials properties is taken into account, picturing the real response of the structure, verified and validated by analytical simplified SDOF model. The case study demonstrates that the proposed approach might constitute an efficient tool to optimize seismic performance in terms of forces applied to columns and deck displacements, in accordance with the limit state requirements described in the Eurocode 8, under various earthquake loads. The capacity curves of the columns gives the forces and displacements corresponding to each of the limit states reflecting the damage occurred. However, this method focuses on the elastic behavior of the structure and the period shift created by the bearings without taking into account the energy dissipation and the increase of damping in the structure. Also all the solutions proposed for limit states LS and NC do not allow to reach the seismic performance objectives expected for the structure. It is then necessary to solicit the bearings in the post-elastic domain, integrating equivalent damping and rigidity. The confrontation of the results of the three methods shows a good agreement for different values of elastomer stiffness's, which allows us to validate the numerical model built with OpenSees. Thereafter, Pareto fronts are generated in the longitudinal and transverse directions, and for different limit states. The first objective function is the acceleration where the second objective function is the displacement.

Conclusions

In this study, we provide a multi-objective optimization method for specifying the isolation elastomer bearings characteristics such that an optimal performance of existing bridges, in terms of both accelerations and displacements, achieved under the elastic spectra specified in the Eurocode 8 for multiple limit states. The linear response of the structure is estimated from the eigenvalue analysis conducted on a 3D OpenSees numerical model. Periods are obtained for the transverse and longitudinal directions. Displacements and accelerations are directly calculated by mean of limit states elastic spectra. The results are compared and validated with the idealization of the structure as an SDOF and 2DOF systems The optimal stiffness of bearings are evaluated by selecting the displacement and accelerations as the objective functions which to be minimized. The goal is finding so called Pareto-optimal solutions by using a fast and elitist non-dominated sorting genetic algorithm (NSGA-II) in MATLAB. From the trends of the results of the present study, following conclusions are drawn:

- Isolation bearings with different stiffness values gives a range number of seismic behaviors to the structures, and optimal solutions tend to decrease displacement and acceleration limits fixed by the seismic demands.
- All the solutions afforded by the NSGA-II optimization algorithm constitutes the best stiffness bearings values to minimize the displacements and accelerations for all the limit states considered.

- A substantial decrease of the forces in the columns is achieved while keeping displacements of the superstructure within acceptable limits.
- It has been observed for non-collapse and life safety limit states that the requirements do not meet for any of the isolation bearings susceptible to be used to the structures. In such a case, a non-linear analysis is needed in order to take into account the post-elastic behavior of the bearings and the columns. An additional damping and dissipation energy must be taken into account consequently.
- This study focuses on the global linear behavior of partially isolated exiting bridges, and constitute a prelude to a more advanced analysis, such as pushover and non-linear time history.

It's of great importance to investigate the robustness of the solutions proposed regarding system uncertainties such as traffic load, stiffness variations, constitutive materials behavior.

References

Abbadi, M.S. & Lamdouar, N. (2018). Structural evaluation updating based on quality control and proof loads. *MATEC Web of Conferences*, *149*, 02014. https://doi.org/10.1051/matecconf/201814902014

Abbadi, M.S. & Lamdouar, N. (2019). Pushover analysis of RC columns subjected to multiple degrees of transverse reinforcement corrosion. *International Journal of Civil Engineering and Technology*, *10*(11), 313-322.

Alhan, C. & Gavin, H.P. (2005). Reliability of base isolation for the protection of critical equipment from earthquake hazards. *Engineering Structures*, *27*(9), 1435-1449.

Alkhamis, M., Ghasemi, M.R., Gholinezhad, A., Shabakhty, N. & Abdullah, W. (2018). Performance-based Optimum Retrofitting Design of Concrete Bridge Piers. *Jordan Journal of Civil Engineering*, *12*(4), 637-653.

Dezfuli, F.H. & Alam, M.S. (2013). Multi-criteria optimization and seismic performance assessment of carbon FRP-based elastomeric isolator. *Engineering Structures*, *49*, 525--540.

Jara, M. & Casas, J.R. (2006). A direct displacement-based method for the seismic design of bridges on bi-linear isolation devices. *Engineering structures*, *28*(6), 869-879.

Kolias, B., Fardis, M.N., Pecker, A. & Gulvanessian, H. (2012). *Designers' guide to Eurocode 8: design of bridges for earthquake resistance.* London: ICE Publishing.

Kwag, S. & Ok, S.Y. (2013). Robust design of seismic isolation system using constrained multi-objective optimization technique. *KSCE Journal of Civil Engineering*, *17*(5), 1051-1063.

Léger, N., Rizzian, L. & Marchi, M. (2017). Reliability-based design optimization of reinforced concrete structures with elastomeric isolators. *Procedia Engineering*, *199*, 1193--1198.

Matsagar, V.A. & Jangid, R.S. (2004). Influence of isolator characteristics on the response of base-isolated structures. *Engineering Structures*, *26*(12), 1735-1749.

Mishra, S.K., Roy, B.K. & Chakraborty, S. (2013). Reliability-based-design-optimization of base isolated buildings considering stochastic system parameters subjected to random earthquakes. *International Journal of Mechanical Sciences*, *75*, 123-133.

Ohsaki, M., Yamakawa, M., Fan, W. & Li, Z. (2019). An order statistics approach to multiobjective structural optimization considering robustness and confidence of responses. Mechanics *Research Communications*, *97*, 33-38.

Pourzeynali, S., Malekzadeh, M. & Esmaeilian, F. (2012). Multi-objective optimization of semi-active control of seismically exited buildings using variable damper and genetic algorithms. *International Journal of Engineering*, *25*(3), 265-276.

Pourzeynali, S., Salimi, S. & Kalesar, H.E. (2013). Robust multi-objective optimization design of TMD control device to reduce tall building responses against earthquake excitations using genetic algorithms. *Scientia Iranica*, *20*(2), 207-221.

Rizzian, L., Léger, N. & Marchi, M. (2017). Multiobjective sizing optimization of seismic-isolated reinforced concrete structures. *Procedia Engineering*, *199*, 372-377.

Roy, B.K. & Chakraborty, S. (2015). Robust optimum design of base isolation system in seismic vibration control of structures under random system parameters. *Structural Safety*, *55*, 49-59.

Scozzese, F., Dall'Asta, A. & Tubaldi, E. (2019). Seismic risk sensitivity of structures equipped with anti-seismic devices with uncertain properties. *Structural Safety*, *77*, 30-47.

Scruggs, J.T., Taflanidis, A.A. & Beck, J.L. (2006). Reliability-based control optimization for active base isolation systems. *Structural Control and Health Monitoring: The Official Journal of the International Association for Structural Control and Monitoring and of the European Association for the Control of Structures*, *13*(2-3), 705-723.

Xie, Y. & Zhang, J. (2018). Design and optimization of seismic isolation and damping devices for highway bridges based on probabilistic repair cost ratio. *Journal of Structural Engineering*, *144*(8), 04018125. https://doi.org/10.1061/(ASCE)ST.1943-541X.0002139

Summary

Multi-objective optimization of elastomeric bearings to improve seismic performance of old bridges using eigen analysis and genetic algorithms. Old bridges present several seismic vulnerabilities and were designed before the emergence of seismic codes. In this context, partial seismic isolation has given a special attention to improve their seismic performance. In particular, elastomeric bearings are the simplest and least expensive mean for this, enabling to resist both non-seismic actions and earthquake loads. In order to assess the initial structural performance and the improvement done by the isolation, this paper attempts to combine multi objective optimization using genetic algorithms with linear and non-linear analysis using FE program OpenSees. A prior screening of the columns states is settled and then a multi objective optimization of a population of standard sized bearings meeting non-seismic and stability requirements is established to optimize the linear and non-linear behavior of the structure, finding the best compromise between displacements and forces at the columns.

Authors' address:
Mohamed Saad Abbadi – corresponding author
(https://orcid.org/0000-0002-9831-9487)
Mohammed V University in Rabat
Mohammadia School of Engineers
Civil Engineering Laboratory
Morocco
e-mail: saadabbadi@research.emi.ac.ma

Nouzha Lamdouar
University in Rabat
Mohammadia School of Engineers Mohammed V Civil Engineering Laboratory
Morocco

Scientific Review – Engineering and Environmental Sciences (2021), 30 (4), 525–536
Sci. Rev. Eng. Env. Sci. (2021), 30 (4)
Przegląd Naukowy – Inżynieria i Kształtowanie Środowiska (2021), 30 (4), 525–536
Prz. Nauk. Inż. Kszt. Środ. (2021), 30 (4)
https://srees.sggw.edu.pl
DOI 10.22630/PNIKS.2021.30.4.44

Erwindy JOSSI, Asdak CHAY, Rahmat BOMBOM, Sapari MOHAMAD

University of Padjadjaran, Graduate School

Integrated assessment of urban land carrying capacity (ULCC) for reducing earthquake risk disaster in Palu City

Key words: land carrying capacity, urban area, earthquake disaster, Palu City

Introduction

The land is one of the main components of the environment, the fundamental matrix of life (Onishi, 1994; Singer, 2014; Xiao et al., 2021). However, land has a limited carrying capacity, therefore must be well maintained to avoid damage or degradation (Stocking & Murnaghan, 2002). The pressure of high population growth in various places has resulted in pressure on land as well beyond its natural carrying capacity (Goldshleger, Ben-Dor, Lugassi & Eshel, 2010). Several studies have shown that land quality is deteriorated due to misuse, one of which includes overuse or over-capacity (Dougill, Twyman, Thomas & Sporton, 2002; Boix & Zinck, 2008). Improper land use requires high costs for repairs; especially when the degradation reaches an irreversible stage (Sudershan, 2003; Gupta & Sharma, 2010). Similar to non-renewable natural resources, rational land use is also an influential indicator of development (Chang & Wu, 2011) and economic growth (Pilvere, Nipers & Upite, 2014). The aforementioned is even related to the concept of sustainable development (Akıncı, Özalp & Turgut, 2013). Sustainable development can be defined as development that meets the needs of the present generation without compromising the ability of future generations to meet their own needs (Atlas Powder Company, 1987; Munasinghe, 1993; Feizizadeh & Blaschke, 2012).

Rapid population growth requires new areas to meet primary needs, especially in urban areas. In turn, this need causes natural resources such as forests, grasslands, wetlands, and agricultural land to be converted into settlements or

industrial estates (Tian & Sun, 2018). This will ultimately lead to land use that is not following its potential and exceeds its carrying capacity (Symeonakis, Calvo-Cases & Arnau-Rosalen, 2007). Land-use planning that allows good inheritance of land resources for future generations is very important to be considered. Thus, an integrated approach is needed for land use planning that takes into account long--term sustainability (Smardon, 2008). Efforts that can be taken for this planning are applying a planned and sustainable land use which is following their capabilities and potential based on urban land carrying capacity (ULCC).

Urban land carrying capacity is part of the evaluation of the environmental carrying capacity which refers to its maximum carrying capacity. Although the carrying capacity of an area is not constant, this suggests a kind of human--environmental lead-lag relationship. Carrying capacity is conceptualized as a load or even full load, an important dimension of it. Projected economic, technological, and social growth rates and the material requirements needed decide the number of people a region can support with its land resources. To live on various time scales (Shi & Chen, 1991; Feng, 1994). Consequently, the carrying capacity of urban land can be defined as the level of human activity, population growth, land use patterns and extent, and physical development that the urban environment can support without significant and irreversible damage (Sarma et al., 2012).

The impact of earthquakes in urban areas is a complete problem that is exacerbated by multi-hazard and significant risk issues, a large inventory of vulnerable physical components, and socioeconomic issues. Given the impact caused by an earthquake is a complex issue, efforts to manage and minimize the effects of this disaster must be considered carefully. In this case, it is very important to predict when and where an earthquake may occur. The foundation and vital rationale for practical risk reduction activities are rational urban risk predictions and projected losses from future significant earthquakes.

Therefore, specific emergency preparedness and procedures should be established, especially in urban centers that were most strongly affected by the earthquakes, i.e. during and before the earthquake where this requires calculating the impact of the earthquake on the physical and social environment. Population, buildings, infrastructure, systems, and socio-economic activities are all "elements at risk" in urban areas (Erdik, Durukal, Aydinoglu, Fahjan & Siyahi, 2006) so that the potential for earthquake hazards must be factored into the measurement of the land's carrying capacity for urban planning.

This research took place in Palu City, a national urban area in Indonesia with limited urban development due to the threat of an earthquake. In the need for sustainable urban development, it is necessary to study the land carrying capacity to reduce the risk of earthquake disasters. This can be done through three stages of analysis, including mapping of earthquake-prone areas through micro-zoning of earthquake vulnerability, assessing the land capability, and conducting a comparative analysis regarding the land capability and spatial planning.

Material and methods

The study area and data source

Palu City is located in Central Sulawesi Province with an area of 395.06 km^2. This city consists of eight districts, namely West Palu District, Tatanga District, Ulujadi District, South Palu District, East Palu District, Mantikulore District, North Palu District, and Tawaeli District. Palu City is one of the national urban areas designed by the national spatial plan (Government Regulation No 26 of 2008 regarding National Territorial Layout Plan) as a center for import-export activities or a gateway to the international area and a center for industrial activities. On the other hand, Palu City is on the Palu-Koro fault line, an active fault that stretches 170 km along the mainland of island of Sulawesi, moving at a speed of 35 ±8 mm per year. Since the 19^{th} century, earthquakes have frequently occurred in Central Sulawesi, some of which were of high magnitude, including in 1968 (6.7 SR), 1993 (5.8 SR), 2005 (6.2 SR), and 2008 (6.7 SR) (7.4 SR) (Bellier et al., 2001).

This research uses applied methods with quantitative and superimpose approaches. The research data was processed using the geographical information systems (GIS) as a tool; field observations support primary and secondary data. To achieve the main purposes of this research, the following stages are taken: (1) mapping of earthquake prone areas with seismic micro-zonation; (2) land capability assessment; and (3) comparative analysis of land capability and spatial planning in Palu up to 2030.

Mapping of earthquake prone areas with seismic micro-zonation

Mapping of earthquake-prone areas of seismic micro-zonation was carried out through microtremor analysis. The aim is to determine the characteristics of the soil layer based on the dominant period parameters and amplification factors. Micro-zonation of microtremor divides an area based on certain parameters by considering characteristics, including ground vibration, amplification factor, and dominant period.

The analysis carried out in this study consisted of (1) analysis of horizontal--vertical spectral ratio (HVSR), namely comparing the spectrum of the horizontal component with the vertical component of the microwave; and (2) analysis of dominant frequency and dominant period, namely determining the frequency value of rock layers in the area so that the type and characteristics of the rock. The microtremor data used in this study were 36 data collection points in Palu City. The data is then processed using the HVSR method to obtain the dominant frequency value. The result will determine the level of earthquake vulnerability. The dominant frequency value will calculate the wave speed value (amplification) to a depth of 30 m (Vs30) which is used to determine the level of disaster risk that occurs through the peak ground acceleration (PGA) value. Furthermore, to obtain a micro-zoning map, data processing uses the overlay technique and GIS weighting by providing the highest earthquake vulnerability value for each PGA parameter, amplification (Vs30), while the maximum period was obtained using the analytical hierarchy process (AHP) method. This earthquake micro-zonation map was then

verified using field survey data showing the location of the destroyed buildings and classified according to the modified Mercalli intensity (MMI) class.

Land capability assessment

To determine the carrying capacity of land in Palu City, a land capability analysis was carried out. This analysis aims to obtain an overview of the level of land capability to be developed as an urban area through the determination of the land capability unit (LCU), which consists of LCU morphology, slope stability LCU, foundation stability LCU, and water availability LCU. The method used in this analysis is a map overlay and input data to each LCU using a thematic map with a scale of 1:25,000, as shown in Table 1.

The total land capability is classification is measured by the overlay of each LCU. It multiplies the final value weight to get the resulting map using the AHP principle (Sharififar, Ghorbani & Karimi, 2013). Digital spatial analysis method using GIS produces a land capability classification map as output.

Comparative analysis of land capability and spatial planning in Palu 2030

The comparative analysis aims to determine land use capability combining land capability analysis, hazard

TABLE 1. Evaluation of land capability unit (LCU)

LCU	Data	Classification of LCU	Score
1. Morphology	a) topography b) morphology	a) very high morphology b) high morphology c) moderate morphology d) low morphology e) very low morphology	1 2 3 4 5
2. Slope stability	a) topography b) morphology c) slope d) geology e) hydrogeology f) rainfall g) land use h) geological hazard	a) high slope stability b) moderate slope stability c) low slope stability d) very low slope stability	1 2 3 4
3. Foundation stability	a) geology b) hydrology c) land use d) geological hazard e) land use	a) low foundation stability b) moderate foundation stability c) high foundation stability	1 2 3
4. Water availability	a) hydrology b) climatology c) morphology d) topography e) geology f) land use existing	a) very low water availability b) low water availability c) medium water availability d) high water availability e) very high water availability	1 2 3 4 5

mapping, and spatial planning 2030. Its result estimates the range of integrated area development. Furthermore, the area estimation leads the strategy to improve spatial planning in Palu based on the carrying capacity of the land. The method was carried out to determine land capability mapping overlay, hazard maps, and spatial planning up to 2030, as stated in the results of land capability analysis of Palu's spatial planning in 2010–2030. In addition, one of the considerations to preparing the spatial planning is the threat of an earthquake in Palu.

Results and discussion

Earthquake hazard mapping with seismic micro-zonation

A micro-zonation process is initiated in the area which is prone to earthquakes. In this study, seismic micro-zonation was used on a 1:25,000 scale detail map. According to microtremor measurements, it leads to the vibration properties in the subsoil layer (Nakamura, 2000). The results of seismic micro-zonation analysis measured three parameters for further calculations by giving the highest class in earthquake-prone areas, with parameters and classification as shown in Table 2.

Based on National Earthquake Hazard Reduction Program (BSSC, 2001), the dominant period values there are in the range of 0.4–0.6 s. This means the entire study area is prone to earthquakes with a very high risk of damage (> 0.6 s), especially in most of Mantikulore District and Tawaeli District. These areas include Ulujadi District, Mantikulore District, and Tawaeli District with a dominant period ranging from 0.4 to 0.6 s. Areas with a dominant period of fewer than 0.4 s indicate a layer of hard soil with a fairly low risk of damage, especially in parts of South Palu District, West Palu District, North Palu District, and Ulujadi District.

The amplification value of Palu ranges from 1.01 to 7.56 $m \cdot s^{-1}$. The harder the soil, the greater the shear wave velocity and the smaller the shock amplification factor will be. Most of the amplification values were 3.18 (alluvial/sediment), especially in Ulujadi

TABLE 2. Parameters for the preparation of the Palu City earthquake micro-zonation map

Parameter	Class division	Score
Dominant period	< 0.4 (alluvial/sediment)	1
	0.4–0.6 (alluvial/sediment)	2
	> 0.6 (granit/metamorf)	3
Amplification	1.01–3.18 (alluvial/sediment)	1
	3.19–5.37 (alluvial/sediment)	2
	5.38–7.56 (granit/metamorf)	3
Peak ground acceleration (PGA)	0.59–0.68 (medium-high)	1
	0.69–0.78 (high)	2
	0.79-0.88 (very high)	3

District, Tatanga District, South Palu District, North Palu District, and Tawaeli District.

The PGA value obtained is the value of the wave acceleration in the bedrock report that occurred due to the earthquake. The value will be smaller since the epicenter distance is caused by the absorption of earthquake energy in the soil medium. The distribution of the PGA values in Palu City consists of: (1) 0.59–0.68 equivalent to the MMI X-scale which causes damage to strong wooden buildings and foundations, most of which are located in the eastern of Mantikulore District and Ulujadi District; (2) 0.69–0.78 is equivalent to MMI XI-scale which causes large soil cracks, landslides, broken bridges, yet wooden buildings standstill, most of which are in the center of Palu City; (3) 0.79–0.88 equivalent to MMI XII-scale which causes damage on a massive scale, blurred vision and discarded objects, most of which are in the center as well as eastern parts of Palu. Figure 1 shows a map of earthquake-prone areas according to both seismic micro-zonation and the damage scale.

Based on the map, 52.09% or 205.81 km^2 of Palu City is dominated by areas with a moderate level of danger located in Tawaeli District, West Palu District, Ulujadi District, North Palu District, Mantikulore District, and Tatanga District; high earthquake hazards were in Tawaeli District, East Palu District, South Palu, West Palu and Ulujadi District with the scale number of 22.47% or 88.76 km^2; while the low earthquake hazard with the scale number of 25.43% or 100.49 km^2 included Mantikulore District, Tawaeli District and Ulujadi District.

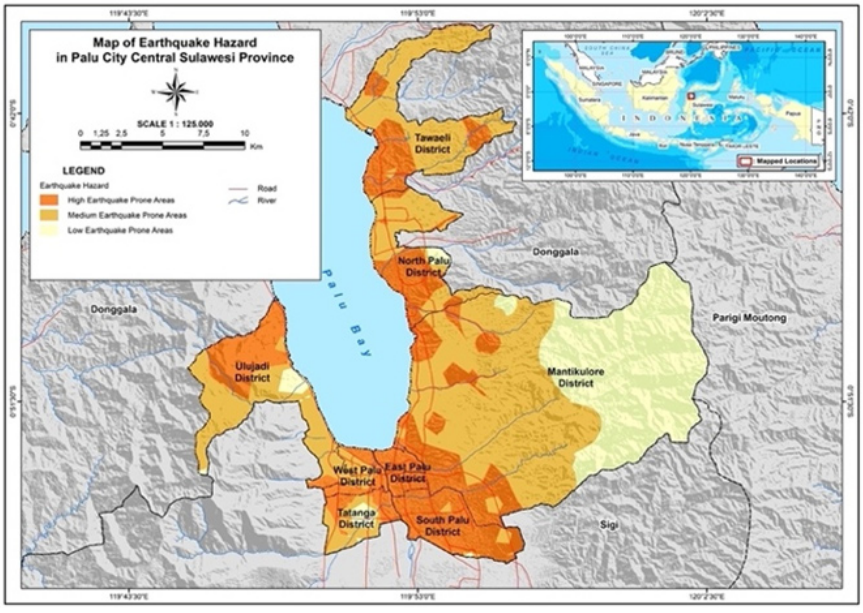

FIGURE 1. The map of earthquake-prone areas in Palu City

Land capability assessment

Land capability assessment proceeds the physical aspects measured by overlaying maps, assigning values, as well as weighting to each parameter. The results stated land capability of Palu grouped into five classes, namely Class A to Class E with proper management with very low to very high-level capability. Class A means to be very low, Class B is the land capability of low, Class C refers to be medium-level capability Class D is high high-level, and Class E means to be very high. This classification is shown in Figure 2.

From the land capability map shown in Figure 3, most of Palu City is dominated by low-level land capability (with the number of 23.92%) to very low (with the number of 31.51%). It indicates Palu has physical limitation in city development.

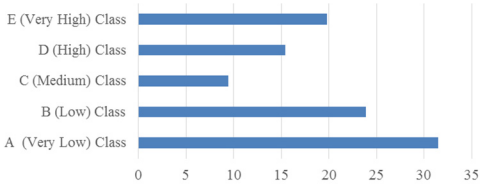

FIGURE 2. Value and class of land capability in Palu City

Integration of land suitability and spatial planning of Palu City 2030

The environment leads the action to evaluate land suitability for spatial planning in Palu. It was done by comparing an area's spatial plan with the land's capability to determine the suitability of the two. The results will show that the area currently under development can be classified as suitable, conditional, and unsuitable land, as shown in Table 3.

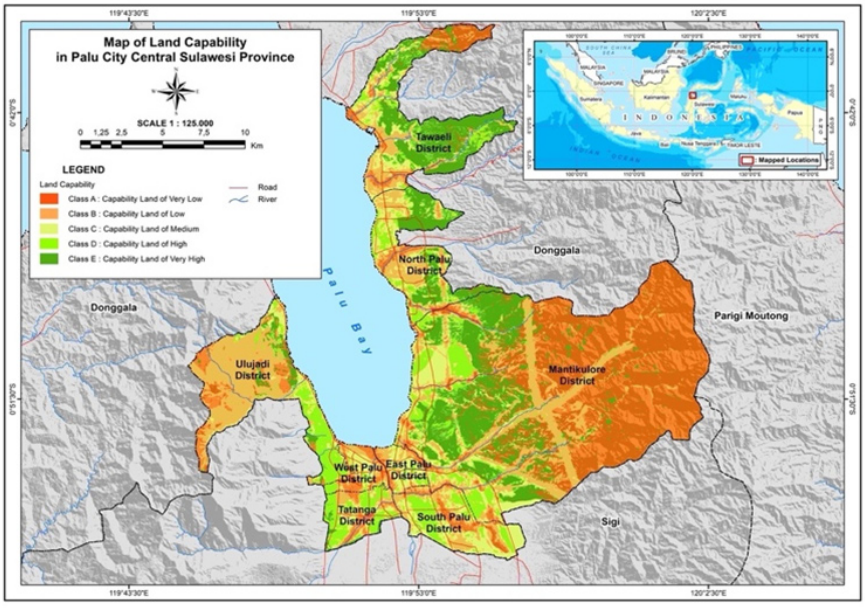

FIGURE 3. Land capability in Palu City

TABLE 3. Compatibility of the Palu spatial plan and ULCC in Palu City

Parameter	Area [%]	Classification
Class A with high earthquake prones with protected areas	9.12	suitable
Class B with medium earthquake prones with protected areas	26.52	suitable
Class C with low earthquake prones with protected areas	20.43	suitable
Class D with high earthquake prones with built-up areas	21.21	unsuitable
Class E with medium earthquake prones with built-up areas	21.57	conditional
Class F with low earthquake prones with built-up areas	1.15	suitable

Palu spatial planning in 2030 is dominated by the land's carrying capacity with proper management for protected areas (with the number of 56.07%). The land carrying capacity was grouped into six classes, namely Class A to Class F with the earthquake-prone area. The classification leads to a high to medium level of earthquake threat, and thus, the 1.15% of the built-up area is acceptable, notably, those in Class F. Conditional land suitability is given to the spatial use plan in built-up areas with the threat of an earthquake but is in Class C land capability class covering 20.43% of the total area of Palu City. The number indicates land development is not suitable for the urban area since it is in the high level of earthquake-prone areas as in Class D (with the number of 21.21%) of the total area of Palu City. A good evaluation of land capability measures the good qual-

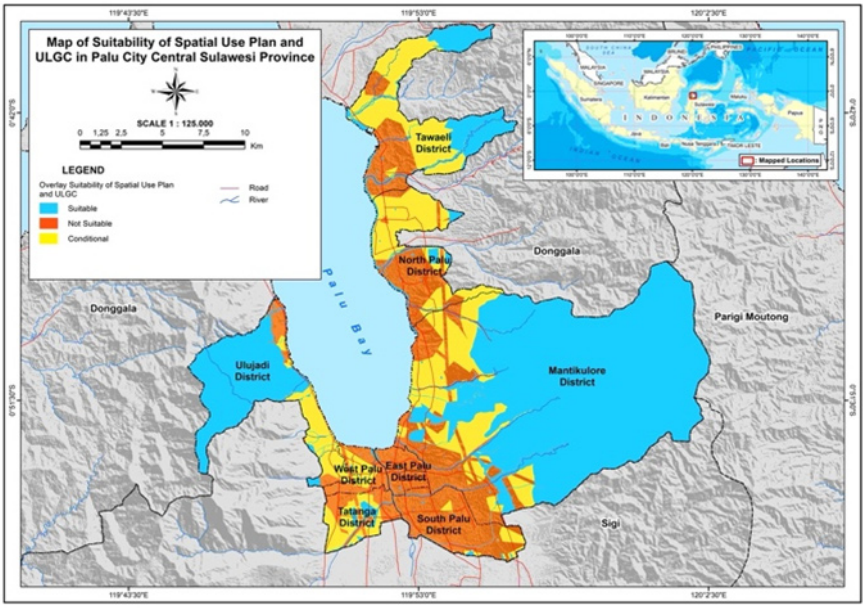

FIGURE 4. Map of suitability of spatial use plan and ULCC in Palu City

ity of spatial planning. This avoids the allocation of spatial use that is inconsistent with the capacity of the land. Thus, it requires special attention for the future development plan of Palu City. Figure 4 shows the land suitability distribution in Palu City.

The type of land use that is unsuitable for urban development, in general, is dominated by residential area land use (with the number of 66.42%), as shown in Figure 5. Good urban spatial planning avoids the allocation of space use that is not under the capacity of the land, hence, this requires a good plan development for the future.

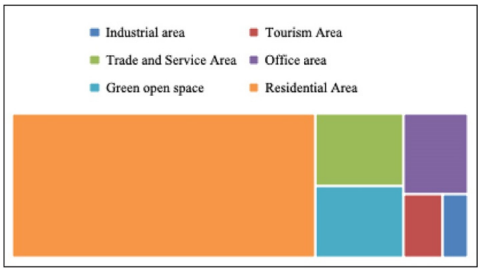

FIGURE 5. Type of land use that is not suitable for urban development in Palu City (Class D)

Conclusions

Improvement and long-term sustainability of the quality of life in human settlements today is the main problem facing urban planners, hence, given the scarcity of natural resources and inadequate infrastructure, one of the strategies is using ULCC. Besides a dynamic city policy to reorganize land carrying capacity is important to improve the state of urban development and the quality of life of human settlements. This study found some "weaknesses" in the spatial planning of Palu to be corrected so that the potential for developing the area is increasingly limited.

The spatial planning Palu City tends to limit regional development by regulating land use and expanding protected areas. There is, however, high demand for both urbanization land and urban development to use land with carrying capacity. Unsuitable land, as a result, the use of land that does not meet the carrying capacity requirements must be regulated and controlled. The limitation of this study devised the carrying capacity of earthquake hazards (excluding other natural disasters) analysis and land capability analysis. Urban land carrying capacity as previous studies has used seismic micro-zonation analysis as a basis for evaluating earthquake-prone areas on a very comprehensive scale.

The application of seismic micro-zonation analysis has been carried out for urban planners in several cities in the world (Chávez-Garcia & Cuenca, 1998; Marcelloni et al., 1998; Lungu, Aldea, Cornea & Arion, 2000; Faccioli & Pessina, 2001; Fäh, Kind, Lang & Giardini, 2001; Ansal et al., 2004). Yokohama City in Japan uses seismic micro-zonation to measure and evaluate industrial as well as population centers by considering various zones, suitable soil conditions, and seismic design coefficients for various types of structures located in different zones; Armenian cities in Colombia using a three-dimensional layers model and combined them with seismic responses to obtain spatial variations in seismic responses were examined by damage assessments of Armenia (Slob, Hack, Scarpas, van Bemmelen & Duque, 2002). Besides, Siliviri City and Istanbul

City in Turkey (Ansal et al., 2004; Gupta & Nair, 2010) have developed seismic micro-zonation maps and assessed damage scenarios.

Furthermore, a land-use development intensity assessment to address the need for optimizing land and utilization is required. The need for comprehensive assessment tends to focus on the current development scale, the identification of factors driving development, temporal-spatial differentiation and patterns of urban land expansion, the productivity and efficiency of construction land use, and the assessment of development potential. To achieve the goal of sustainable development, three indicators (size, efficiency, and potential) need to be considered at the same time.

References

Akıncı, H., Özalp, A.Y. & Turgut, B. (2013). Agricultural land use suitability analysis using GIS and AHP technique. *Computers and Electronics in Agriculture*, *97*, 71-82.

Ansal, A., Erdik, M., Studer, J., Springman, S., Laue, J., Buchheister, J., Giardini, D., Faeh, D. & Koksal, D. (2004). Seismic microzonation for earthquake risk mitigation in Turkey. In *13th World Conference on Earthquake Engineering: Vancouver 1-6 August* [on-line, Paper 1428].

Atlas Powder Company (1987). *Explosives and rock blasting*. Dallas: Atlas Powder Company.

Bellier, O., Sébrier, M., Beaudouin, T., Villeneuve, M., Braucher, R., Bourles, D., Siame, L., Putranto, E. & Pratomo, I. (2001). High slip rate for a low seismicity along the Palu-Koro active fault in central Sulawesi (Indonesia). *Terra Nova*, *13*(6), 463-470.

Boix, L.R. & Zinck, J.A. (2008). Land-use planning in the Chaco plain (Burruyacu, Argentina). Part 1: Evaluating land-use options to support crop diversification in an agricultural frontier area using physical land evaluation. *Environmental Management*, *42*(6), 1043.

Chang, I.S. & Wu, J. (2011). Review on natural resources utilization in China. *Management Science and Engineering*, *5*(2), 16-21.

Chávez-García, F.J. & Cuenca, J. (1998). Site effects and microzonation in Acapulco. *Earthquake Spectra*, *14*(1), 75-93.

Dougill, A.J., Twyman, C., Thomas, D.S. & Sporton, D. (2002). Soil degradation assessment in mixed farming systems of southern Africa: use of nutrient balance studies for participatory degradation monitoring. *Geographical Journal*, *168*(3), 195-210.

Erdik, M., Durukal, E., Aydinoglu, N., Fahjan, Y. & Siyahi, B. (2006). Urban earthquake loss assessment. In *Geohazards – Technical, Economicial and Social Risk Evaluation: Lillehammer, 18-21 June 2006* [on-line]. Retrieved from: http://dc.engconfintl.org/geohazards/17

Faccioli, E. & Pessina, V. (2001). *The Catania Project: earthquake damage scenarios for a high risk area in the Mediterranean*. Retrieved from: https://www.earth-prints.org/bitstream/2122/12181/1/FACTCP_99.pdf

Fäh, D., Kind, F., Lang, K. & Giardini, D. (2001). Earthquake scenarios for the city of Basel. *Soil Dynamics and Earthquake Engineering*, *21*(5), 405-413.

Feizizadeh, B. & Blaschke, T. (2012). Uncertainty analysis of GIS-based ordered weighted averaging method for landslide susceptibility mapping in Urmia Lake Basin, Iran. In *Seventh International Geographic Information Science Conference* (pp. 18-21). [s.l.]: Springer.

Feng, Z.M. (1994). Land bearing capacity research of past, present, and future. *China Land Science*, *8*, 1–9.

Goldshleger, N., Ben-Dor, E., Lugassi, R. & Eshel, G. (2010). Soil degradation monitoring by remote sensing: examples with three degradation processes. *Soil Science Society of America Journal*, *74*(5), 1433-1445.

Gupta, A.K. & Nair, S.S. (2010). Flood risk and context of land-uses: Chennai city case. *Journal of Geography and Regional Planning*, *3*(12), 365-372.

Gupta, S. & Sharma, R.K. (2010). Dynamics of land utilisation, land degradation and factors

determining land degradation in Himachal Pradesh. *Indian Journal of Agricultural Economics*, *65*(2), 245-260.

Lungu, D., Aldea, A., Cornea, T. & Arion, C. (2000). Seismic micro-zonation of the City of Bucharest. In *6th International Conference on Seismic Zonation*. Oakland: Earthquake Engineering Research Institute.

Marcellini, A., Daminelli, R., Pagani, M., Riva, F., Crespellani, T., Madiai, C., Vannucchi, G., Frassineti, G., Martelli, L., Palumbo, D. & Viel, G. (1998). Seismic micro-zonation of some municipalities of The Rubicone Area (Emilia-Romagna Region). In *Proceedings of the 11th European Conference on Earthquake Engineering: 6-11 September 1998, Paris, France* (pp. 339-350). Rotterdam: Balkema Retrieved from: https://geotecnica.dicea.unifi.it/parigi98.pdf

Munasinghe, M. (1993). *Environmental economics and sustainable development*. Washington: World Bank.

Nakamura, Y. (2000, January). Clear identification of fundamental idea of Nakamura's technique and its applications. In *Proceedings of the 12th World Conference on Earthquake Engineering*, *2656*, 1-8.

Onishi, T. (1994). A capacity approach for sustainable urban development: an empirical study. *Regional studies*, *28*(1), 39-51.

Peraturan Pemerintah Nomor 26 Tahun 2008 tentang Rencana Tata Ruang Wilayah Nasional. Lembaran Negara Republik Indonesia Tahun 2008 Nomor 48, Tambahan Lembaran Negara Republik Indonesia Nomor 4833 [Government Regulation No 26 of 2008 regarding National Territorial Layout Plan. State Gazette of the Republic of Indonesia of 2008 Number 48, Supplement to the State Gazette of the Republic of Indonesia Number 4833].

Pilvere, I., Nipers, A. & Upite, I. (2014). Agricultural land utilization efficiency: the case of Latvia. *International Journal of Trade, Economics and Finance*, *5*(1), 65-71.

Sarma, A.K., Mahanta, C., Bhattacharya, R., Dutta, S., Kartha, S., Kumar, B. & Sreeja, P. (2012). *Urban carrying capacity: concept and calculation*. Assam: Centre of Excellence.

Sharififar, A., Ghorbani, H. & Karimi, H. (2013). Integrated land evaluation for sustainable agricultural production by using analytical hierarchy process. *Agriculture*, *59*(3), 131--140.

Shi, L.Y. & Chen, B.M. (1991). *Production capacity of land resources and population bearing capacity study in China*. Beijing, China: China Renmin University Press.

Singer, M.J. (2014). Land capability analysis. In Y. Wang (Ed.) *Encyclopedia of Natural Resources: Land*. Vol. 1 (pp. 295-298). New York: Taylor and Francis.

Slob, S., Hack, R., Scarpas, T., Bemmelen, B. van & Duque, A. (2002). A methodology for seismic microzonation using GIS and SHAKE a case study from Armenia, Colombia. In *Engineering Geology for Developing Countries-Proceedings of 9th Congress of the International Association for Engineering Geology and the Environment: Durban 16-20 September 2002* (pp. 2843-2852). Pretoria: South African Institute of Engineering and Environmental Geologists.

Smardon, R. (2008). A comparison of Local Agenda 21 Implementation in North American, European, and Indian Cities. *Management of Environmental Quality: An International Journal*, *19*(1), 118-137.

Stocking, M.A. & Murnaghan, N. (2002). *Field assessment of land degradation*. London: Earthscan.

Sudershan, I. (2003). Environmental damage to land resources – need to improve land use data base. *Economic and Political Weekly*, *38*(34), 3596-3604.

Symeonakis, E., Calvo-Cases, A. & Arnau--Rosalen, E. (2007). Land use change and land degradation in southeastern Mediterranean Spain. *Environmental Management*, *40*(1), 80-94.

Tian, Y. & Sun, C. (2018). A spatial differentiation study on comprehensive carrying capacity of the urban agglomeration in the Yangtze River Economic Belt. *Regional Science and Urban Economics*, *68*(1), 11-22.

Xiao, H.B., Shi, Z.H., Li, Z.W., Chen, J., Huang, B., Yue, Z.J. & Zhan, Y.M. (2021). The regulatory effects of biotic and abiotic factors on soil respiration under different land-use types. *Ecological Indicators*, *127*, 107787. https://doi.org/10.1016/j.ecolind.2021.107787

Summary

Integrated assessment of urban land carrying capacity (ULCC) for reducing earthquake risk disaster in Palu City. Assessment of the carrying capacity of urban land is very important to evaluate and obtain an overview of the level of land capability through the classification of the carrying capacity of the area so that it becomes the basis for future urban development. This research was conducted in Palu City, which is national city in Indonesia with limited urban development due to its prone to earthquakes. For urban development, it is necessary to study the carrying capacity of land to reduce the risk of earthquake disasters, through three stages of analysis, namely mapping of earthquake-prone areas using the earthquake hazard mapping with seismic micro-zonation; land capability assessment; and integration of land suitability with planning and spatial planning of Palu City. Based on the findings of this study, 74.56% of Palu City is an earthquake-prone area dominated by land capability Classes A to B, namely low to very low land capability classes (55.43%), implying that they have urban physical constraints. However, if it is integrated with the Palu City spatial plan until 2030, most (78.79%) are already in accordance with the carrying capacity of their land, especially in protected areas, but there are still land developments that are not suitable for carrying capacity (21.21%), especially in cultivation areas with risks earthquake disaster. Land use plans that are not in accordance with their carrying capacity must be managed strictly as a tool for disaster mitigation that is urgently needed.

Authors' address:
Erwindy Jossi – corresponding author
(https://orcid.org/0000-0002-8021-5911)
University of Padjadjaran
Graduate School
Department of Environmental Studies
Jl. Dipati Ukur 35, Bandung City
West Java, Indonesia, 40132
e-mail: jossi18001@mail.unpad.ac.id

Scientific Review – Engineering and Environmental Sciences (2021), 30 (4), 537–551
Sci. Rev. Eng. Env. Sci. (2021), 30 (4)
Przegląd Naukowy – Inżynieria i Kształtowanie Środowiska (2021), 30 (4), 537–551
Prz. Nauk. Inż. Kszt. Środ. (2021), 30 (4)
https://srees.sggw.edu.pl
DOI 10.22630/PNIKS.2021.30.4.45

Saja S. ALKHATTAT, Munaf A. Al-RAMAHEE
University of Al-Qadisiyah, College of Engineering

Shear performance of reinforced self-compacting concrete beams incorporating steel and polypropylene fibers

Key words: steel fiber, lightweight concrete, polypropylene fiber, shear strength

Introduction

Concrete improvement is an important aspect of modern construction development. Self-compacting concrete (SCC) is characterized as concrete that can flow on its weight without any compaction effort and can fill voids in all corners and gaps. The use of superplasticizers, mineral additives, high content of fine materials and mortars, contributes to greater cohesion and fluidity of the paste, on the other hand, concrete absorbs less energy (Rahman, Usman & Al-Ghalib, 2012). With the use of SCC, fewer construction workers are required during the casting stage, and the noise level created by mechanical vibration equipment is minimized, resulting in reduced sound impacts on the environment (Okamura & Ozawa, 1996). Improving working conditions and the climate and has been created commonly used to create complex-shaped beams or structures with a high density of reinforcement (Barros, Gomes & Barboza, 2011). However, when a regular weight and high specific gravity aggregate in some cases have a concern regarding the structural weight, the lighter weight aggregates are needed. In this case, the coarse aggregates are partially or completely replaced by lightweight aggregate (Siva Rama Prasad, 2017). Aside from its structural uses, lightweight aggregate concrete (LWAC) primarily increases building thermal conductivity and sound insulation properties (Ahmad, Chen & Shah, 2019). Artificial LWA, such as sintered fly ash, expanded clay, and expanded shale, are commonly used in the manufacture of LWC as they have a lower density, greater longevity, and higher specific strength. Lightweight self-compacting concrete (LWSCC) is rendered by replacing the usual coarse aggregates in SCC with lighter coarse aggregates which produce a new type of high-performance material that incorporates

the benefits of both SCC and LWC (Liu, Wu, Yang & Wei, 2019). The LWSCC is expected to have good workability without segregation and high reliability despite being lighter. The use of aggregates is essential to the development of high-quality LWSCC. Expanded clay (LECA) is a ceramic medium made by rotary kiln expansion and verification of selected clay. Other lightweight aggregates such as expanded shale, pumice, granite, perlite, bottom ash, and others have been used successfully in the manufacture of lightweight concretes (LWCs) (Hwang & Hung, 2005; Wu, Zhang, Zheng & Ding, 2009; Alkhattat & Al-Ramahee, 2021). The incorporating of fibers in concrete can improve both the physical properties of the concrete and the structural performance (Sahmaran, Yurtseven & Yaman, 2005). Fibers can also help strengthen the bond between lightweight concrete and the reinforcing bar. Hybrid fibers are fibers that are also added to concrete by mixing various kinds of fibers such as polypropylene and steel fibers. The SCC is affected by the type of powder that is added to its mix such as limestone powder and fly ash. Topcu, Bilir and Uygunoğlu (2009) have been studied different dosages of powder and found that when its amount more than: 200 $kg \cdot m^{-3}$, the workability was not affected while the compressive strength decreased. The fresh mix properties such as slump flow, L-box, and v-funnel test were improved when the used amount of powder was less than 200 $kg \cdot m^{-3}$ (Mazaheripour, Ghanbarpour, Mirmoradi & Hosseinpour, 2011). The compressive strength increased at the late age by using fly ash while the limestone powder increased the compressive strength at the early and the late ages (Topcu et al., 2009). Ramanathan, Baskar, Muthupriya and Venkatasubramani (2013) examined the effects of various mineral admixtures, such as fly ash, ground granulated blast furnace slag, and silica fume, on the fresh and hardened properties of SCC. These minerals had a passable impact on the fresh properties. With successful execution on the fresh state of SCC, blast furnace slag has higher workability than fly ash and silica fume. When using a 30% mineral admixture replacement ratio and water/powder ratio of 0.35 to minimize the segregation, the mechanical properties compressive, splitting, and flexural strength was improved significantly. Vijayalakshmi and Ramanagopal (2018) found that the specific weight of LWC was around (16–48%) less than that of normal-weight concrete with high water absorption and strength ranging from 24 to 60 MPa after 28 days of curing. The density of concrete was also decreased, ranged from 1,290 to 2,044 $kg \cdot m^{-3}$. Rashad (2018) found that when LECA was used as a coarse aggregate, the compressive strength decreased by 12.5–38%, the density decreased by 16.36–36.51%, and all other properties, such as chloride attack, shrinkage, and resistance to melting and freezing, decreased by 12.5–38%. The shear behavior of LWC beams was investigated and compared to that of normal concrete beams. It was discovered that the overall maximum shear strength of LWSCC beams was 15.8% lower than that of normal concrete beams. This reduction in strength was due to the use of LWC (expanded clay). It was also discovered that increasing the main reinforcement increase the shear strength (Garcia, Lannes, Carneiro & Lara, 2020). Raman-

janeyulu, Srigiri and Rao (2018) examined the impact of expanded clay on the LWSCC's strength and durability. The results showed that LWSCC had a lower density than standard concrete, ranged from 1,870 to 1,950 $kg \cdot m^{-3}$. However, increasing the amount of LECA caused segregation, and increasing the dosage of superplasticizer led to less resistance to the effects of sulfate and acids than natural aggregate self-compacting concrete. The impact of steel fiber on the fresh and hardened properties of LWSCC with 0.5% steel fiber was investigated, and it was discovered that workability decreased while compressive strength and elasticity modules – improved. The mixes reinforced with steel fiber had greater energy absorption ability and soften performance (Gao, Sun & Marino, 1997). Gencel, Ozel, Brostow and Martinez-Barrera (2011) examined the effect of the addition of polypropylene to self-compacting concrete and found that when the fiber is distributed evenly, there is no issue with followability. Increasing fiber content contributes to an increase in fracturing, compressive, and Young's modules. Compressive strength is improved when 0.6% steel fiber and 0.3% polypropylene were added. As the hybrid content was increased, the tensile and flexural strength increased by around 129 and 206%, respectively with keeping the polypropylene ratio constant at 0.3% (Ibrahim & Abbas, 2019). Karimipour, Ghalehnovi, de Brito and Attari (2020) performed a study on polypropylene fiber and its effect on SCC and discovered that the optimal ratio for improving tensile and flexural strength, as well as impact and heat resistance, was 0.3%. However, this resulted in a decrease in compressive strength. The lightweight concrete is week in compression and tension, so to enhance the performance of such beam, steel and polypropylene fiber were added in this study. The steel and hybrid (polypropylene with steel) fibers were added as 1% volumetric a to study their effect on the shear behavior of lightweight self-compacting reinforced beams that made with partial and full replacement of coarse aggregate using LECA.

Experimental program

In the experimental program, seven simply supported beams with dimensions of 150 × 250 × 1,650 mm, as listed in Table 1, were cast to investigate various factors that can influence the structural behavior. In the specimen nomenclature, the two digits that follow the letters SR refer percentage of coarse aggregate replacement by LECA (0 for no replacement, 50 for partial replacement, and 100 for full replacement), followed by 00 to refer no fiber added, letters SF which refers to 1% steel fiber, or letters SP refers to 0.75% steel and 0.25% polypropylene fiber (hybrid fiber). The first beam (SR00-00) was used as a control beam for comparison purposes and was fabricated entirely using SCC (no LECA replacement and no fibers). Expanded clay has been employed to make two lightweight reinforced concrete RC beams in place of coarse aggregate. The first lightweight beam (SR50-00) was cast with 50% coarse aggregate replacement, while the second (SR100-00) was prepared with 100% replacement. After that, steel fibers and hybrid fibers were added to each form of LWSCC. Based on the findings

of a previous report (Mazaheripour et al., 2011), the volumetric percentage of used fiber was set at 1%. The steel fiber had a percentage of 0.75% and the polypropylene fiber had a percentage of 0.25% in the hybrid fiber, Figure 1 shows the steel and polypropylene fiber. Other materials that used in this research were Portland cement that follows the Iraqi specification the IQS No 5/1984 (Central Organization for Standardization and Quality Control [COSQC], 1984), coarse aggregate with a max size of 10 mm and, fine aggregate with sulfate content (SO_3) of 0.34 from Al-Najaf inquire, limestone powder (LP) with a specific gravity of 1.07 kg·m^{-3}, superplasticizer Sika ViscoCrete®-5930L, expanded clay (LECA) with a maximum size of 10 mm and bulk density of 260 kg·m^{-3}. The water-cement ratio (w/c) was 0.35 for all mixes. These mixes were based on the results of Abo Dhaheer, Al-Rubaye, Alyhya, Karihaloo and Kulasegaram studies. The details and mix proportions of all used materials are listed in Table 1.

The properties of fibers used in this experiment are listed in Table 2. All beams were reinforced with 2Φ16 steel bars as main tensile reinforcement and 2Φ10 steel bars as compressive reinforcement for practical consideration. To ensure shear failure, shear reinforcement was provided using closed Φ10 at 250 mm c/c. Figure 2 depicts the cross-section and steel reinforcement. Slump flow and L-box tests were performed before beam casting, as shown in

TABLE 1. Mix proportions

Specimen mix	LECA [kg]	Cement [kg·m^{-3}]	Sand [kg·m^{-3}]	Gravel [kg·m^{-3}]	Steel fiber [%]	Polypropylene [%]
SR00-F0	0	468	754	858	0	0
SR50-00	100	468	754	429	0	0
SR100-00	200	468	754	0	0	0
SR50-SF	100	468	754	429	1	0
SR100-SF	200	468	754	0	1	0
R50-SP	100	468	754	429	0.75	0.25
SR100-SP	200	468	754	0	0.75	0.25

FIGURE 1. Steel and polypropylene fiber

Figure 3, in accordance with the limitations presented in "The European guidelines for self-compacting concrete" (European Federation of National Associations Representing for Concrete [EFNARC], 2005). The compressive strengths of SCC and LWSCC average 28-day based on 150 × 150 × 150 mm cubes, splitting tensile strength of a cylinder (dimensions: 20 mm diameter, 200 mm height), flexural strength for a 100 × 100 × 500 mm prism, and density for all mixes are described in Table 3. Also, fresh properties for all mixes in terms of slump flow and L-box results are listed in Table 4. The average density of partial replacement of aggregate mix (for all types of fibers) was around 1,930 kg·m^{-3} while it was around 1,630 kg·m^{-3} for full replacement specimens mix. These values agree with the definition of the report ACI 213R-03 (American Concrete Institute [ACI], 2003). The experimental work was performed at the Civil Engineering Structural Lab at the Al-Qadisiyah University.

TABLE 2. Properties of steel and polypropylene fibers

Property	Steel fiber	Polypropylene fibers
Diameter [mm]	0.2–0.25	0.032
Length [mm]	12–14	12
Tensile strength [MPa]	2 850	600–700

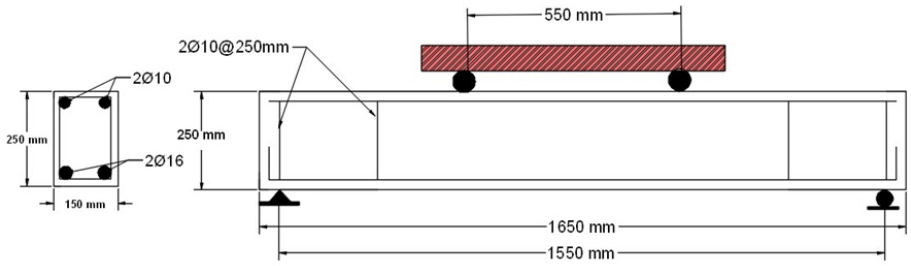

FIGURE 2. Specimens reinforcement details

FIGURE 3. Slump flow and L-box test

TABLE 3. Mechanical properties

Sample	Compressive strength [MPa]	Tensile strength [MPa]	Flexure strength [MPa]	Density [kg·m^{-3}]
SR00-00	50	3.5	7.5	2 220
SR50-00	34	2.8	5.12	1 915
SR100-00	24	2.16	3.5	1 620
SR50-SF	44	4.4	6.78	1 950
SR100-SF	34	3.4	5.8	1 750
SR50-SP	35	4.2	7	1 912
SR100-SP	29	3.19	5.87	1 650

TABLE 4. Slump flow and L-box results

Sample	Slump flow [mm]	BR = h_2 / h_1
SR00-00	740	0.857
SR50-00	737.5	0.88
SR100-00	750	0.92
SR50-SF	733	0.88
SR100-SF	730	0.85
SR50-SP	735	0.87
SR100-SP	742	0.8

Experimental tests

A four-point load configuration has been used to test all specimens. The tests were carried out with a 1,000 kN hydraulic jack at a constant rate of 5 kN·min^{-1} as shown in Figure 4. The central deflection was recorded using an electronic dial gauge attached to the mid-span bottom face. The instrumentation was connected to automated data acquisition devices. Based on visual inspection, cracks were found during the loading stages. If there

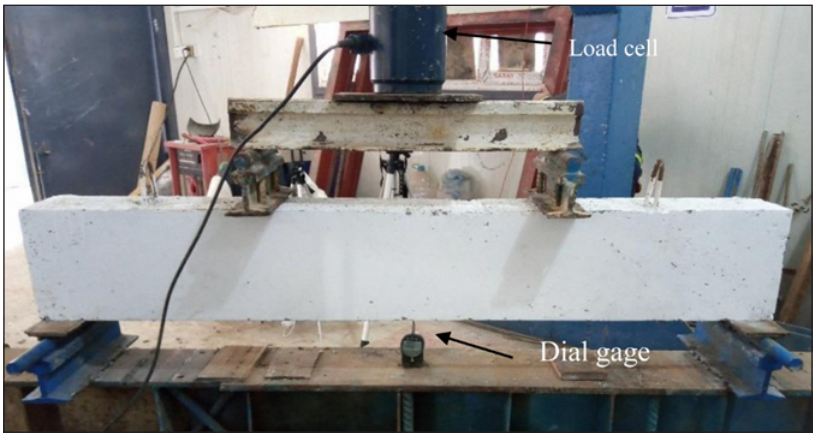

FIGURE 4. Beam with testing machine

is an excessive deflection or the load has fallen dramatically, beams are deemed to have failed.

Results and discussion

The control beam (SR00-00) has been made using standard SCC without the addition of any fibers. The first crack was discovered at a load level of 33 kN, with a central deflection of 1.05 mm. However, at a load level of 131 kN, the first shear crack appeared with 5.44 mm central deflection. The maximum load applied to this specimen was 215 kN, with a central deflection of 12.83 mm. The load-vertical displacement relation for SR00-00 is shown in Figure 5. Figure 6 shows the crack pattern at failure.

Effect of using lightweight concrete

Two different percentages of lightweight aggregate LECA (50 and 100%) replacement have been used. For the (SR50-00) beam with partial replacement (50% LECA), the first crack appeared at load level of 13 kN with a central deflection of 0.54 mm. The first shear crack appeared at 63 kN with 2.94 mm central deflection. This beam reached an ultimate load level of 165 kN with a corresponding central deflection of 11 mm.

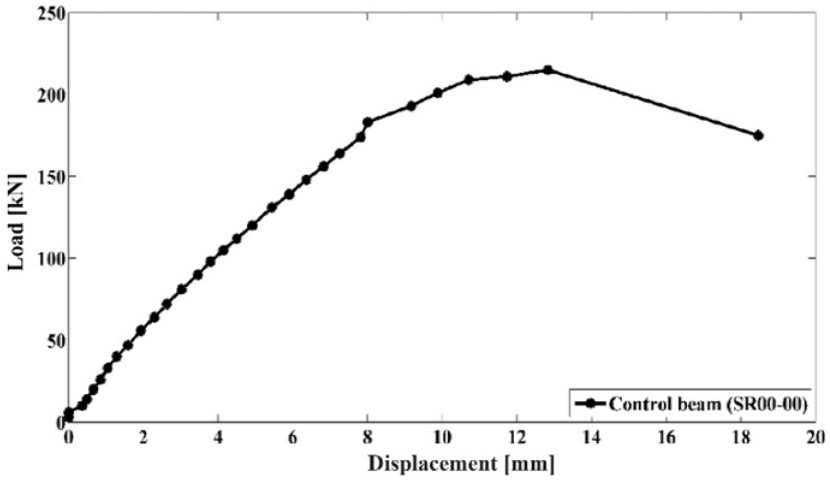

FIGURE 5. Load-displacement relationship for control beam

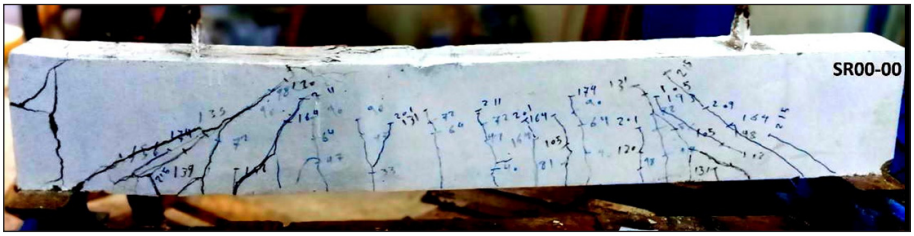

FIGURE 6. Crack pattern in the beam

Figure 7 shows the crack pattern at the ultimate load level which clearly indicates the shear failure of the beam.

For the (SR100-00) beam that was cast with full coarse aggregate replacement (100% LECA), the first crack was noticed at a load level of 18 kN, with a central deflection of 1.23 mm. However, at a load of 75 kN, the shear crack was observed with a central deflection of 3.79 mm. Moreover, the maximum capacity of this specimen was 175 kN, with a corresponding mid-span deflection of 11.2 mm. Figure 8 depicts the crack pattern for this beam with shear failure at the ultimate load.

Figure 9 shows the comparison in load-displacement response for a beam with LECA replacement with the control beam. From this figure, the ultimate loads

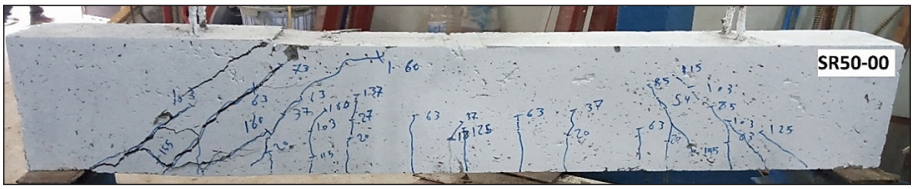

FIGURE 7. Crack pattern for 50% LECA

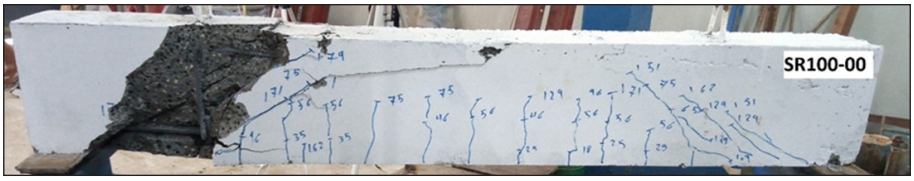

FIGURE 8. Crack pattern for 100% LECA

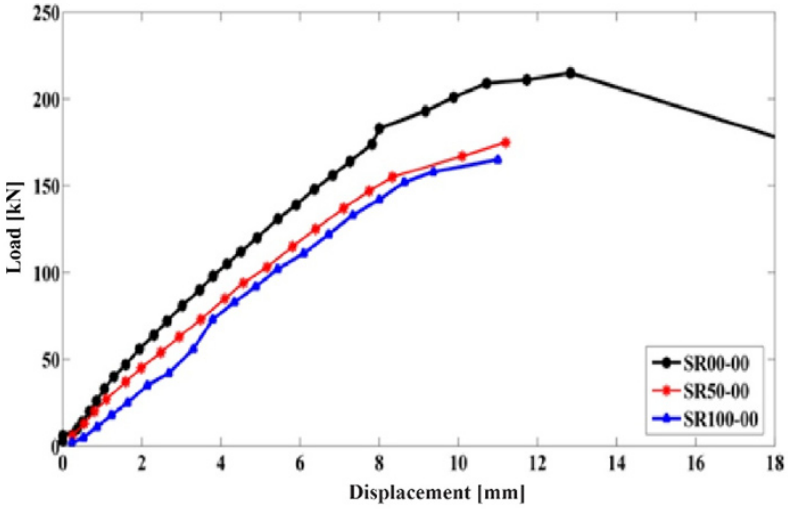

FIGURE 9. Effect of using LECA in SCC beams

for beam with LECA replacement are reduced by 23 and 30% for partial and full replacement, respectively when compared with the control beam. It is also worth noting that the SR50-00 when compared to the control beam, there is little difference in its stiffness. While the SR100-00 has a noticeable difference in its stiffness compared to the control beam.

Effect of steel fiber

The influence of steel fibers on the performance of the LWSCC reinforced beam has been investigated. Steel fiber was used at a volumetric ratio of 1% for both partial and full LECA substitution. For the SR50-SF beam which represents the SCC beam with partial aggregate replacement and 1% steel fiber, the ultimate load was 227 kN which represents a 30% increase compared to the ultimate load for SR50-00 (without steel fiber). The deflection that corresponding to the ultimate load level was 16.17 mm. The first crack for SR50-SF was recorded at a load level of 40 kN with a deflection of 1.64 mm. However, the first shear crack was noticed at a load level of 117 kN with a corresponding deflection of 5.45 mm. The use of steel fiber contributed to enhancing the shear strength of the beam and correspondingly changed the failure mode. The eventual collapse of the beams appeared to be caused by a combination of diagonal

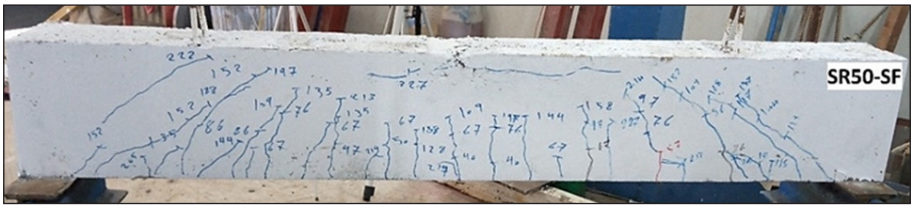

FIGURE 10. Crack pattern for SR50-SF

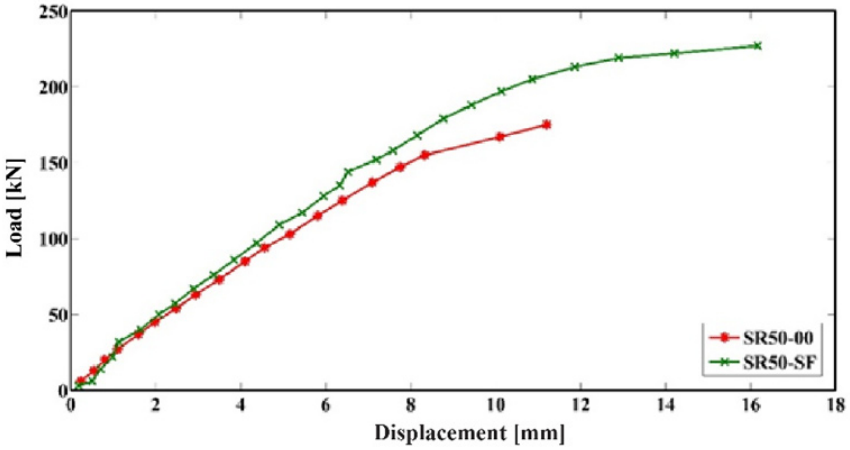

FIGURE 11. Effect of steel fiber on LWSCC beam with partial replacement

tension failure, flexural cracking at the mid-span, and concrete crushing in the compression area as shown in Figure 10. Figure 11 shows the load-displacement relationship. It was found that the steel fiber made the beam more ductile with reduced the crack width.

The ultimate load level for the beam with full replacement of coarse aggregate and 1% steel fiber (SR100-SF) was 207 kN which represents a 25% increase in the load level compared to SR100-00 (without steel fiber). The deflection that corresponding to the ultimate load level was 15.7 mm. The first crack was recorded at a load of 28 kN with 0.85 mm mid-span deflection. Moreover, the first shear crack was noticed at a load level of 116 kN with 5.11 mm mid-span deflection. Figures 12 and 13 show the crack pattern and load-displacement relation. Steel fiber usage improves beam stiffness, post-cracking behavior, and load-carrying capacity, as compared to SR100-00. The beams collapsed due to a combination of diagonal tension failure and flexural cracking at the mid-span, as well as concrete crushing in the compression area, which was attributed to the steel fiber's high tensile strength, which increased the beam's shear resistance.

FIGURE 12. Crack pattern of SR100-SF

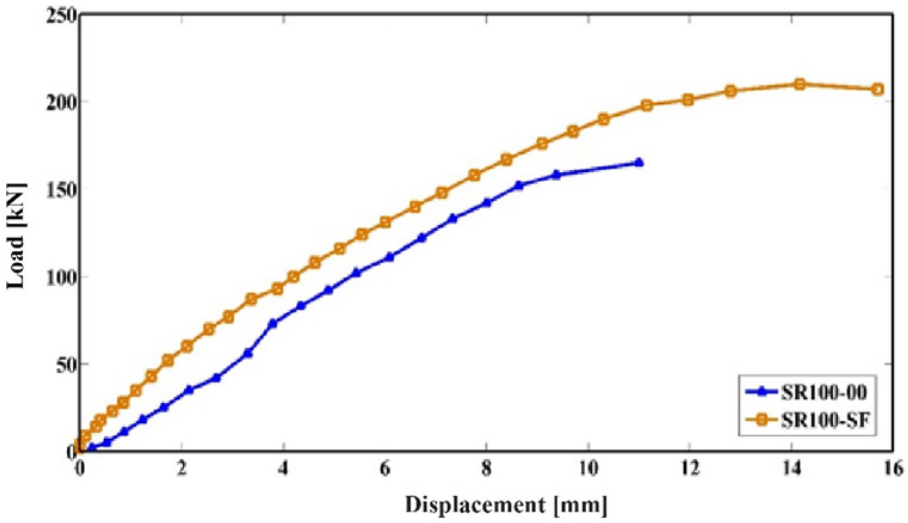

FIGURE 13. Effect of steel fiber on the failure mode for full replacement

Effect of using polypropylene fibers

The impact of hybrid fibers on the LWSCC beam's action has been investigated. In this test, the hybrid fibers contain 0.75% steel fibers and 0.25% polypropylene fibers as a volumetric ratio. Both partial and full LECA replacement beams incorporating hybrid fibers were investigated. With 12 mm corresponding central deflection, the SR50-SP beam (50% replacement contain hybrid fibers) achieved an ultimate load level of 185 kN. The first crack was recorded at load level 42 kN with 1.95 mm central deflection. At a load level of 108 kN, the shear crack was observed with a central deflection of 5.37 mm. Figure 14 shows the crack pattern and failure mode for SR50-SP. In contrast to beams with only steel fibers, it can be seen the shear failure is the dominant failure in lightweight beams with hybrid failure. Figure 15 shows the load-displacement and results in comparison for a beam with partial replacement.

The SR100-SP beam (full LECA replacement and hybrid fibers) has an ultimate strength of 187 kN with a central deflection of 13.48 mm which represents an increase of about 13% compared to

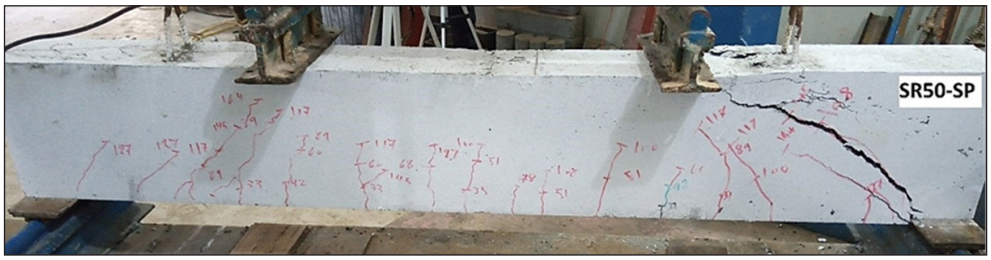

FIGURE 14. Effect of hybrid fiber on the LWSCC beam

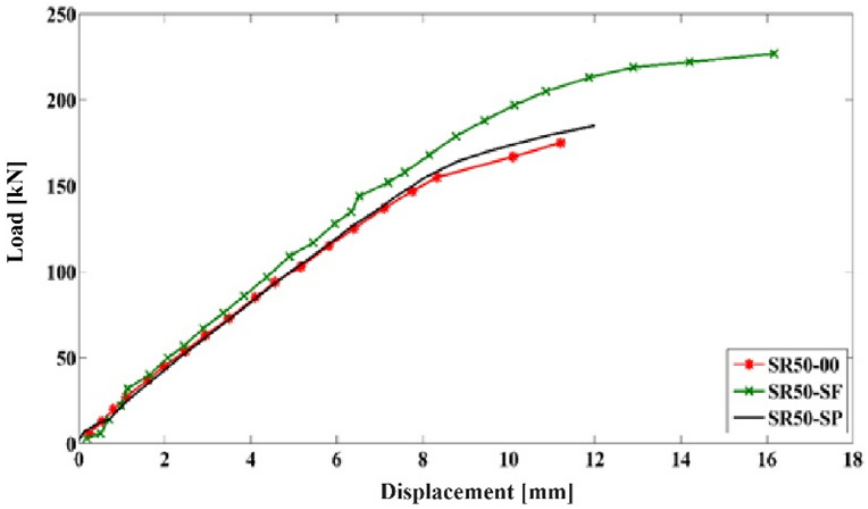

FIGURE 15. Effect of hybrid fiber on the LWSCC beam for 50% and 100% replacement

SR100-00 (beam with full replacement of coarse aggregate and fibers). The first crack was shown at a load level of 30 kN with a central deflection of 1.52 mm. However, the shear crack was observed at a load level of 84 kN with a 4.33 mm central deflection. Figure 16 shows the crack pattern and failure mode for the SR100-SP beam and Figure 17 shows the load-displacement relationship and the effect of using hybrid (polypropylene and steel) fiber with LWSCC. Similar to beams with partial and hybrid fibers, there was a significant change in the ultimate load with an improvement in the crack pattern, and beam stiffness, and tensile and shear strength of the beam compared to the beam with full replacement and without any type of fibers.

Conclusions

The performance of lightweight self--compacting concrete (LWSCC) employing two types of fibers was investigated

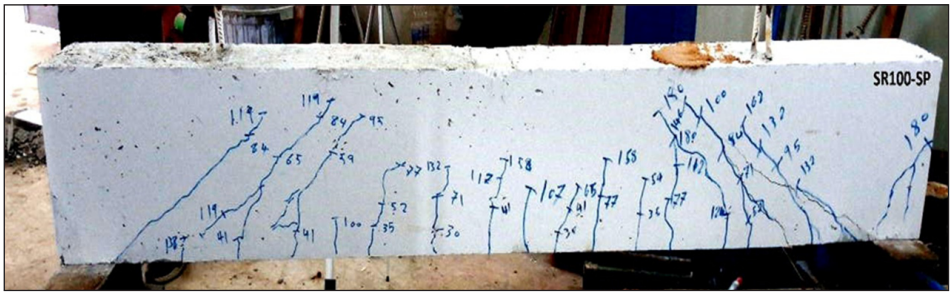

FIGURE 16. Effect of using polypropylene and steel fiber on LWSCC beam

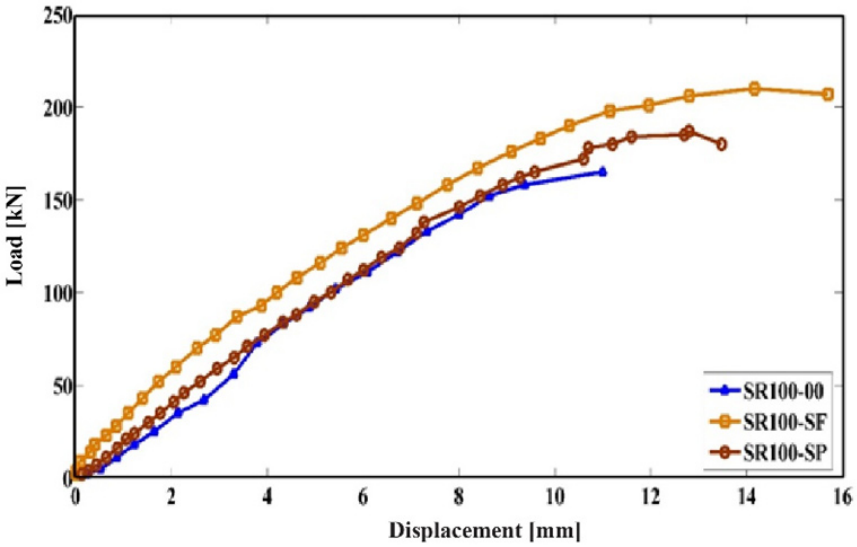

FIGURE 17. Effect of steel and hybrid fiber with 100% LECA

in this research. The experimental results of seven beams were discussed in terms of the crack patterns, ultimate load, and deflection and compared with each other. The following are the study's main points and conclusions:

1. When using light weight aggregate in the concrete mix as a partial or full replacement with coarse aggregate led to decreases the density of the structure about 13% for a partial replacement and about 27% for full replacement and that make it a lightweight concrete according to the specification of the report ACI 213R-03 definition (ACI, 2003).
2. Lightweight concrete has a greater capacity to bend than conventional concrete, but it also has a greater tendency to segregate. All of the cracking patterns that appeared were identical. For the control beam with a thinner fracture, the crack displayed dispersion followed a similar pattern. Finally, using pre-wetted aggregate had no effect on the self-compatibility or stability of the mixtures.
3. The steel fiber used as 1% volumetric ratio led to an increase in the compressive, tensile, and flexural strength about 29, 43, and 32%, respectively for partial replacement (50% LECA), and 41, 57, and 65%, respectively for full replacement (100% LECA).
4. Using steel fiber led to an increase in the shear strength of LWSCC beam and changing the failure mode from shear to flexure due to the high tensile strength of the steel fiber combined with stirrups, with additional fractures spread over the length of the beam steel fiber increased the stiffness of the beam, improving its ultimate load and beam behavior.
5. The use of hybrid fiber (steel and polypropylene) enhanced the tensile strength by 50 and 48% for the partial and full coarse aggregate replacement, respectively. Also, it increased the flexural strength by about 37 and 68% for the partial and full coarse aggregate replacement, respectively compared to lightweight beams without fibers.
6. Beams with fibers have well stiffened, less crack width, and improved load mid-span deflection, increasing shear capacity. Hybrid beams demonstrated a ductile post-cracking behavior since beams without fiber showed considerable deformation before the collapse.

References

Abo Dhaheer, M.S., Al-Rubaye, M.M., Alyhya, W.S., Karihaloo, B.L. & Kulasegaram, S. (2016). Proportioning of self-compacting concrete mixes based on target plastic viscosity and compressive strength: Part II – experimental validation. *Journal of Sustainable Cement-Based Materials*, *5*(4), 217-232.

Ahmad, M.R., Chen, B. & Shah, S.F.A. (2019). Investigate the influence of expanded clay aggregate and silica fume on the properties of lightweight concrete. *Construction and Building Materials*, *220*, 253-266.

Alkhattat, S.S. & Al-Ramahee, M.A. (2021). Flexural strength of fibrous light-weight self-compacted concrete beams. *Journal of Physics: Conference Series*, *1973*(1), 012221. https://doi.org/10.1088/1742-6596/1973/1/012221

American Concrete Institute [ACI] (2003). *Guide for structural lightweight aggregate concrete*.

Specification, production and use. ACI Committee 213 report (ACI 213R-03). Farmington Hills: American Concrete Institute.

Barros, A.R., Gomes, P.C.C. & Barboza, A.S.R. (2011). Steel fibers reinforced self-compacting concrete: behavior to bending. *Revista IBRACON de Estruturas e Materiais*, *4*, 49--78.

Central Organization for Standardization and Quality Control [COSQC] (1984). *Portland cement* (IQS No 5/1984). Baghdad: Central Organization for Standardization and Quality Control.

European Federation of National Associations Representing for Concrete [EFNARC] (2005). *The European guidelines for self--compacting concrete*. Surrey: European Federation of National Associations Representing for Concrete.

Gao, J., Sun, W. & Morino, K. (1997). Mechanical properties of steel fiber-reinforced, high--strength, lightweight concrete. *Cement and Concrete Composites*, *19*(4), 307-313.

Garcia, S.L.G., Lannes, C.V., Carneiro, L.A.V. & Lara, R.C. (2020). Shear behavior of lightweight self-consolidating reinforced concrete beams without transverse reinforcement. *Latin American Journal of Solids and Structures*, *17*(4), 1-13.

Gencel, O., Ozel, C., Brostow, W. & Martinez--Barrera, G. (2011). Mechanical properties of self-compacting concrete reinforced with polypropylene fibres. *Materials Research Innovations*, *15*(3), 216-225.

Hwang, C.L. & Hung, M.F. (2005). Durability design and performance of self-consolidating lightweight concrete. *Construction and Building Materials*, *19*(8), 619-626.

Ibrahim, H.A. & Abbas, B.J. (2019). Influence of hybrid fibers on the fresh and hardened properties of structural light weight self-compacting concrete. *IOP Conference Series: Materials Science and Engineering*, *518*(2), 022022. https://doi.org/10.1088/1757-899X/518/2/022022

Karimipour, A., Ghalehnovi, M., Brito, J. de & Attari, M. (2020). The effect of polypropylene fibres on the compressive strength, impact and heat resistance of self-compacting concrete. *Structures*, *25*, 72-87.

Liu, X., Wu, T., Yang, X. & Wei, H. (2019). Properties of self-compacting lightweight concrete reinforced with steel and polypropylene fibers. *Construction and Building Materials*, *226*, 388-398.

Mazaheripour, H., Ghanbarpour, S., Mirmoradi, S.H. & Hosseinpour, I. (2011). The effect of polypropylene fibers on the properties of fresh and hardened lightweight self-compacting concrete. *Construction and Building Materials*, *25*(1), 351-358.

Okamura, H. & Ozawa, K. (1996). Self-compactable high-performance concrete in Japan. *Special Publication*, *159*, 31-44.

Rahman, M.M., Usman, M. & Al-Ghalib, A.A. (2012). Fundamental properties of rubber modified self-compacting concrete (RMSCC). *Construction and Building Materials*, *36*, 630-637.

Ramanathan, P., Baskar, I., Muthupriya, P. & Venkatasubramani, R. (2013). Performance of self-compacting concrete containing different mineral admixtures. *KSCE Journal of Civil Engineering*, *17*(2), 465-472.

Ramanjaneyulu, N., Srigiri, K. & Rao, M.S. (2018). Strength and durability studies on light weight self-compacting concrete with LECA as partial replacement of coarse aggregate. *CVR Journal of Science and Technology*, *15*, 1-9.

Rashad, A.M. (2018). Lightweight expanded clay aggregate as a building material – an overview. *Construction and Building Materials*, *170*, 757-775.

Sahmaran, M., Yurtseven, A. & Yaman, I.O. (2005). Workability of hybrid fiber reinforced self-compacting concrete. *Building and Environment*, *40*(12), 1672-1677.

Siva Rama Prasad, C.V. (2017). Light Weight Concrete using Fly Ash Aggregate. *International Journal of Innovative Technologies*, *5*(3), 460-463.

Topcu, I.B., Bilir, T. & Uygunoğlu, T. (2009). Effect of waste marble dust content as filler on properties of self-compacting concrete. *Construction and Building Materials*, *23*(5), 1947-1953.

Vijayalakshmi, R. & Ramanagopal, S. (2018). Structural concrete using expanded clay aggregate: a review. *Indian Journal of Science and Technology*, *11*(16), 1-12.

Wu, Z., Zhang, Y., Zheng, J. & Ding, Y. (2009). An experimental study on the workability of self-compacting lightweight concrete. *Construction and Building Materials*, *23*(5), 2087-2092.

Summary

Shear performance of reinforced self--compacting concrete beams incorporating steel and polypropylene fibers. The impact of steel and polypropylene fibers on the performance of lightweight self-compacting concrete (LWSCC) beams was investigated in this study. Seven beams with various parameters were cast and tested. Partial (50%) and full (100%) replacement of coarse aggregate with lightweight aggregate expanded clay (LECA) were considered. In addition, a 1% volumetric ratio of steel or hybrid (steel and polypropylene) fiber was added to LWSCC beams to study their effect on the shear performance. The LWSCC beams had a decrease in ultimate load and stiffness of 23 and 30% for partial and full replacement, respectively when compared to normal weight beam. The addition of steel fiber improved the efficiency of LWSCC beams in terms of crack formation, failure mode, crack width, and ultimate load, as well as changed the failure mode from shear to flexure. The ultimate load for hybrid LWSCC was increased by around 6% for a partial replacement and 13% for full replacement as compared to beams without fibers. However, hybrid beams had a larger bearing capacity, little more cracks with smaller size, and ductile failure.

Authors' address:
Munaf A. Al-Ramahee – corresponding author
(https://orcid.org/0000-0002-1922-9871)
(Web of Science ResearcherID W-7313-2018)
University of Al-Qadisiyah
College of Engineering
e-mail: Munaf.alramahee@qu.edu.iq

Scientific Review – Engineering and Environmental Sciences (2021), 30 (4), 552–560
Sci. Rev. Eng. Env. Sci. (2021), 30 (4)
Przegląd Naukowy – Inżynieria i Kształtowanie Środowiska (2021), 30 (4), 552–560
Prz. Nauk. Inż. Kszt. Środ. (2021), 30 (4)
https://srees.sggw.edu.pl
DOI 10.22630/PNIKS.2021.30.4.46

Nur Muizzah NAWI, Doris Asmani MAT YUSOF, Siti Shahidah SHARIPUDIN, Nora Farina MOHD HALIM, Nor Mayuze MOHAMAD

Universiti Teknologi MARA, College of Engineering

Study on potential of soil stabilization using concrete sludge of batching plant (CSBP)

Key words: CBR value, concrete sludge, organic soil, maximum dry density, subgrade

Introduction

Malaysia's construction sector is fast developing as it moves closer to being a developed country. The expansion of new buildings and infrastructure in this country aided the expansion of manufacturing factories to meet the demand for materials for such projects. As concrete is one of the primary materials used in most construction projects, the number of batching plants in Malaysia will grow as ready-mix concrete is preferred to be used by the construction industry.

Traditionally, concrete mix design for casting in-situ must include a certain amount of allowable wastage for the materials as well as ready-mix concrete. The ready-mix concrete was one of the most wasteful materials, estimated to be 12% and will eventually be returned to the batching plants as concrete sludge (Arshad, Qasim, Thaheem & Gabriel, 2017). Unfortunately, the batching plant lacks an appropriate disposal solution for the returning concrete sludge. A research conducted in 2016 that looked at the current techniques for using fresh concrete waste returning to batching plants may have solved the problem. Kazaz and Ulubeyli (2016) concluded that there are nine techniques for benefitting batching plant returned concrete sludge. Discharging to the ground is the most common method utilized by batching plants out of all the options.

As a solution, several studies have been conducted to recycle the returned concrete sludge of batching plants (Arunvivek, Maheswaran, Senthil Kumar, Senthilkumar & Bragadeeswaran, 2015; Vieira & de Figueiredo, 2016; Thorneycroft, Orr, Savoikar & Ball, 2018). According to a study conducted by Vieira and de Figueiredo (2016) in Brazil, crushing

hardened concrete to generate recycled aggregates is one of the ways that may be utilized to tackle the problem (Vieira & de Figueiredo, 2016). On the other hand, Arunvivek et al. (2015) found that concrete containing 15–30% recycled fresh concrete waste is excellent for generating standard strength concrete.

There is a global need for developments of method used to utilize the waste that came from the batching plant. The search for environmentally, sustainably, and economically solution for the final disposal of concrete sludge from the batching plant is a challenge. At present the main concern is to dispose this waste correctly and reducing the storage costs hence promote sustainable waste management (Tewar, Shah & Patel, 2017). Many studies have shown that this concrete sludge can be used as recycled concrete (Arunvivek et al., 2015; Vieira & de Figueiredo, 2016; Thorneycroft et al., 2018; Nawi et al., 2019).

Three type of cementitious materials was tested and the result show that the combination of fly ash and Portland cement was the most effective stabilizer to acquire higher strengths (Tavakol, Hossain & Tucker-Kulesza, 2019). As the characteristics of CSBP and fly ash are almost the same which more on cementitious behavior, this research is to aim for the potential of soil-CSBP mixture to be use as subgrade soil stabilizer (Chattaraj & Sengupta, 2017; Tewar et al., 2017).

The strength behavior of soil with fly ash is identified by examining the influence of fly ash on the consistency, compactness, acidic characteristics, and strength of organic soil, according to Nath, Molla, Ali and Sarkar (2017). The plasticity index of organic soil is considerably reduced by fly ash, but the liquid and plastic limits rise. Aside from that, the properties of organic soil are enhanced, but the extent of the improvement is dependent on the organic soil's features as well as the properties and amount of fly ash (Nath et al., 2017).

Anupam, Kumar, Ransinchung and Shah (2017) has conducted a study to investigate the usefulness of industrial waste which are fly ash and bagasse ash as a soil admixture. The physical and chemical properties of these waste was examined by using California bearing ratio test, unconfined compressive strength and triaxial test. It shows that combination of fly ash and bagasse ash increased the unconfined compressive strength of the soil significantly thus can improve the load bearing capacity of the soil (Anupam et al., 2017).

The use of additional material for subgrade improvement was extend not only to roadwork but also on airfield pavements. Basically, lime, fly ash, cement and several combinations of these material were utilized as the stabilized agent for the soils. The best stabilized agent was depending on the soil characteristics itself, but nevertheless fly ash was use at two of the airports with the addition of 12–14% and the CBR value is reported to increase approximately 20. Plus, the fly ash is cheaper and easier to find compare to produce cement (Ward, Taylor & Grubbs, 2017). This supports the usage of recycle material as fly ash and CSBP has a problematic issue related to the disposal method of the material.

Preliminary study shows that the replacement of cement by 20% of CSBP in concrete achieved the favorable compressive strength (Nawi et al., 2019).

According to the findings, CSBP has the potential to be employed as a sustainable recycled material in traditional concrete. To extend the potential of CSBP as the recycled material in construction industry, it is to be proposed to use as the subgrade stabilization agent for pavement construction. A study conducted by Bandara, Binoy, Aboujrad and Sato (2015) has used cement, lime, and fly ash as the recycled material for subgrade stabilization to identify long term benefit for optimizing pavement design yet also lessen landfill problems. Since the properties of CSBP are comparable to those of fly ash, it is proposed in this study that CSBP be used as a recycled material for subgrade stabilization in pavement construction.

As CSBP can be categorized as one of the sustainable recycled materials, it is expected that by adding certain amount of CSBP in soil can increase the strength of the proposed soil. This study evaluates the use of CSBP as an additive for soil in subgrade layer for pavement construction as CSBP will act as a stabilizing agent of the soil mixture. At the same time, it promotes the proper and sustainable way to dispose CSBP rather than dispose them to landfill as well as reducing the cost of stabilizer agent for soil improvement as CSBP is a recycled material which incurred low processing cost.

Material and methods

The purpose of this study was to look at the performance of stabilized-organic soil at various CSBP percentages which are 0, 5, 10 and 15% based on the earlier study that performed by Kumar and Harika (2021). Instead of using fly ash, CSBP were used as it gives the similar cementitious characteristic as fly ash. In that study, the combination of 10% of fly ash gives the optimum value of CBR to the treated soil (Kumar & Harika, 2021). This study then was further tested to identify the index properties of the soil, compaction characteristic and California bearing ratio (CBR) characteristics.

Organic soils

The organic soil sample was collected at a depth of 0.5–1.0 m below the present ground surface from a local source in Pasir Gudang, Johor, Malaysia. The soil sample was then transferred to the laboratory and oven-dried at 105°C for about 48 h before laboratory testing is conducted.

Concrete sludge of batching plant (CSBP)

Concrete sludge of batching plant is a fresh concrete waste that returned to the batching plants and was collected from Lafarge concrete batching plant which located at Pengerang, Kota Tinggi Johor. The CBSP was transported to the laboratory and oven-dried at 105°C for about 48 h. Then, the dry CSBP was manually crushed with a rubber hammer and sieved through a 0.475 mm sieve (in powder form) as in Figure 1.

FIGURE 1. Physical appearance of CSBP after sieved

General laboratory testing method

In general, multiple laboratory experiments were conducted in this study to assess the efficiency of CSBP in improving the performance of local problematic organic soil in Pasir Gudang, Johor. To identify and categorize the soil characteristic, the particle size distribution (PSD), Atterberg limit test, and specific gravity test were used. The materials were then subjected to a standard proctor compaction test to establish their optimum moisture content (OMC) and maximum dry density (MDD) values. Finally, a California carrying ratio (CBR) test was performed to assess the soil's load bearing capability in an unsoaked condition. All tests were carried out in accordance with the British standard BS 1377--2:1990 (British Standards Institution [BSI], 2004).

Results and discussion

Index properties of soil

Table 1 summarizes the index properties of organic soil that were used in this investigation to identify and classify soil characteristics. Atterberg limit test is conducted to determine the plasticity index (PI) value based on plastic limit (PL) and liquid limit (LL) result data. Table 1 shows that the LL and the PL of the soil used throughout this study are 69 and 62%, respectively. Hence, the PI data is verified as 7%. Based on the plasticity chart for soil classification given in Figure 2, the soil was classified as an organic of high plasticity (OH). The specific gravity of soil used is 2.3, which was classified as organic soil as outlined in the British standard BS 1377-2:1990.

TABLE 1. Index properties of organic soils

Index properties	Value
Liquid limit (LL) [%]	69.00
Plastic limit (PL) [%]	62.00
Plasticity index (PI) [%]	7.00
Specific gravity	2.30

Compaction characteristic

The optimum moisture content (OMC) and maximum dry density (MDD) relationships for the various percentages of CSBP (0, 5, 10, and 15%) were determined using the standard proctor compaction test. As in Figure 3, it shows the results of the standard proctor compaction test comparing dry density and moisture content at various percentages of CSBP. While data shows that the original organic soil sample has OMC value of 38.05%, while the OMC value of stabilized soil with 5, 10, and 15% of CSBP are 36.94, 35.33, and 31.58%, respectively (Table 2). However, the MDD value of the original organic soil sample is 1.12 $Mg \cdot m^{-3}$ while for stabilized soil with 5, 10, and 15% of CSBP are 1.13, 1.15, and 1.22 $Mg \cdot m^{-3}$, respectively. The OMC value decreases with the addition of CSBP, whereas the MDD value increases. However, the increases of MDD values does not show such a significant difference.

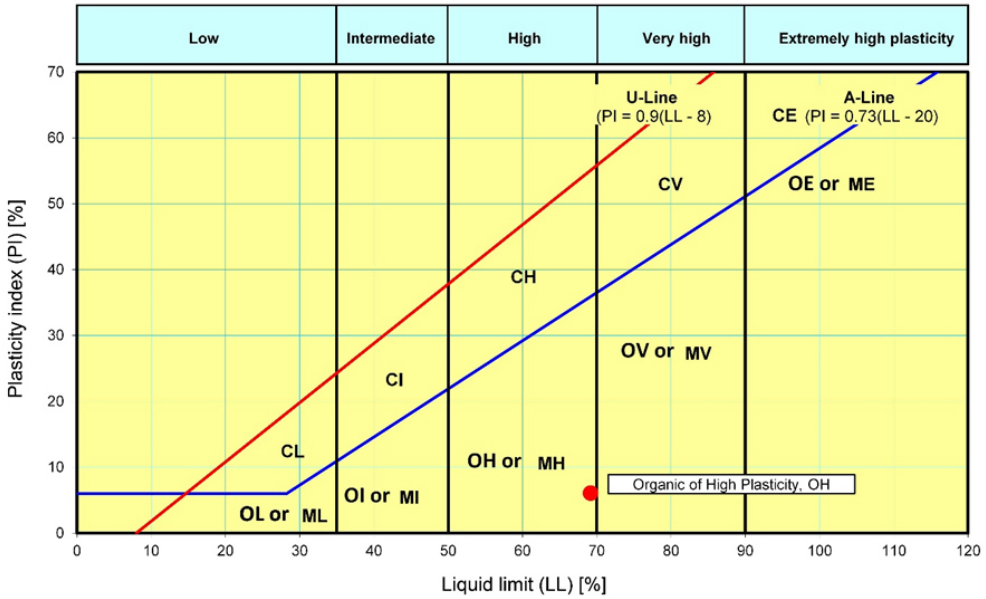

FIGURE 2. Plasticity chart for the soil classification

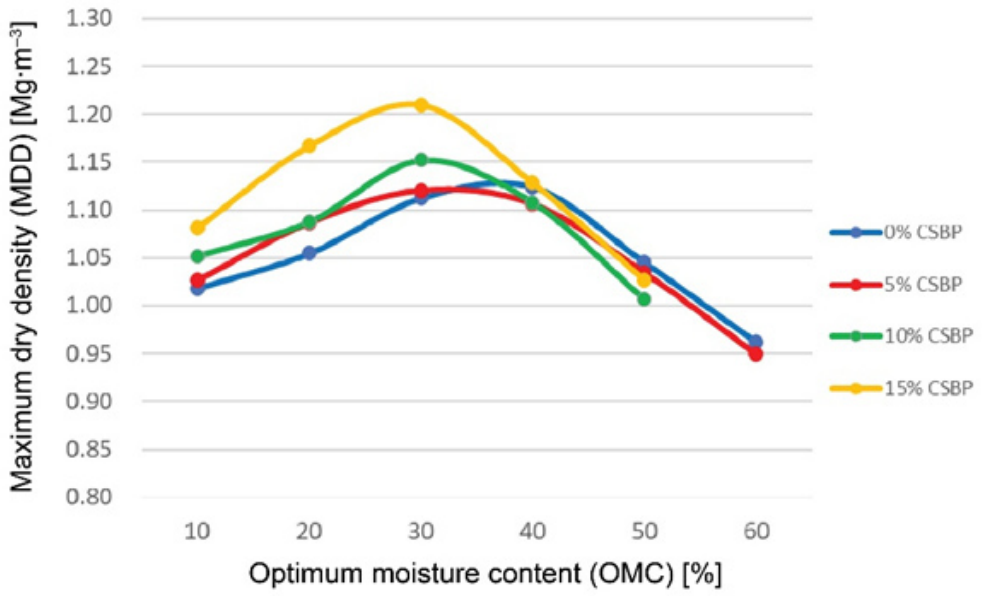

FIGURE 3. Optimum moisture content (OMC) and maximum dry density (MDD) relationship compaction curve

TABLE 2. Optimum moisture content (OMC) and maximum dry density (MDD) values of compaction test

CSBP ratio [%]	OMC value [%]	MDD value [$Mg \cdot m^{-3}$]
0	38.05	1.12
5	36.94	1.13
10	35.33	1.15
15	31.58	1.22

California bearing ratio (CBR) characteristics

The CBR characteristic was used to analyse the effect of CSBP on stabilised soil strength. The CBR test was carried out in unsoaked conditions by measuring the force required to penetrate a soil sample with a plunger in order to estimate the soil's load bearing capability. The CBR values for the load that corresponds to the 2.5 mm and 5.0 mm penetration are recorded as summarized in Table 3, and generally the greater value has been accepted as CBR value. Thus, according to the findings the CBR values at 5.0 mm penetration are found to be greater than those at 2.5 mm penetration.

Figure 4 shows the relationship between load and penetration at various CSBP percentages. From the plotted graph, the load and penetration curve show that the CBR value at 5.0 mm has increased by 4.8, 7.4, 13.2, and 20.7% with the addition in CSBP percentages of 0, 5, 10, and 15%, respectively. According to the data obtained, the subgrade category, SG for organic soil change from SG1 to SG2 and SG3 due to increases amount percentage of CSBP (Malaysia Public Work Department, 2008). Because of the cement content in the sludge, which is made of lime, silica, and alumina, which gives specific features in soil stabilisation, it can be deduced that the strength of stabilised soil increased with the elevation percentage of CSBP (Shalabi et al., 2019). Furthermore, Akbar et al. (2020) has concluded that concrete sludge waste has the potential to modify the engineering behaviour of high plasticity soil and significantly increase the CBR value of stabilised soil to meet the requirement for road-base material.

TABLE 3. California bearing ratio (CBR) value at 2.5 mm and 5.0 mm penetration

CSBP ratio [%]	CBR at 2.5 mm penetration [%]	CBR at 5.0 mm penetration [%]
0	3	4.8
5	4.3	7.4
10	8.4	13.2
15	15.6	20.7

Conclusions

This study offers the preliminary results of using concrete sludge of batching plant (CSBP) for soil stabilization and modification of an organic soil sample. An organic soil sample used can be graded as an organic of high plasticity (OH). Thus, soil improvement needs to meet specific requirement in subgrade pavement design in standard specification for road work of Malaysia Public Work Department (2008). Compacted soil samples with various CSBP percentages were tested to see if CSBP has the ability to change the engineering behavior of organic soil and make it suitable for subgrade.

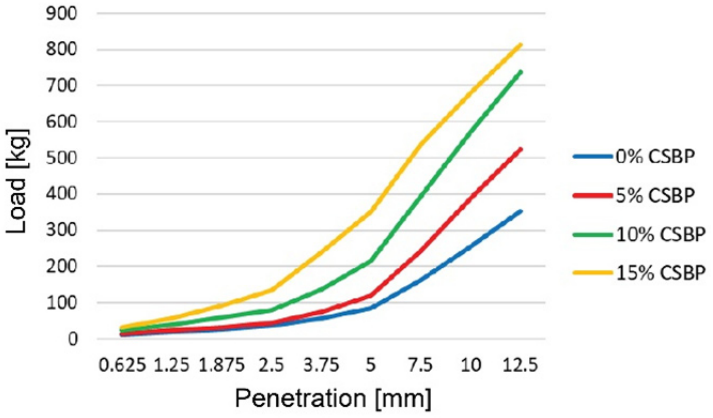

FIGURE 4. Load and penetration curve at different concrete sludge of batching plant (CSBP) percentages

With the growth in CSBP percentages from 0 to 15%, the CBR value increases considerably from 4.8 to 20.7%. The CBR values have revealed a possible increasing trend of strength of stabilised soil samples as the percentage of CSBP has increased. In this study, CSBP has shown its potential as a stabilization material in increasing CBR value for subgrade pavement. Subsequently, the utilize of CSBP in organic soil stabilization is an inventive thought due to a couple of reasons, counting being able to retain water, and sustainable practice where it is great for the environment impacts as well as to diminish costs at batching plant. Other than that, utilize of CSBP will advance the natural motivating forces to supply a way to reuse huge amounts of waste materials for highway engineering resolutions.

Acknowledgements

The authors are grateful to Universiti Teknologi MARA, Cawangan Johor for providing research funding through Geran Bestari Phase 1/2020 and Lafarge Concrete Industries Sdn Bhd, Malaysia, for providing the materials for the study.

References

Akbar, N.A., Ismail, T.N.H.T., Adnan, S.H., Yusop, F.M., Khosran, H. & Saji, N. (2020). Improvement in CBR Value of Sub-Base Soil using Concrete Slush Waste (CSW). *Journal of Advanced Industrial Technology and Application*, *1*(1), 48-56.

Anupam, A.K., Kumar, P., Ransinchung, G.D. & Shah, Y.U. (2017). Study on performance and efficacy of industrial waste materials in road construction: fly ash and bagasse ash. *Airfield and Highway Pavements*, *2017*, *45-56*.

Arshad, H., Qasim, M., Thaheem, M.J. & Gabriel, H.F. (2017). Quantification of material wastage in construction industry of Pakistan: An analytical relationship between building types and waste generation. *Journal of Construction in Developing Countries*, *22*(2), 19-34.

Arunvivek, G.K., Maheswaran, G., Senthil Kumar, S., Senthilkumar, M. & Bragadeeswaran, T. (2015). Experimental study on influence of recycled fresh concrete waste coarse aggregate on properties of concrete. *International*

Journal of Applied Engineering Research, *10*(11), 29809-29815.

Bandara, N., Binoy, T.H., Aboujrad, H.S. & Sato, J. (2015). Pavement subgrade stabilization using recycled materials. *Airfield and Highway Pavements*, *2015*, 605-616.

British Standards Institution [BSI] (2004). *Methods of test for soils for civil engineering purposes*. *Part 2: Classification tests* (BS 1377-2:1990). Chiswick: British Standards Institution.

Chattaraj, R. & Sengupta, A. (2017). Dynamic properties of fly ash. *Journal of Materials in Civil Engineering*, *29*(1), 04016190. https://doi.org/10.1061/(ASCE)MT.1943-5533.0001712

Kazaz, A. & Ulubeyli, S. (2016). Current methods for the utilization of the fresh concrete waste returned to batching plants. *Procedia Engineering*, *161*, 42-46.

Kumar, P.G. & Harika, S. (2021). Stabilization of expansive subgrade soil by using fly ash. *Materials Today: Proceedings*, *45*, 6558-6562.

Malaysia Public Work Department (2008). *Standard Specification for Road Works*. *Section 4. Flexible Pavement*. Kuala Lumpur: Kerja Raya Malaysia.

Nawi, N.M., Mat Yusof, D.A., Sharipudin, S.S., Mohd Halim, N.F., Mohamad, N.M. & Shafie, M.Z. (2019). The utilization of concrete sludge of batching plant (CSBP) as a partial cement replacement in concrete. *International Journal of Engineering & Technology*, *8*(3), 257-260.

Nath, B.D., Molla, M., Ali, K. & Sarkar, G. (2017). Study on Strength Behavior of Organic Soil Stabilized with Fly Ash. *International Scholarly Research Notices*, *2017*, 5786541. https://doi.org/10.1155/2017/5786541

Shalabi, F.I., Mazher, J., Khan, K., Alsuliman, M., Almustafa, I., Mahmoud, W. & Alomran, N. (2019). Cement-stabilized waste sand as sustainable construction materials for foundations and highway roads. *Materials*, *12*(4), 600. https://doi.org/10.3390/ma12040600

Tavakol, M., Hossain, M. & Tucker-Kulesza, S.E. (2019). Subgrade soil stabilization using low-quality recycled concrete aggregate. In *Geo-Congress 2019: Geotechnical Materials, Modeling, and Testing* (pp. 235-244). Reston, VA: American Society of Civil Engineers.

Tewar, B., Shah, P.M. & Patel, P.B. (2017). Effect of Partial Replacement of Sand with Wastage of Manufactured AAC Block in Concrete. *Materials Today: Proceedings*, *4*(9), 9817--9821.

Thorneycroft, J., Orr, J., Savoikar, P. & Ball, R.J. (2018). Performance of structural concrete with recycled plastic waste as a partial replacement for sand. *Construction and Building Materials*, *161*, 63-69.

Vieira, L.D.B.P. & Figueiredo, A.D. de (2016). Evaluation of concrete recycling system efficiency for ready-mix concrete plants. *Waste Management*, *56*, 337-351.

Ward, T., Taylor, A. & Grubbs, J. (2017). A comparison of subgrade improvement methods. *International Conference on Highway Pavements and Airfield Technology*, *2017*, 173-184.

Summary

Study on potential of soil stabilization using concrete sludge of batching plant (CSBP). More than 8 t of fresh concrete waste may be created and returned to the batching plants throughout Malaysia, where it will degrade into concrete sludge. Most batching plants will dump their concrete sludge on the ground or at a landfill which is not eco-friendly at all. Consequently, this study is to investigate the potential of concrete sludge of batching plant (CSBP) to be used as the stabilized material for organic soil which indirectly can help to recycle CSBP from end up at the landfill. The Atterberg limit test was conducted to identify the characteristic of soil used in this study. Four different percentages of CSBP were used which are 0, 5, 10 and 15%. Then, the standard Proctor test and California bearing ratio test were performed, and it shows that the CBR value remarkably increases from 4.8 to 20.7%, with the rise of CSBP percentages from 0 to 15%. The finding shows that CSBP can be used as the potential material to

enhance the trend of strength value of CBR. Thus, using CSBP as a stabilized material for organic soil would alleviate the problem of overflowing landfills with concrete sludge and encourage a more sustainable approach in the construction industry.

Authors' address:
Nur Muizzah Nawi – corresponding author
Universiti Teknologi MARA
College of Engineering
School of Civil Engineering
Cawangan Johor, Pasir Gudang Campus
81750 Masai, Johor
Malaysia
e-mail: nmuizzah@uitm.edu.my

Doris Asmani Mat Yusof
Universiti Teknologi MARA
College of Engineering
School of Civil Engineering
Cawangan Johor, Pasir Gudang Campus
81750 Masai, Johor
Malaysia
e-mail: dorisasmani@uitm.edu.my

Siti Shahidah Sharipudin
Universiti Teknologi MARA
College of Engineering
School of Civil Engineering
Cawangan Johor, Pasir Gudang Campus
81750 Masai, Johor
Malaysia
e-mail: shahidahs@uitm.edu.my

Nora Farina Mohd Halim
Universiti Teknologi MARA
College of Engineering
School of Civil Engineering
Cawangan Johor, Pasir Gudang Campus
81750 Masai, Johor
Malaysia
e-mail: norafarina@uitm.edu.my

Nor Mayuze Mohamad
Universiti Teknologi MARA
College of Engineering
School of Civil Engineering
Cawangan Johor, Pasir Gudang Campus
81750 Masai, Johor
Malaysia
e-mail: norma7544@uitm.edu.my

Scientific Review – Engineering and Environmental Sciences (2021), 30 (4), 561–572
Sci. Rev. Eng. Env. Sci. (2021), 30 (4)
Przegląd Naukowy – Inżynieria i Kształtowanie Środowiska (2021), 30 (4), 561–572
Prz. Nauk. Inż. Kszt. Środ. (2021), 30 (4)
https://srees.sggw.edu.pl
DOI 10.22630/PNIKS.2021.30.4.47

BAKHTIAR[1], SUKOSO[2], SAIDA[1]

[1] Universitas Muslim Indonesia, Faculty of Agriculture
[2] Universitas Brawijaya, Faculty of Fisheries and Marine Science

Use of sulfate-reducing bacteria and different organic fertilizer for bioremediation of ex-nickel mining soils

Key words: organic matter, pH, sulfate, nickel

Introduction

Indonesia plays a very important role in the world coal and mineral industry. In 2019, Indonesia was ranked first as a nickel exporting country with a total share of around 37%. While mining and mineral extraction contributed significantly to the development and national economies, they also caused serious impact on environmental degradation. Mineral extraction and its resultant need for the disposal of wastes, slurry, and water can result in a negative impact on the environmental (Jain, Cui & Domen, 2016). The increasing number of businesses in the mining sector led to the problem of post-mining critical lands. Mining often causes exposure to sulfur-containing minerals such as pyrite, pyrotite, chalkopyrite, arsenopyrite, and cobaltite. Ex-mining land often exhibits a low pH character. Decreasing pH will increase the solubility of minerals in soil and water. The high content of sulfates and the solubility of heavy metals in the soil are the main limiting factors for plants grown on soils that exhibit low or acidic pH (Sánchez-Andrea, Sanz, Bymans & Stams, 2014; Pistelli et al., 2017).

One of the nickel mining areas in Indonesia is located in the Sorowako area, South Sulawesi. The nickel mining area in this area is approximately 118,300 ha; the area that has been managed only reached 10,000 ha. Nickel reserves amounted to 107.7 million t of ore, with an average grade of 1.83% Ni. With a production capacity of 200 million t of nickel per year, these reserves

will be mined for 18.9 years. The high concentration of heavy metal (nickel) in the ex-mining area can cause high levels of poisoning, which can endanger all aspects of life. Another study reported that in the coastal waters of the nickel mining location in Pomala, Kolaka Regency, Southeast Sulawesi, heavy metal pollution occurs (Fe, Cr, Ni, Pb, and Zn), which exceeded the threshold for assimilation capacity waters (Syahrir, Yaqin, Landu & Tambaru, 2019).

Industrial development has led to generation of large volumes of wastewater containing heavy metals, which need to be removed before the wastewater is released into the environment. This is of great environmental concern as some heavy metals are highly toxic. Chemical and electrochemical methods are traditionally applied to treat this type of wastewater. These conventional methods have several shortcomings, such as secondary pollution and cost (Xu & Chen, 2020). Efforts to improve the quality of ex-mining soil can be carried out by using a bioremediation process using micro-organisms. Within a number of possibilities, biological treatment applying SRB is an attractive option to treat acid mine drainage and to recover metals. The SRB may reduce heavy metal in soil and water such as sulphate, cadmium copper, nickel, ferro, plumbum, zinc, and arsenic (Kiran, Pakshirajan & Das, 2016; Kiran, Pakshirajan & Das, 2017; Serrano & Eduardo, 2017; Zhang, He, Zhao, Kou & Huang, 2020). One type of microorganism that is commonly used is SRB (Li et al., 2018). These bacteria can be used for treating mining wastewaters and recovering metals in several bioreactor configurations (Papirio, Villa-Gomez, Esposito, Pirozzi & Lens, 2013). In the process of reducing the sulfate ion, in addition to producing hydrogen sulfide (H_2S), a hydroxyl ion (OH^-) is also released. The more sulfate ions that are reduced, the more hydroxyl ions are produced, so that the pH increases. The resulting sulfides will react with dissolved metals to form metal sulfides which precipitate, so that their toxicity is reduced. SRB that grow in anoxic sediments or the bottom of the marine sediment, in this case the pond bottom soil, may exhibit different characteristics and characteristics from SRB that grow in normal environments. Thus, these bacteria exhibit the potential to be utilized in overcoming unfavorable conditions in ex-mining soil, be it for the management of ex-mining soil in relation to plants or in relation to other organisms, namely by reducing the solubility of sulfate ions, hydrogen ions, and metal ions (Gavrilescu, 2004).

The application of SRB plays an important role in reducing pollutant content in the environment characterized by changes in pH and C-organic. The SRB is able to neutralize the acidity of water bodies close to neutral (pH 6–7) and reduce the content of dissolved heavy metals in the waters. Other studies showed that this option is effective for the precipitation of the dissolved metals (copper and iron), for the reduction and removal of sulfates, and even for the alkalizing of the waters. The SRB's ability to remove up to 9,000 ppm of sulfate ion efficiently, to grow in the presence of up to 100 ppm of copper and 30 ppm of iron, and alkalize the medium makes it a potential bioremediation agent (Garciá,

Moreno, Ballaster, Blázquez & González, 2001). The SRB facilitate the conversion of sulfate to sulfide with the sulfides reacting with heavy metals to precipitate toxic metals as metal sulfide. These metal sulfides are stable and can easily be removed from acid mine tailings waste (Cohen, 2006). This process facilitates the removal of toxic metals from tailing waste by SRB. Research conducted in ex-coal mining showed that SRB was able to reduce 84.25% sulfate content in 20 days. In consequence, the soil pH was increased from 4.15 to 6.66 during the process. However, no research exists on the application of the SRB carried out by the former nickel mining land. The purpose of this study was to examine the ability of SRB in several organic matters to reduce sulfate and nickel ions, and to increase pH of soil from nickel in mining areas.

Material and methods

This study used the bacteria consortium collection of the Soil Laboratory of the Faculty of Agriculture, Universitas Muslim Indonesia. Those were previously isolated from two cultivating pond of milkfish in the Kuri area of Maros Regency, South Sulawesi, Indonesia. The soil samples were collected from ex-mining areas of the Vale Indonesia Enterprise in Sorowako, South Sulawesi, Indonesia. Those were mixed with organic fertilizer, generated from sugarcane sludge, cow manure and Quickstick leaves. These three types of fertilizers were selected because of their high nutrient content for the soil remediation process (Juradi, Tando & Saida, 2020). Other materials used are chemicals used in the propagation of SRB isolates, analysis of sulfate levels, and heavy metal analysis of nickel.

Propagation of sulfate-reducing bacteria

The SRB isolates were cultured on liquid media, namely Postgate B media. The composition of the per one-liter media is sodium lactate 3.5 g, $MgSO_4 \cdot 7H_2O$ 2.0 g, NH_4Cl 0.2 g, KH_2PO_4 0.5 g, $CaSO_4$ 0.2 g, $FeSO_4 \cdot 7H_2O$ 0.5 g, yeast extract 1, 0 g, 0.1 g ascorbic acid, 0.1N NaOH, and 0.1N HCl to determine the pH of the media. The screw tube contains a liquid medium, inoculated with SRB. The media were incubated in an incubator at 35°C. The multiplication of the SRB isolates was successful when the media forming a black color. This black color is an indicator of sulfate reduction in the media.

Preparation of planting media

Examining soil samples obtained were air-dried and then cleaned of plant debris, stones, and gravel; then, they were sieved with a sieve hole diameter of 2 mm. After that, the soil sample was autoclaved at a temperature of 121°C, 1 atm pressure for 20 min. Furthermore, the 5 kg soil samples were put into a pot and mixed evenly with organic fertilizers. The doses of the organic fertilizer were 50 and 100 g per pot. The mixtures were stagnated with the water as high as 10 cm. Then, the SRB isolate solution was poured in the treatment mixture.

Sulfate content analysis

Sulfate contents were measured on 0, 10, 20, and 30 days after treatment (DAT). The mixture of soil, organic fertilizer, and SRB were extracted and filtered. The 5 ml results of the filtering were taken and then put into a test tube. After that, 1 ml of tween and $BaCl_2$ was added. Next, it was homogenized by shaking and let stand for 15 min. After that, the sample was measured with a spectrophotometer at a wavelength of 494 nm. The absorbance measurement results of the sample were adjusted to the standard curve for sulfate. From the standard curve, the sulfate ion concentration contained in the sample is obtained. Each solution in the test tube was stirred slowly before measuring.

Analysis of nickel heavy metal content in the planting medium was carried out before application of sulfate-reducing bacteria and after application. Then, an average of 5 g of the sample was taken and stored in a tube with a capacity of 100 and 20 ml of 1M HCl was added and shaken until blended. Furthermore, the samples were stored at room temperature for 24 h.

Samples were filtered using Whatman filter paper 42. The filtered sample is taken as much as 5 ml and then put into a 50 ml volumetric tube, and then 45 ml of distilled water was added. Next, 2 ml was taken and dissolved in 18 ml 0.1M HCl in a 20 ml volumetric tube. Then, the sample was analyzed to determine the concentration of heavy metal Ni, using a Perkin Elmer Analyst 300 Atomic Absorption Spectrometer. The nickel concentration was measured merely on the 30 DAT.

Experiment design and data analysis

This research was arranged based on block design. It consists of three factors, treatment of SRB inoculum, the type, and dose of organic matter. The first factor of the SRB inoculum consists of no SRB inoculum (control) and the SRB inoculum (treatment). The two factors of organic matter were sugarcane sludge, manure, and Quickstick leaves, each with doses of 50 and 100 g. The combination of these three factors obtained 12 treatments. Each treatment was repeated three times. By adopting a general linear model repeated measures analysis of variance (ANOVA), we tested the sulfate concentration and pH level differences among the treatments over time, with SRB treatment, fertilizer type, and fertilizer doses as between--subject factors and measurement time as a within-subject factor and with three replicates. Meanwhile, the concentration of nickel was analyzed by multivariate ANOVA. The tests were performed using SPSS® version 25 software (SPSS Inc. Chicago, IL, US), and the results of the F-statistic test were considered significant when $p < 0.05$.

Results and discussion

This study indicated that the effect of SRB treatment was significant on the decrease in the concentration of sulfate ($F = 438.3$, $p < 0.001$), nickel ($F = = 1026.6$, $p < 0.001$), and change in pH level ($F = 4.7$, $p < 0.05$). The effect of fertilizer type was also significant for the three dependent variables. The fertilizer dose resulted in a significant effect on

reducing sulfate ($F = 38.7$, $p < 0.001$) and nickel ($F = 32.1$, $p < 0.001$) but not a significant change in the pH level ($p > 0.05$). Sulfate concentrations and pH differed significantly between test times, indicating a change over time. The interaction between factors did not significantly affect the dependent variables, except of interaction between SRB treatment and fertilizer dose for nickel remediation (Table 1).

TABLE 1. Summary of F-statistic followed by probability of the effect of time, the SRB inundation, fertilizer type, and fertilizer dose

Parameter	Sulfate	pH	Nickel
Time (t)	438.3***	58.6***	not performed
SRB treatment (b)	102.8***	4.7*	1 026.6***
Fertilizer type (f)	44.4***	38.7***	3.8*
Fertilizer doses (c)	38.7***	4.1^{ns}	32.1***
Interaction (b × f)	1.3^{ns}	0.2^{ns}	84.2***
Interaction (b × c)	1.2^{ns}	0.4^{ns}	3.6^{ns}
Interaction (f × c)	1.7^{ns}	1.6^{ns}	0.0^{ns}
Interaction (b × f × c)	2.7^{ns}	0.9^{ns}	0.7^{ns}

Note: ns = not significant; *$p < 0.05$; ***$p < 0.001$; data of sulfate and pH means were analyzed by repeated measures ANOVA; while nickel was measured by multivariate ANOVA

In general, soils treated with organic matter and SRB contained lower levels of sulfate than those treated with organic matter without BPS. The effect of SRB treatment was significant in reducing sulfate levels in all organic fertilizer treatments. Among the three types of organic fertilizers used, manure exhibited a more effective reduction rate. At 10 DAT, the sulfate concentration decreased from 2,530 ppm to 1,443 ppm in treatment of SRB and manure with dose of 50 g and 1,363 ppm with that of 100 g. At the end of the observation (30 DAT), those were decreased to 1,217 ppm in the treatment of SRB and manure with dose of 50 g and 1,167 ppm with that of 100 g. Meanwhile, the lowest effect of the SRB treatment was found in that with sugarcane sludge fertilizer application. At 10 DAT, the sulfate concentration decreased from 2,530 ppm to 1,553 ppm in treatment of SRB and manure with dose of 50 g and 1,510 ppm with that of 100 g. At the end of the observation (30 DAT), those were decreased to 1,273 ppm in treatment of SRB and manure with either 50 or 100 g doses (Fig. 1).

The results of the observations indicated that the pH concentration of ex-mining soil increased from the initial pH of 5.52. The increase in pH occurred in all treatments, both those treat with SRB and control. Ex-mining soil pH increased toward neutral condition. In addition, at 10 DAT, the average pH in all treatments exceeds 7 and then decreases toward an average approaching 7. Among the three types of organic fertilizers used, Quickstick exhibits the more effective reduction rate. At 10 DAT, pH increased in SRB treatment to 7.06 at a concentration of 50 g and 7.01 at a concentration of 50 g. At the end of the observation (30 DAT), the pH became 6.67 at a concentration of 50 g and 6.82 at a concentration of 50 g. Meanwhile, the organic fertilizer application that generates the lowest pH is sugarcane sludge. At 10 DAT, pH in

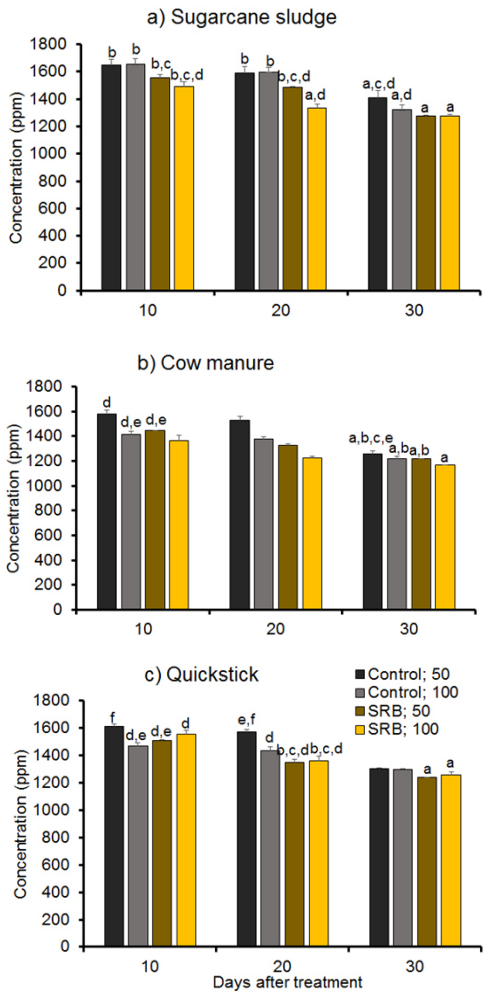

FIGURE 1. Changes in sulfate concentration in ex-nickel mining soil treated with SRB with the addition of sugarcane sludge (a), cow manure (b) and Quickstick fertilizers (c) from 10 DAT to 30 DAT. Error bars followed by different alphabet mean that the averages are significantly different

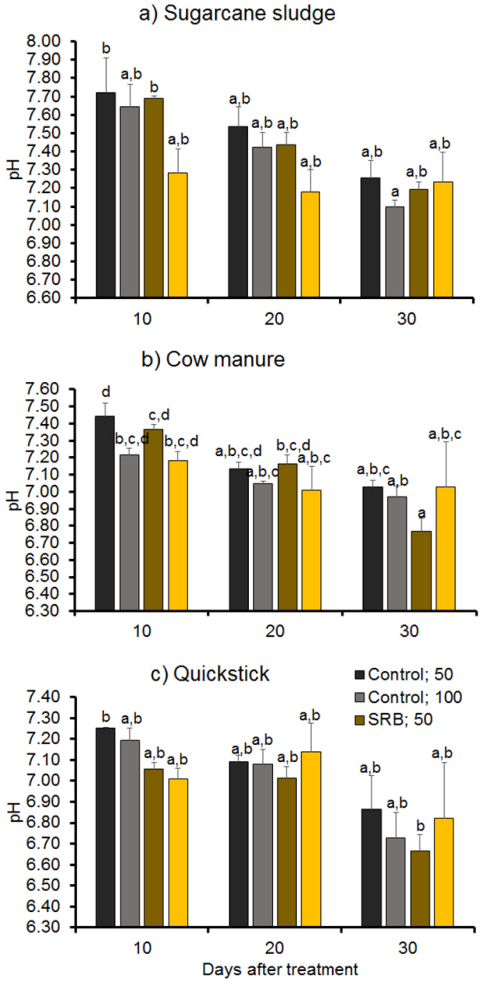

FIGURE 2. Changes in pH level in ex-nickel mining soil treated with SRB with the addition of sugarcane sludge (a), cow manure (b) and Quickstick fertilizers (c) from 10 to 30 DAT. Error bars followed by different alphabet mean that the averages are significantly different

creased in SRB treatment by 7.69 at a concentration of 50 g and 7.28 at a concentration of 50 g. At the end of the observation (30 DAT), the pH became 7.19 at a concentration of 50 g and 7.23 at a concentration of 50 g (Fig. 2).

Treatment with SRB exhibits a very significant effect on nickel concentration. The initial nickel concentration of 4,720 ppm decreased to an average of below 3,000 ppm in the treatment of all types of fertilizers added by SRB. The best decrease occurred in the treatment

of SRB with manure fertilizer. The nickel concentration decreased from origin concentration to 1,950 ppm in the treatment of SRB and manure with dose of 50 g and 1,690 ppm with that of 100 g. The lowest reduction was found in the treatment of SRB with Quickstick fertilizer. The nickel concentration decreased from the origin concentration to 2,560 ppm in treatment of SRB and manure with dose of 50 g and 2,370 ppm with that of 100 g (Fig. 3).

The ex-mining soil is characterized by its high acidity and lower fertility. Degradation of chemical properties such as acid soil and high nickel content are the factors that limit the level of soil fertility as a planting medium. The addition of fertilizers in the bioremediation process of ex-mining soil plays an important role in increasing the input of organic matter. Organic matter increases the activity of microorganisms for nitrogen fixation and transfer of certain nutrients such as nitrogen, phosphor and sulphure. The role of organic matter on soil chemical properties is to increase cation exchange capacity so that it may affect nutrient uptake by plants. Cow manure"s ability to reduce sulfate and nickel may be due to the high levels of nitrogen and carbon in the material (Halifah, Soelistyono & Santoso, 2014). The availability of nitrogen and carbon is very supportive to increase the activity of microorganisms including SRB in reducing sulfate and nickel. However, in increasing the pH, the ability of sugarcane sludge fertilizer was better than the other two fertilizers. This is probably because sugarcane sludge has high levels of phosphorus and calcium, so it has a more neutral pH. In addition, the process of decomposition of organic matter in soils made of high organic matter, such as with cow manure, is always found in acidic soils with low pH, this is due to the decomposition process of organic matter which in the process will expel and remove elements of calcium from the soil (Palupi, 2015).

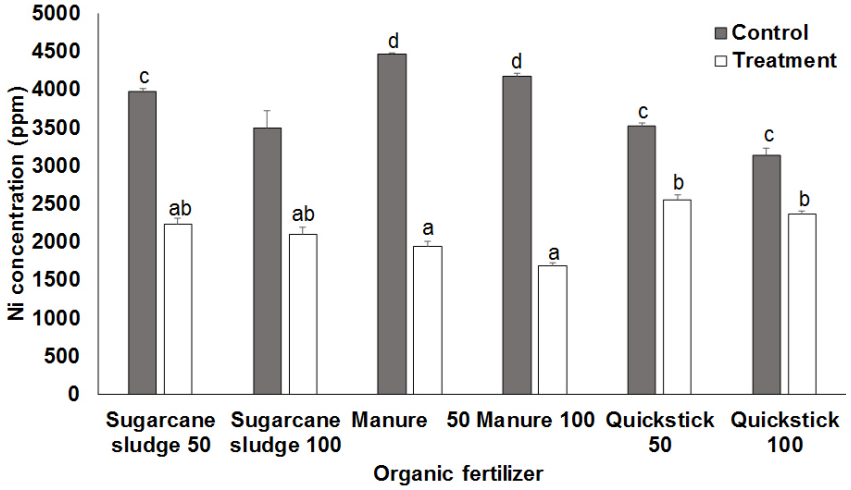

FIGURE 3. Effect of fertilizer application and the addition of SRB on nickel concentration. Error bars followed by different alphabet mean that the averages are significantly different

According to Ansari and Malik (2010), the high heavy metal content in soil like zinc, copper, nickel, lead, chromium, and cadmium, low pH, and low nutrients are factors that limit plant growth. During extreme conditions, mining activities destruct soil quality such as poor nutrients, toxic due to heavy metal, physical properties alteration. Therefore, to improve the quality, new technology is required such as bioreactor (Dikinya & Areola, 2010; Papirio et al., 2013), bed reactor (Liu, Liu, Zhou & He, 2017), or semi-continuous stirred tank reactors (Kieu, Müller & Horn, 2011).

Soil pH value

In this study, the initial pH of ex-mining soil was acidic; however, the level of acidity increased after being inundated with water and organic matter. Inundation with water caused the release of hydroxyl ions which bind H^+ ions. In addition, the increase in pH to neutral occurs because organic matter has a buffering capacity so that it can increase or decrease the pH of its environment. The activity of SRB greatly increases the effluent pH. Even at an influent pH of 3.0, 60.8% of sulfate, 41.3% of COD and 91.2% of heavy metals could be removed, and the effluent quality can meet the national discharge standard (Liu et al., 2017). In the natural environment, the pH of the soil has an enormous influence on soil biogeochemical processes. Soil pH is, therefore, described as the "master soil variable" that influences myriads of soil biological, chemical, and physical properties and processes that affect plant growth and biomass yield (Neina, 2019).

An increase in pH may occur due to the presence and activity of SRB. Therefore, SRB is often used as bioremediation of ex-acid mining land because it exhibits the ability to increase soil pH (Winch, Mills, Kostka, Fortin & Lean, 2009). The results of research by (Sandrawati, Suryatmana, Putra & Kamaluddin, 2019) showed an increase in pH after inundation, provision of organic matter and SRB. The initial pH, which ranges from 3.6–5.2, increased to 6.6–8.1. SRB utilize organic material as a source of electron donors in reducing sulfate to sulfide and produce bicarbonate so that the soil pH increased from 4.15 to 6.66 during the process (Widyati, 2007). Bioremediation was rapid once the initial pH increased to > 4.5, as SRB's are known to perform better in more neutral environments (Koschorreck, 2008).

Sulfate concentration

The sulfate content in the ex-mining area is reduced after 30 days of inundation. Decreasing sulfate content occurred in relation with increasing soil pH levels. Next, the sulfate reduction process produced metal sulfide deposits and increased the alkalinity. The increase in pH occurred because SRB used sulfate as an electron acceptor and carbon of organic matter as an electron donor by producing hydrogen sulfide. Meanwhile, SRB uses an electron donor H_2 and a C (CO_2) source, which can be obtained from organic materials. Hydrogen sulfide immediately binds with metal to form metal sulfide, which is insoluble so that metal availability decreases (Widyati, 2007). The type of organic material affects the rate of sulfate reduction because each

organic material exhibits a different amount of carbon (Sandrawati et al., 2019). The SRB is more efficient than chemical reduction due to saturation and addition of organic matter. However, the addition of organic material and saturation is still required because the sulfate reduction reaction by SRB to sulfide can be increased by adding moisture content and addition of soil organic matter (Cao et al., 2020).

The sulfate content of the soil soaked with organic matter without giving bacteria showed higher sulfate levels (0.141–0.122) than the organic matter added with SRB (0.127–0.117). This is in accordance with previous study whom stated that the addition of SRB can increase the rate of reduction of sulfate to hydrogen sulfide (Sandrawati et al., 2019). The more the amount of SRB in the soil, the lower the sulfate concentration, even reducing heavy metals such as Fe in the soil (Reyes et al., 2017). The problems faced by ex-nickel mining areas are the acidic soil pH concentration, high Ni content, and low phosphate availability. If ex-mining land is developed for agricultural activities, it becomes a limiting factor and possibly an obstacle in the production process. Furthermore, plants that live in ex-mining areas are deficient in nutrients such as K, Ca, Fe, Cu, and Mn. In addition, nickel mining soils are formed from basic or ultra-alkaline igneous rock base materials which contain heavy metals that reach toxic levels in plants, including Ni and Cr. Meanwhile, Pb and Cd metals are in relatively safe concentrations (Singh, Upadhyay, Pathak & Gupta, 2011). The nickel content of ex-mining soil, which was given organic matter and SRB accompanied by water inundation for 30 days, showed a lower Ni content than the application of organic matter to the ex-mining soil without being given bacteria. Providing organic materials such as compost and manure is an alternative solution for the supporting of life in the soil to reduce nickel levels in the soil. The nickel content was provided organic matter and soaked for 30 days and was still high, namely 3.14–4.47%, while the nickel content treated with organic matter and the addition of SRB ranged from 1.69–2.56%. Land with a nickel content between 3–5% are unable to be used as a medium for growing plants. The level of nickel content in ex-mining land became lower after treatment with SBR and manure. This occurred because it was suspected that the amount of C-organic from manure was very high so the sulfate reduction process carried out by SRB was more optimal. In addition, the rate of nickel reduction carried out by sulfate bacteria occurs due to water immersing. When inundation is carried out, O_2 deficiency occurs so that the SRB population increases thousands of times in approximately two weeks.

Conclusions

The results of this study indicate that the application of fertilizer and the addition of SRB exhibits an effect on reducing levels of sulfate and nickel. Among the three types of organic fertilizers, manure was effective to reduce of sulfate and nickel concentrations, while Quickstick fertilizer was the more effective to stabilize pH level. Fertilizer doses exhibited a significant effect on

decreasing sulfate and nickel concentrations, but it exhibited no significant effect on stabilizing pH levels. Thus, the application of manure fertilizer and the addition of SRB is recommended for bioremediation of sulfate and nickel from ex-mining soil.

Acknowledgements

We would like to thank the Ministry of Research Technology and Higher Education (KEMENRISTEKDIKTI) of Indonesia for funding this research in 2018.

References

Ansari, M.I. & Malik, A. (2010). Seasonal variation of different microorganisms with nickel and cadmium in the industrial wastewater and agricultural soils. *Environmental Monitoring and Assessment*, *167*(1), 151-163. https://doi.org/10.1007/s10661-009-1038-y

Cao, Q.Q., Liu, B., Ren, Z., Xiao, H.B., Cheng, J.M. & Xue, W.N. (2020). Temporal distribution characteristic and risk analysis of heavy metals in greenhouse vegetable soils. *Polish Journal of Environmental Studies*, *29*(3), 2071-2079. https://doi.org/10.15244/pjoes/111318

Cohen, R.R.H. (2006). Use of microbes for cost reduction of metal removal from metals and mining industry waste streams. *Journal of Cleaner Production*, *14*(12-13), 1146-1157. https://doi.org/10.1016/j.jclepro.2004.10.009

Dikinya, O. & Areola, O. (2010). Comparative analysis of heavy metal concentration in secondary treated wastewater irrigated soils cultivated by different crops. *International Journal of Environmental Science and Technology*, *7*(2), 337-346. https://doi.org/10.1007/BF03326143

García, C., Moreno, D.A., Ballester, A., Blázquez, M.L. & González, F. (2001). Bioremediation of an industrial acid mine water by metal-tolerant sulphate-reducing bacteria. *Minerals Engineering*, *14*(9), 997-1008. https://doi.org/10.1016/S0892-6875(01)00107-8

Gavrilescu, M. (2004). Removal of heavy metals from the environment by biosorption. *Engineering in Life Sciences*, *4*(3), 219-232. https://doi.org/10.1002/elsc.200420026

Halifah, U.N., Soelistyono, R. & Santoso, M. (2014). The effect of application of organic (Blotong) and anorganic fertilizer (Za) on plant shallot (*Allium ascalonicum* L.). *Jurnal Produksi Tanaman*, *2*(8), 665-672.

Jain, R.K., Cui, Z.C. & Domen, J.K. (2016). *Environmental impacts of mining and mineral processing: management, monitoring and auditing strategies*. Oxford: Butterworth-Heinemann. https://doi.org/10.1016/B978-0-12-804040-9.00004-8

Juradi, M.A., Tando, E. & Saida (2020). Innovation Technology of Blotong Compos to Repair Soil Fertility and Increasing Plant Sugarcane Productivity. *Jurnal Agrotek*, *4*(1), 24-36.

Kieu, H.T.Q., Müller, E. & Horn, H. (2011). Heavy metal removal in anaerobic semi-continuous stirred tank reactors by a consortium of sulfate-reducing bacteria. *Water Research*, *45*(13), 3863-3870. https://doi.org/10.1016/j.watres.2011.04.043.

Kiran, M.G., Pakshirajan, K. & Das, G. (2016). Heavy metal removal using sulfate-reducing biomass obtained from a lab-scale upflow anaerobic-packed bed reactor. *Journal of Environmental Engineering*, *142*(9), C4015010. https://doi.org/10.1061/(ASCE)EE.1943-7870.0001005

Kiran, M.G., Pakshirajan, K. & Das, G. (2017). Heavy metal removal from multicomponent system by sulfate reducing bacteria: Mechanism and cell surface characterization. *Journal of Hazardous Materials*, *324*, 62-70. https://doi.org/10.1016/j.jhazmat.2015.12.042

Koschorreck, M. (2008). Microbial sulphate reduction at a low pH. *Microbiology Ecology*, *64*(3), 329-342. https://doi.org/10.1111/j.1574-6941.2008.00482.x

Li, X., Lan, S.M., Zhu, Z.P., Zhang, C., Zeng, G.M., Liu, Y.G., Cao, W.C., Song, B., Yang, H., Wang, S.F. & Wu, S.H. (2018). The bioenergetics mechanisms and applications of sulfate-reducing bacteria in remediation of pollutants in drainage: A review. *Ecotoxicology and Environmental Safety*, *158*, 162-170. https://doi.org/10.1016/j.ecoenv.2018.04.025

Liu, H.H., Liu, G.H., Zhou, Y.F. & He, C. (2017). Spatial distribution and influence analysis of soil heavy metals in a hilly region of sichuan Basin. *Polish Journal of Environmental Studies*, *26*(2), 725-732. https://doi.org/10.15244/pjoes/65152

Neina, D. (2019). The role of soil pH in plant nutrition and soil remediation. *Applied and Environmental Soil Science*, *2019*, 5794869. https://doi.org/10.1155/2019/5794869

Palupi, N.P. (2015). Soil Acidity and C Organic Analysis On Cogon Grass Land (*Imperata cylindrica* L.) by chicken and Goat manure's Application. *Media Sains*, *8*(2), 182-188.

Papirio, S., Villa-Gomez, D.K., Esposito, G., Pirozzi, F. & Lens, P.N.L. (2013). Acid mine drainage treatment in fluidized-bed bioreactors by sulfate-reducing bacteria: A Critical Review. *Critical Reviews in Environmental Science and Technology*, *43*(23), 2545-2580. https://doi.org/10.1080/10643389.2012.694328

Pistelli, L., D'Angiolillo, F. & Morelli, E., Basso, B., Rosellini, I., Posarelli, M. & Barbafieri, M. (2017). Response of spontaneous plants from an ex-mining site of Elba island (Tuscany, Italy) to metal(loid) contamination. *Environmental Science Pollution Research*, *24*(8), 7809-7820. https://doi.org/10.1007/s11356-017-8488-5

Reyes, C., Schneider, D., Thürmer, A., Kulkarni, A., Lipka, M., Sztejrenszus, S.Y., Böttcher, M.E., Daniel, R. & Friedrich, M.W. (2017). Potentially Active Iron, Sulfur, and Sulfate Reducing Bacteria in Skagerrak and Bothnian Bay Sediments. *Geomicrobiology Journal*, *34*(10), 840-850. https://doi.org/10.1080/01490451.2017.1281360

Sánchez-Andrea, I., Sanz, J.L., Bijmans, M.F.M. & Stams, A.J.M. (2014). Sulfate reduction at low pH to remediate acid mine drainage. *Journal of Hazardous Materials*, *269*, 98-109. https://doi.org/10.1016/j.jhazmat.2013.12.032

Sandrawati, A., Suryatmana, P., Putra, I.N. & Kamaluddin, N.N. (2019). Pengaruh jenis bahan organik dan bakteri pereduksi sulfat terhadap konsentrasi Fe dan Mn dalam remediasi air asam tambang. *Soilrens*, *17*(1), 1-8.

Serrano, J. & Eduardo, L. (2017). Removal of arsenic using acid/metal-tolerant sulfate reducing bacteria: A new approach for bioremediation of high-arsenic acid mine waters. *Water*, *9*(12), 994. https://doi.org/10.3390/w9120994

Singh, J., Upadhyay, S.K., Pathak, R.K. & Gupta, V. (2011). Accumulation of heavy metals in soil and paddy crop (*Oryza sativa*), irrigated with water of Ramgarh Lake, Gorakhpur. *India, Toxicological & Environmental Chemistry*, *93*(3), 462-473. https://doi.org/10.1080/02772248.2010.546559

Syahrir, Yaqin, K., Landu, A. & Tambaru, R. (2019). Analysis of mercury and nickel content in fish and shrimp a result aquaculture of ponds in Pomalaa, Kolaka Regency. *IOP Conference Series: Earth and Environmental Science*, *382*(1), 012025. https://doi.org/10.1088/1755-1315/382/1/012025

Widyati, E. (2007). The use of sulphate-reducing bacteria in bioremediation of ex-coal mining soil. *Biodiversitas*, *8*(4), 283-286. https://doi.org/10.13057/biodiv/d080408

Winch, S., Mills, H.J., Kostka, J.E., Fortin, D. & Lean, D.R.S. (2009). Identification of sulfate-reducing bacteria in methylmercury--contaminated mine tailings by analysis of SSU rRNA genes. *FEMS Microbiology Ecology*, *68*(1), 94-107. https://doi.org/10.1111/j.1574-6941.2009.00658.x

Xu, Y.N. & Chen, Y. (2020). Advances in heavy metal removal by sulfate-reducing bacteria. *Water Science Technology*, *81*(9), 1797-1827. https://doi.org/10.2166/wst.2020.227

Zhang, F.W., He, Y.L., Zhao, C.M., Kou, Y.B. & Huang, K. (2020). Heavy metals pollution characteristics and health risk assessment of farmland soils and agricultural products in a mining area of Henan Province, China. *Polish Journal of Environmental Studies*, *29*(5), 3929-3941. https://doi.org/10.15244/pjoes/115273

Summary

Use of sulfate-reducing bacteria and different organic fertilizer for bioremediation of ex-nickel mining soils. The microbiological activity associated with ex-mining soil remediation can be considered useful to accelerate the contaminant degradation. The use of sulfate-reducing bacteria (SRB) and organic matter exhibits potential in improving ex-nickel mining soil quality. The purpose of this study was to examine the ability of SRB in several organic fertilizers to reduce sulfate and nickel ions, and to increase pH of soil from nickel in mining areas. This study used the bacteria collection of the Soil Laboratory of the Faculty of Agriculture, Universitas Muslim Indonesia. Those were previously isolated from two cultivating pond of milkfish in the Kuri area of Maros Regency, South Sulawesi, Indonesia. The soil samples were collected from ex-mining areas of the Vale Indonesia Enterprise in Soroako, South Sulawesi, Indonesia. Those were mixed with organic fertilizers, generated from sugarcane sludge, manure, and Quickstick (*Gliricidia sepium*) leaves, each with 50 and 100 g doses. The 5 kg soil samples were put into a pot and mixed evenly with organic fertilizers. A general linear model (GLM) repeated measures analysis of variance (ANOVA) was adopted to analyze the data. The results of this study indicate that the application of SRB and fertilizer was effective in reducing concentration of sulfate and nickel. Among the three types of organic fertilizers, manure was effective in reducing sulfate and nickel concentrations, while Quickstick fertilizer was the more effective in stabilizing pH level. Fertilizer doses exhibited a significant effect on decreasing sulfate and nickel concentrations, but it exhibited no significant effect on stabilizing pH levels. At 10 days after treatment (DAT), the sulfate concentration decreased from 2,530 ppm to 1,443 ppm in treatment of SRB and manure with dose of 50 g and 1,363 ppm with that of 100 g. At the end of the observation (30 DAT), those were decreased to 1,217 ppm in treatment of SRB and manure with doses of 50 g and 1,167 ppm with that of 100 g. Among the three types of organic fertilizers used, Quickstick demonstrates the more effective reduction rate. At 10 DAT, pH increased in SRB treatment by 7.06 at a concentration of 50 g and 7.01 at a concentration of 50 g. At the end of the observation (30 DAT), the pH became 6.67 at a concentration of 50 g and 6.82 at a concentration of 50 g. The nickel concentration decreased from an origin concentration to 1,950 ppm in treatment of SRB and manure with doses of 50 g and 1,690 ppm with that of 100 g. Thus, the application of manure fertilizer and the addition of SRB is recommended for bioremediation of sulfate and nickel from ex-mining soil.

Authors' address:
Bakhtiar – corresponding author
Universitas Muslim Indonesia
Faculty of Agriculture
90231 Makassar
Indonesia
e-mail: ibakhtiarumi@gmail.com

Sukoso
Universitas Brawijaya
Faculty of Fisheries and Marine Science
65145, Malang
Indonesia

Saida
Universitas Muslim Indonesia
Faculty of Agriculture
90231 Makassar
Indonesia

Scientific Review – Engineering and Environmental Sciences (2021), 30 (4), 573–584
Sci. Rev. Eng. Env. Sci. (2021), 30 (4)
Przegląd Naukowy – Inżynieria i Kształtowanie Środowiska (2021), 30 (4), 573–584
Prz. Nauk. Inż. Kszt. Środ. (2021), 30 (4)
https://srees.sggw.edu.pl
DOI 10.22630/PNIKS.2021.30.4.48

Karina PAREDES PÁLIZ[1, 2], Ana María CUNACHI[3], Edwin LICTA[2]

[1] Universidad Nacional de Chimborazo, Facultad de Ciencias de la Salud, Grupo de Investigación en Estudios Interdisciplinarios
[2] Escuela Superior Politécnica de Chimborazo, Facultad de Ciencias, Grupo de Investigación en Materiales Avanzados (GIMA)
[3] Escuela Superior Politécnica de Chimborazo, Facultad de Recursos Naturales, Laboratorio de Ciencias Biológicas

Reduction of the soil environmental impact caused by the presence of total petroleum hydrocarbons (TPH) by using *Pseudomona*s sp.

Key words: bioaugmentation, biodegradation, total petroleum hydrocarbons, efficiency, bacterium

Introduction

Fossil fuels are limited resources that are used to obtain energy. Within these, we can find oil, natural gas, and liquefied petroleum gas, which have been formed from the accumulation of large quantities of organic remains from plants and animals (Abas, Kalair & Khan, 2015). The use of fossil fuels causes atmospheric pollution, generators greenhouse gases, acid rain and respiratory diseases (Singh, 2017; Herndon & Whiteside, 2019).

The hydrocarbon activity in Ecuador is one of the main engines that move the economy of the country and therefore it is impossible to stop or replace the use of this type of resource (Merchán-Rivera & Chiogna, 2017).

Thanks to biotechnology, various methodologies have been developed that allow the restoration of soil, water, and even air, according to the needs and dimensions of the problem (Kuppusamy et al., 2017). One of the techniques used today for recovery of hydrocarbon contaminated soils is bioremediation in which bacteria are used for effective biodegradation of total petroleum hydrocarbons (TPH) (Quintella, Mata & Lima, 2019). Today, due biological and technological advances, it is much easier to

resort to any of the bioremediation processes such as phytoremediation, biostimulation, bioaugmentation, among others; where they use living organisms to treat environmental pollutants (Paredes-Páliz et al., 2016a; Anza et al., 2019).

In this context, bioaugmentation arises from the need to reduce the environmental impact of an area affected or contaminated by the presence of hydrocarbons to detoxify pollutants in different environments (soils and water) through the strategic use of microorganisms, plants, or enzymes (Arora, 2015). This mechanism involves the artificial introduction of viable populations through bioaccumulation using live cells and biosorption by dead microbial biomass (Paredes-Páliz et al., 2016b).

Within the bacterial groups mostly used for bioremediation purposes, *Pseudomonas* sp. is considered as one of the most heterogeneous and ecologically important groups of hydrocarbon-degrading bacteria (Rabus et al., 2016).

The first studies about this microorganism date back to the late 50s, when Leadbetter and Foster (1959) observed that *Pseudomonas methanica* oxidized ethane but could not use it as a carbon source. This was the first of a series of articles by the Foster group, who subsequently observed that this bacterium, growing in a medium with methane, could transform different hydrocarbons. Also, currently, *Pseudomonas aeruginosa* is one of the most used and studied microorganisms in bioremediation and presents a series of natural activities on xenobiotics. Unfortunately, it is also known to be an opportunistic pathogen in humans and causes serious complications in human health (Safdari, Kariminia, Nejad & Fletcher, 2017).

To evaluate the biodegradation of the TPH in soil, we isolated selective bacteria, using optimal environmental conditions for bacterial growth (Jiang et al., 2016). These studies were made in the Laboratory of Analysis and Environmental Assessment (AqLab), located in the city of El Coca, Orellana Province, Ecuador.

The aim of this study was to evaluate the bioremediation capacity of *Pseudomonas* sp. to propose economic and efficient solutions to treat soils contaminated with hydrocarbons with the finality of promoting the interest of companies specialized in bioremediation in the use of this bacteria as a potent degrader of oil contaminants.

Material and methods

Location of the study

This research was carried out in the province of Francisco de Orellana, Ecuador, in the AqLab laboratory, with the geo-referential coordinates 279265 m E and 9948497 m S located in zone 18M, WGS-84 S - UTM, extracted from Google Earth.

Experiment design

The completely randomized design (DCA) was used, which helped us to know if one treatment is different from the other treatment about native bacteria vs. commercial bacteria, with four repetitions. Our methodol-

ogy included: first group of buckets: S1.a, S1.b, S1.c, S1.d corresponding to the sterile native soil with its respective four replicates (a, b, c, and d) were inoculated with the bacterial colonies of *Pseudomonas aeruginosa* (S1). The second group of buckets: S2.a, S2.b, S2.c, S2.d, which corresponds to the sterile native soil with its respective four aftershocks (a, b, c, and d) were inoculated with *Pseudomonas* sp. bacteria previously isolated from same soil (S2). The standard soil called S3 (native non-sterile soil) which was not carried out replicas with the purpose to finalize the total contaminated soil, was bioaugmented with the bacterium *Pseudomonas* sp. (Table 1).

Unlike the previous physicochemical results, the TPH of the soil to be treated was above the permissible limits in Ecuador established in the Ecuadorian Executive Decree 1215 (RAOHE). To execute the treatments with their respective repetitions, the division into eight cubes was carried out with 2 kg of contaminated soil each, divided into two variables: the bacteria used for inoculation and the biodegraded TPH in the 80 days of treatment. For the test it was necessary to homogenize the soil and its sterilization avoiding the presence of other microorganisms at the time of bioaugmentation with the isolated bacteria (*Pseudomonas* sp.) and the commercial bacteria (*Pseudomonas aeruginosa*).

Physicochemical analysis of soil samples

A total of 6 kg of soil was extracted for the initial physical-chemical analysis and the isolation of *Pseudomonas* sp. The sterilization of native soil was carried out utilizing an autoclave at 120°C for 15 min for three times. Physicochemical parameters such temperature (T°), pH, humidity, electrical conductivity (EC), organic matter (MO), total organic carbon (COt), nitrogen (N), phosphorus (P) was measured using the methodology based on the "Standard methods for examination of water and wastewater" (American Public Health Association, American Water Works Association, Water Environment Federation [APHA, AWWA, WEF], 2017), EPA and ASTM methods, standardized methods private laboratory AqLab, duly

TABLE 1. Design and characteristics of the treatments (own studies)

Treatment	Description	Inoculation	Repetition
Soil 1 (S1)	native sterile soil	commercial bacteria (*Pseudomonas aeruginosa*)	S1.a S1.b S1.c S1.d
Soil 2 (S2)	native sterile soil	autochthonous bacteria isolated (*Pseudomonas* sp.)	S2.a S2.b S2.c S2.d
Soil 3 (S3)	native non-sterile soil	autochthonous bacteria isolated (*Pseudomonas* sp.)	no repetitions were realized

accredited by Ecuadorian service of accreditation – Servicio de Acreditación Ecuatoriano (SAE).

Isolation and massification of *Pseudomonas* sp. and *Pseudomonas aeruginosa*

To verify the presence of *Pseudomona*s sp. in native soil, media were prepared for the isolation of colonies. Selective medium Difco™ Pseudomonas Isolation Agar (DPI) was used as a first media for subsequent incubation in broth infusion brain-heart (BHI) at 35°C for 24 h. After 24 and 48 h, the cultures in Petri dishes were examined, using always a blank to verify that the medium is not contaminated with any type of microorganisms. Also, peptone water was used to reduce the microbial concentration by dilution (10^{-1}, 10^{-3}, 10^{-5}, 10^{-8}). Those isolates that presented blue/green or yellowish-brown pigmentation (Palleroni, 2005), due to the production of pyocyanin or pyoverdine were considered positive for the biodegradation treatment (APHA, AWWA, WEF, 2017).

The procedure for the isolation of *Pseudomonas* sp. (Native Strain No AqLab-001) and activation of *Pseudomonas aeruginosa* (Commercial Strain: ATCC@ 15442™* Catalogue No 0693, Lot No 693-1323) was done according to the methodology used in the laboratory AqLab and its comprehensive provider of commercial bacteria MEDILAB, laboratories accredited by the SAE, based on the book of Standard Methods No 9213E and the Association of Official Analytical Chemists (AOCA, 2003.07.2005). The reactivation and massification of the *Pseudomonas aeruginosa* was made using the isolation method proposed by Morales-Guzmán et al. (2017) to isolate petroleum degrading and emulsifying bacteria were performed with the addition of the nutrient broth for *Pseudomonas* sp. in the procedure standardized by the AqLab laboratory, whose massification is in agitation at 180 rpm for 72 h.

Bacteria efficiency and TPH biodegradation

The efficiency of the bacteria was determined based in the levels of biodegradation of TPH after some days of treatments (80 days), with data measured in $mg \cdot kg^{-1}$ in samples every 20 days. The methodology used for extraction measurement was made according to Schwartz, Ben-Dor and Eshel (2012). Consequently, no specific identification was carried out in this study, since only the presence of total oil-pollutants hydrocarbons (TPHs), was reported.

RESULTS AND DISCUSSION

Characterization of soil samples

The optimization and control of bioremediation processes is a complex system of many factors that include: the existence of a microbial population capable of degrading the pollutants; the availability of contaminants to the microbial population; the environment factors (temperature, type of soil, the presence of oxygen or other electron acceptors, pH, and nutrients) (Hlihor, Gavrilescu, Tavares, Favier & Olivieri, 2017).

Physical chemical parameters such organic carbon (TOC), organic matter (MO), phosphorus (P), nitrogen (N), humidity, pH, electrical conductivity (EC), temperature and irrigation were daily monitoring for a total of 80 days. At the same time, TPH and the presence of *Pseudomonas* were also measured. The collection of data through the control generates statistical data that will allow us to perform the efficiency calculations and maintain the soil conditions in optimal conditions for the bacterium to work in the biodegradation of TPH.

The parameters analyzed in the investigation of environmental liabilities contaminated with TPH are presented in Table 2, whose results showed that the physicochemical conditions of the soil, are in midpoint of the permissible limits of the current legal regulations of Ecuador. Also, reference was made in the quality criterion of the minimum parameters of soil fertility in TULSMA book VI, Ecuadorian Executive Decree 3516. Studies have shown that crude oil removal was improved in the presence of sufficient nitrogen and considerably reduced by insufficient nitrogen levels, by the other hand, lack of phosphorus can significantly decrease TPH removal (Sun et al., 2021). Besides, microorganisms produce enzymes in the presence of carbon sources which are responsible for attacking the hydrocarbon molecules. Many of these enzymes have different pathways involved to degrade a hydrocarbon contained in petroleum. Lack of an appropriate enzyme will either prevents attack or will act as a barrier to

TABLE 2. Physical-chemical parameters (own studies)

Parameter	Reference	Unit	Analysis results			Permissible limits		
			initial (0 days)	medium (40 days)	final (80 days)	min.	half	max.
pH	EPA9045C	–	7.32	7.3	7.64	6	–	8
Electric conductivity	EPA9050A	$mmho \cdot cm^{-1}$	240	248	252	–	–	< 2 000
Humidity	ASTM D3976-92	%	73	67	68	50	–	70
Organic material	gravimetric	%	4.12	2.6	1.74	≤ 1.0	1.0–2.0	≥ 2
Total organic carbon*	EPA9060	%	2.5	1.5	one	≤ 0.6–1.5	1.5–3.0	3.0–≥ 6.0
Total nitrogen*	Kjeldahl, EPA351.2	%	0.216	0.13	0.09	0–0.15	0.16–0.3	≥ 0.31
Phosphorus	Booker Tropical Soil Manual (Landon, 1991)	$mg \cdot kg^{-1}$	206.7	257.3	447.2	0–10.0	11–20	≥ 21

*Percentage ratio of C / N 11.6 is within the parameters since the regulations do not determine the accuracy of the permissible limit of the amount of organic matter, nitrogen and phosphorus in terms of the C / N ratio will be < 30 maximum for agricultural land according to current legal regulations (TULSMA book VI, Ecuadorian Executive Decree 3516).

complete hydrocarbon degradation (Barboza, Guerra-Sá & Leão, 2016). For this reason, it is essential that there is an adequate carbon balance for the removal of pollutants, as we can see in our results.

Morphological characterization of *Pseudomonas* sp.

Pseudomonas sp. showed a yellow-brown pigmentation in the first 24 h of incubation at 35°C (Fig. 1), changing to fluorescent red after 48 h of observation in incubation. The presence of polar flagella was also verified, so a minimum displacement of the colonies was observed at the end of the 7 days of observation. *Pseudomonas* oxidatively degrades glucose, which is why it is considered oxidase and catalase positive (Luján, 2019). Specifically, cytochrome monoxygenase enzymes allow the catalytic oxidation of THPs, degrading up to 100% of aromatic fractions (Araujo-Blanco et al., 2016; Cevallos Paguay & García Díaz, 2018).

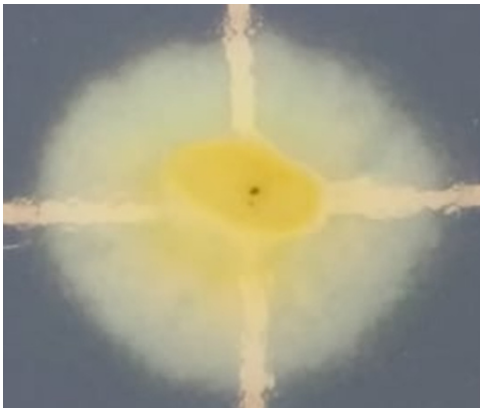

FIGURE 1. Isolation and growth of a colony from dilution 10^{-1} of *Pseudomonas* sp. after 24 h incubation at 35°C (own studies)

These characteristics helped confirm that the isolated bacterium belongs to the genus *Pseudomonas* (Powell et al., 2016). Because in the sponsoring company AqLab it does not have the accreditation of the SAE for molecular characterization, however, using API tests we were able to carry out the biochemical characterization of the native and commercial strains. Considering that only molecular tests can define the bacterial species to 100%, we prefer to describe the native strain only up to genus.

Control of the presence of *Pseudomonas sp.*

For an efficient bioremediation process, it is essential that the quantity and quality of the bacteria used are always optimal (Ojuederie & Babalola, 2017). For this reason, verification of *Pseudomonas* sp. colonies present in the contaminated soil was carried out at the beginning, during and at the end of the treatment of the biodegradation of TPH. The results were beneficial due the periodic control of the bacterial presence every 20 days during the entire treatment, making two massification: at the beginning and 60 days since the presence in colonies of *Pseudomonas* sp. and *P. aeruginosa* began to suffer a decrease in the CFU.

At 40 days of bioaugmentation in the native soil sterile using *Pseudomonas* sp. and *Pseudomonas aeruginosa*, CFUs are maintained with a high number of colonies in the dilution 10^{-3} to 10^{-8}. After 60 days, a deficit was observed in the CFUs in dilution 10^{-1} of the eight treatment cubes, so a count was made in some

cases by sectioning it into quadrants, obtaining between 89 and 373 CFU per Petri dish so that the activation of the bacteria in cryogenics was carried out and its massification in BHI broth, which is necessary a new bioaugmentation of the soil with the bacteria investigated thus without affecting the analysis of the degradation of the TPH.

Evaluation of TPH in soil samples

Biodegradation of total petroleum hydrocarbons (TPHs) is particularly limited by the low availability of contaminant compounds due to their low water solubility and strong absorption in inorganic and organic soil components. However, many studies associated with TPH biodegradation have focused on the use of single strains or an artificial microbial consortium constructed by mixing several known strains, which can grow on TPHs as the only carbon source (Harmsen & Rietra, 2018; Safdari et al., 2018). In our case, we used a native and commercial bacteria of genus *Pseudomonas* sp. Bioaugmentation carried out with *Pseudomonas* sp. is one of the most ecological and economical methods, since they convert hydrocarbons into innocuous subproducts such as CO_2 and H_2O (Prakash & Irfan, 2011; Luján, 2019). This bacterium uses and degrades N alkanes between 11 and 40 carbon atoms reaching 60% effectiveness, using C_{20} as a substrate (Brito, Flores, Howard, Cedillo & Hu, 2008).

Due the sterilization, the TPH can be significantly reduced in the samples evaluated, resulting in an average reduction of 56% at the initial TPH concentration of the standard sample; this occurs because they have different volatile organic compounds and boiling temperatures. Therefore, the initial results of the treatment show a reduction of an average from 20,640 $mg \cdot kg^{-1}$ in a sample of TPH (S3) to an initial of 9,366 and 8,977 $mg \cdot kg^{-1}$ (S1 and S2) without bacteria inoculation (Table 3).

Pseudomonas aeruginosa reduces the initial TPH to 1,996 $mg \cdot kg^{-1}$ and *Pseudomonas* sp reduces the initial TPH to 994 $mg \cdot kg^{-1}$ after 80 days of treatments (Fig. 2).

We can note that the highest concentration of TPH decreased at the first 20 days of treatment in the soil bioaugmented with *Pseudomonas* sp. (S2), unlike

TABLE 3. TPH quantity during treatment

Soil sample	TPH in the samples			Permissible limits in Ecuador			Unit
	initial (0 days)	medium (40 days)	final (80 days)	agricultural use	industrial use	sensitive ecosystems	
S1*	9 366	5 150	1 996	< 2 500	< 4 000	< 1 000	$mg \cdot kg^{-1}$
S2*	8 977	2 992	994	< 2 500	< 4 000	< 1 000	$mg \cdot kg^{-1}$
S3*	20 640	7 710	739**	< 2 500	< 4 000	< 1 000	$mg \cdot kg^{-1}$

*The representation of the acronyms S1 is the bioaugmented native sterile soil with *Pseudomonas aeruginosa*; S2: it is the bio-augmented native sterile soil with *Pseudomonas* sp.; S3: it is the bio-augmented non-sterile standard soil with *Pseudomonas* sp.

**They are the final TPH after 100 days of treatment to give final disposal to the total soil.

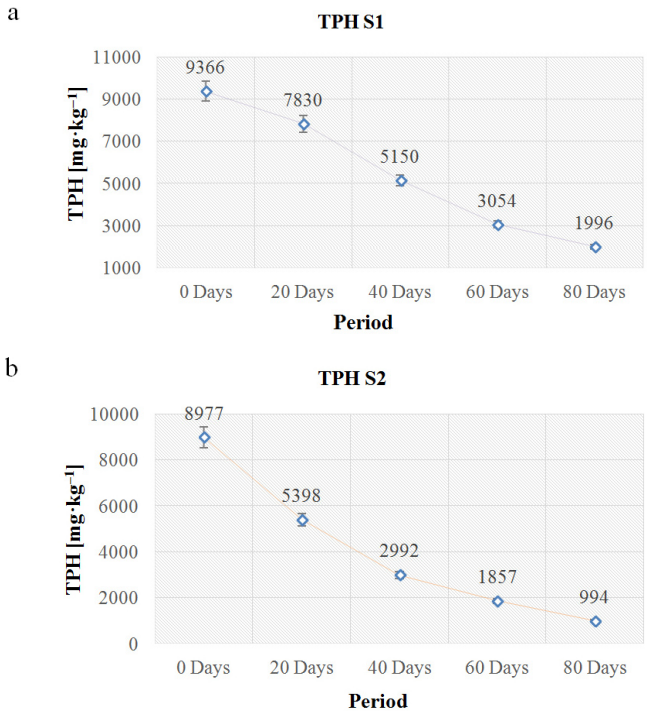

FIGURE 2. TPH biodegradation in soils inoculated with commercial and native bacteria (values are mean ±*SE* of four replicates): a – TPH biodegradation after 80 days of treatment with *Pseudomonas aeruginosa* (S1); b – TPH biodegradation after 80 days of treatment with *Pseudomonas* sp. (S2) (own studies)

the soil inoculated with *Pseudomonas aeruginosa* (S1) that decreased the TPH, but in a smaller percentage compared to the second S2 treatment. From here, the bioaugmentation proceeded only using *Pseudomonas* sp. since the purpose of the research is to reduce costs that generate high socio-economic benefits.

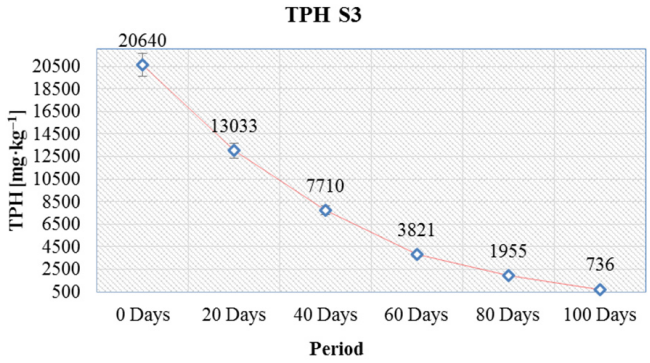

FIGURE 3. TPH biodegradation of the non-sterile standard sample in 100 days of treatment with *Pseudomonas* sp. (S3) (own studies)

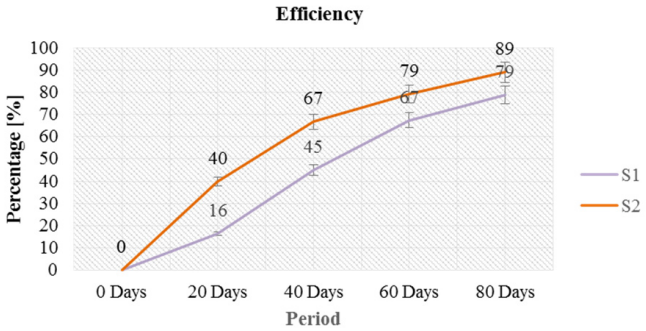

FIGURE 4. Efficiency growth by degrading TPH of *P. aeruginosa* (S1) and *Pseudomonas* sp. (S2) bacteria in sterile native soil during 80 days of treatment (own studies)

Because the laboratory permissible limit must be < 1,000 mg·kg^{-1} exclusive for sensitive ecosystems, according to Ecuadorian Executive Decree 1215, the evaluation of the biodegradation of TPH in the standard not sterilized sample was extended for 20 days over 80 days of treatment. At the end of the treatment, the soil complies with the permissible limits of current legal regulations having a result of TPH in a sample of 736 mg·kg^{-1} (Fig. 3).

Efficiency analysis

The degradation efficiency was calculated, allowing continuity to the statistical analysis and in this way to verify the hypothesis raised at the beginning of the study. As a result, the treatment with the native bacterium *Pseudomonas* sp. (S2) obtained a degradation percentage of 89% compared to commercial bacterium *Pseudomonas aeruginosa* (S1) that reached 79%, having a range of amplitude from one to the other of 10% (Fig. 4) whose average is a biodegradation of 84%. Data that could be compared with efficiency studies reported by Safdari et al. (2017) that show that the removal of hydrocarbons of up to 10 carbons reaches an efficiency of up to 90%, while for hydrocarbons of 20 carbons or more, the efficiency is of about 69%.

Conclusions

Bioaugmentation with isolated and massive native bacteria belonging to the Pseudomonadaceae family, specifically the *Pseudomonas* genus, reduced the concentration of initial total oil hydrocarbons (TPH) in contaminated soils to a final percentage of 4–12%. These results show an efficiency compared to the biodegradation rate of the commercial bacterium *Pseudomonas aeruginosa* that showed a final concentration of 20–22% of TPH in the agglomerates or environmental liabilities stored in the AqLab laboratory that was used in this research. The use of native bacteria in the area is decisive to ensure accelerated and efficient biodegradation due to the innate adaptability that these strains have compared to others that are not native to the site to be remedied.

References

Abas, N., Kalair, A. & Khan, N. (2015). Review of fossil fuels and future energy technologies. *Futures*, *69*, 31-49.

Anza, M., Salazar, O., Epelde, L., Becerril, J.M., Alkorta, I. & Garbisu, C. (2019). Remediation of organically contaminated soil through the combination of assisted phytoremediation and bioaugmentation. *Applied Sciences*, *9*(22), 4757. https://doi.org/10.3390/app9224757

American Public Health Association, American Water Works Association, Water Environment Federation [APHA, AWWA, WEF] (2017). *Standard methods for the examination of water and wastewater*. Washington: American Public Health Association.

Araujo-Blanco, J., Rojas, Y., Depool, B., Antequera, A., Rodríguez, J. & Yegres, F. (2016). Microanálisis de una cepa de *Aspergillus niger* biocatalizadora de hidrocarburos policíclicos aromáticos HPA [Microanalysis of a strain *Aspergillus niger* catalyzing polycyclic hydrocarbons aromatics HPA]. *Acta Microscopica*, *25*(2), 98-110.

Arora, N.K. (ed.). (2015). *Plant microbes symbiosis: applied facets*. New Delhi: Springer India.

Barboza, N.R., Guerra-Sá, R. & Leão, V.A. (2016). Mechanisms of manganese bioremediation by microbes: an overview. *Journal of Chemical Technology & Biotechnology*, *91*(11), 2733-2739.

Brito, R.S., Flores, G.P., Howard, A.M.M., Cedillo, F.D. & Hu, E.T.W. (2008). Degradación de n-alcanos por *Pseudomonas aeruginosa* MGP-1 [Degradation of n-alkanes by *Pseudomonas aeruginosa* MGP-1]. *Investigación Universitaria Multidisciplinaria: Revista de Investigación de la Universidad Simón Bolívar*, *7*(11), 123-132.

Cevallos Paguay, T.C. & García Díaz, J.D. (2018). *Evaluación de la biodegradación de suelos contaminados con hidrocarburos utilizando* Aspergillus niger*,* Pleurotus ostreatus *y* Pseudomonas aeruginosa [*Evaluation of the biodegradation of soils contaminated with hydrocarbons using* Aspergillus niger, Pleurotus ostreatus *and* Pseudomonas aeruginosa]. Quito: Politecnica Salesiana University.

Decreto Ejecutivo 1215. Reglamento sustitutivo del reglamento ambiental para las operaciones hidrocarburíferas en el Ecuador. Registro Oficial 265, 13.02.2001, ultima modificación 29.10.2010 [Executive Decree 1215. Replacement regulation of the environmental regulation for hydrocarbon operations in Ecuador. Official Registry 265, 13.02.2001, last modified 10.29.2010].

Decreto Ejecutivo 3516. Reforma texto unificado legislacion secundaria, medio ambiente. Registro Oficial, suplemento 2, TULSMA libro VI, anexo 2, ultima modificación 04.05.2015 [Executive Decree 3516. Reform of the unified text of secondary legislation, environment. Official Register, supplement 2, TULSMA book VI, annex 2, last modified 04.05.2015].

Harmsen, J. & Rietra, R.P. (2018). 25 years monitoring of PAHs and petroleum hydrocarbons biodegradation in soil. *Chemosphere*, *207*, 229-238.

Herndon, J.M. & Whiteside, M. (2019). Further evidence that particulate pollution is the principal cause of global warming: humanitarian considerations. *Journal of Geography, Environment and Earth Science International*, *21*(1), 1-11.

Hlihor, R.M., Gavrilescu, M., Tavares, T., Favier, L. & Olivieri, G. (2017). Bioremediation: an overview on current practices, advances, and new perspectives in environmental pollution treatment. *BioMed Research International*, *2017*, 6327610. https://doi.org/10.1155/2017/6327610

Jiang, Y., Brassington, K.J., Prpich, G., Paton, G.I., Semple, K.T., Pollard, S.J. & Coulon, F. (2016). Insights into the biodegradation of weathered hydrocarbons in contaminated soils by bioaugmentation and nutrient stimulation. *Chemosphere*, *161*, 300-307.

Kuppusamy, S., Thavamani, P., Venkateswarlu, K., Lee, Y.B., Naidu, R., & Megharaj, M. (2017). Remediation approaches for polycyclic aromatic hydrocarbons (PAHs) contaminated soils: technological constraints, emerging trends and future directions. *Chemosphere*, *168*, 944-968.

Landon, J.R. (1991). *Booker Tropical Soil Manual. A Handbook for Soil Survey and Agricultural Land Evaluation in the Tropics and Subtropics*. London: Routledge.

Luján, D. (2019). Uso de *Pseudomonas aeruginosa* en biorremediación [Use of *Pseudomonas aeruginosa* in bioremediation]. *Bio Tecnología*, *23*(1), 32-42.

Merchán-Rivera, P. & Chiogna, G. (2017). *Assessment of contamination by petroleum hydrocarbons from oil exploration and production activities in Aguarico, Ecuador*. Munich: Technical University of Munich.

Morales-Guzmán, G., Ferrera-Cerrato, R., Carmen Rivera-Cruz, M. del, Torres-Bustillos, L. G., Arteaga-Garibay, R.I., Mendoza--López, M.R., Esquivel-Cote, R. & Alarcón, A. (2017). Diesel degradation by emulsifying bacteria isolated from soils polluted with weathered petroleum hydrocarbons. *Applied Soil Ecology*, *121*, 127-134.

Ojuederie, O.B. & Babalola, O.O. (2017). Microbial and plant-assisted bioremediation of heavy metal polluted environments: a review. *International Journal of Environmental Research and Public Health*, *14*(12), 1504. https://doi.org/10.3390/ijerph14121504

Paredes-Páliz, K.I., Caviedes, M.A., Doukkali, B., Mateos-Naranjo, E., Rodríguez-Llorente, I.D. & Pajuelo, E. (2016a). Screening beneficial rhizobacteria from *Spartina maritima* for phytoremediation of metal polluted salt marshes: comparison of gram-positive and gram-negative strains. *Environmental Science and Pollution Research*, *23*(19), 19825--19837.

Paredes-Páliz, K.I., Pajuelo, E., Doukkali, B., Caviedes, M.Á., Rodríguez-Llorente, I.D. & Mateos-Naranjo, E. (2016b). Bacterial inoculants for enhanced seed germination of Spartina densiflora: Implications for restoration of metal polluted areas. *Marine Pollution Bulletin*, *110*(1), 396-400.

Powell, L.C., Khan, S., Chinga-Carrasco, G., Wright, C.J., Hill, K. E. & Thomas, D.W. (2016). An investigation of *Pseudomonas aeruginosa* biofilm growth on novel nanocellulose fibre dressings. *Carbohydrate Polymers*, *137*, 191-197.

Prakash, B., Irfan, M. (2011). *Pseudomonas aeruginosa* is present in crude oil contaminated sites of Barmer Region (India). *Journal of Bioremediation and Biodegradation*, *2*(5), 129. https://doi.org/10.4172/2155-6199.1000129

Quintella, C.M., Mata, A.M. & Lima, L.C. (2019). Overview of bioremediation with technology assessment and emphasis on fungal bioremediation of oil contaminated soils. *Journal of Environmental Management*, *241*, 156-166.

Rabus, R., Boll, M., Heider, J., Meckenstock, R.U., Buckel, W., Einsle, O., Ermler, U., Golding, B.T., Gunsalus, R.P., Kroneck, P.M.H., Krüger, M., Lueders, T., Martins, B. M., Musat, F., Richnow, H. H., Schink, B., Seifert, J., Szaleniec, M., Treude, T., Ullmann, G.M., Vogt, C., Bergen, M. von & Wilkes, H. (2016). Anaerobic microbial degradation of hydrocarbons: from enzymatic reactions to the environment. *Journal of Molecular Microbiology and Biotechnology*, *26*(1-3), 5-28.

Safdari, M.S., Kariminia, H.R., Nejad, Z.G. & Fletcher, T.H. (2017). Study potential of indigenous *Pseudomonas aeruginosa* and *Bacillus subtilis* in bioremediation of diesel-contaminated water. *Water, Air, & Soil Pollution*, *228*(1), 1-7.

Safdari, M.S., Kariminia, H.R., Rahmati, M., Fazlollahi, F., Polasko, A., Mahendra, S., Wilding, W.V. & Fletcher, T.H. (2018). Development of bioreactors for comparative study of natural attenuation, biostimulation, and bioaugmentation of petroleum-hydrocarbon contaminated soil. *Journal of Hazardous Materials*, *342*, 270-278.

Schwartz, G., Ben-Dor, E. & Eshel, G. (2012). Quantitative analysis of total petroleum hydrocarbons in soils: comparison between reflectance spectroscopy and solvent extraction by 3 certified laboratories. *Applied and Environmental Soil Science*, *2012*, 751956. https://doi.org/10.1155/2012/751956

Singh, R.L. (ed.). (2017). *Principles and applications of environmental biotechnology for a sustainable future*. Singapore: Springer.

Sun, Y., Chen, W., Wang, Y., Guo, J., Zhang, H. & Hu, X. (2021). Nutrient depletion is the main limiting factor in the crude oil bioaugmentation process. *Journal of Environmental Sciences*, *100*, 317-327.

Summary

Reduction of the soil environmental impact caused by the presence of total petroleum hydrocarbons (TPH) by using *Pseudomonas* sp. This research focuses on the bioaugmentation with *Pseudomonas* sp. (native) and *Pseudomonas aeruginosa* (commercial) for the biodegradation of total petroleum hydrocarbons (TPH) of the environmental soil samples of the AqLab laboratory in Orellana, Ecuador. Two treatments of sterilized soil (one inoculated with the native strain and the other inoculated with the commercial strain), where used for physical--chemical analyzes as well as the degradation of TPH. They were evaluated every 20 days for a total period of 80–100 days. The native bacterium was isolated from the laboratory agglomerates in a selective culture medium specific for *Pseudomonas* sp. The biodegradation of the TPH exhibited a positive result after 80 and 100 days of treatment, with a reduction of 84 and 96% of initial TPH after the bacterial inoculation. The comparison between the two strains evaluated, commercial and native, showed a greater efficiency of biodegradation by the native strain isolated directly from the agglomerates, suggesting working with native strains of the place that have a greater adaptability to the contaminated environment that would ensure bioremediation processes faster and more efficient, low cost and environmentally friendly.

Authors' address:
Karina Paredes Páliz – corresponding author
(https://orcid.org/0000-0002-5474-2566)
Universidad Nacional de Chimborazo
Facultad de Ciencias de la Salud
Avenida Antonio José de Sucre, Vía a Guano
EC060155 Riobamba
Ecuador
e-mail: kparedespaliz@gmail.com
karina.paredes@unach.edu.ec

Ana María Cunachi
Escuela Superior Politécnica de Chimborazo
Facultad de Recursos Naturales
Panamericana Sur km 1½
EC060155 Riobamba
Ecuador
e-mail: amcunachip@espoch.edu.ec

Edwin Licta
AqLab, Environmental Analysis and Evaluation Laboratories
Francisco de Orellana. Juan Huncite y Fray Gregorio
Ecuador
e-mail: edwin.licta@espoch.edu.ec

Instruction for Authors

The journal publishes in English languages, peer-reviewed original research, critical reviews and short communications, which have not been and will not be published elsewhere in substantially the same form. Author of an article is required to transfer the copyright to the journal publisher, however authors retain significant rights to use and share their own published papers. The published papers are available under the terms of the principles of Open Access Creative Commons CC BY-NC license. The submitting author must agree to pay the publication charge (see Charges).

The author of submitted materials (e.g. text, figures, tables etc.) is obligated to restricts the publishing rights. All contributors who do not meet the criteria for authorship should be listed in an Acknowledgements section of the manuscript. Authors should, therefore, add a statement on the type of assistance, if any, received from the sponsor or the sponsor's representative and include the names of any person who provided technical help, writing assistance, editorial support or any type of participation in writing the manuscript.

Uniform requirements for manuscripts

Manuscript should be sent with tables, graphs and abstract on separate pages by e-mail: iks_pn@sggw.edu.pl. All figures and tables should be placed near their reference in the main text and additionally sent in a form of data files (e.g. Excel, Visio, Adobe Illustrator, Adobe Photoshop, CorelDRAW). Figures are printed in black and white on paper version of the journal (color printing is combined with an additional fee calculated on a case-by-case basis), while on the website are published in color.

The size of the manuscript should be limited up to 10 pages including overview, summary, references and figures (the manuscript more than 13 pages is unacceptable); Please set the text format in single column with paragraphs (A4 paper format), all margins to 25 mm, use the font Times New Roman, typeface 12 points and line spacing one and half.

The submitted manuscript should include the following parts:

- name and SURNAME of the author(s) – up to 5 authors
- affiliation of the author(s), ORCID Id (optional)
- title of the work
- key words
- abstract (about 500 characters)
- text of the paper divided into: Introduction, Material and Methods, Results and Discussion, Conclusions, References and Summary
- references in APA style are listed fully in alphabetical order according to the last name of the first author and not numbered; please find the details below
- post and mailing address of the corresponding author:

  Author's address:
  Name, SURNAME
  Affiliation
  Street, number, postal code, City
  Country
  e-mail: adress@domain

- Plagiarism statement (https://srees.sggw.edu.pl/copyright)

Reference formatting

In the Scientific Review Engineering and Environmental Sciences the APA 6th edition style is used.

Detailed information

More information can be found: https://srees.sggw.edu.pl